NPS ARCHIVE
1966
JOHNSON, S.

A TRANSISTORIZED RELAY SERVO

STEPHEN JOHNSON
and
ROBERT HUNTLEY PIDGEON

Library
U. S. Naval Postgraduate School
Monterey, California

This document has been approved for public release and sale; its distribution is unlimited.

A TRANSISTORIZED RELAY SERVO

by

Stephen Johnson, Jr.
Lieutenant, United States Navy
B.S., Purdue University, 1961

and

Robert Huntley Pidgeon
Lieutenant, United States Navy
B.S., United States Naval Academy, 1958

[redacted]

Submitted in partial fulfillment
for the degree of

MASTER OF SCIENCE IN ELECTRICAL ENGINEERING

from the

UNITED STATES NAVAL POSTGRADUATE SCHOOL
May 1966

NPS ARCHIVE
1966
JOHNSON, S.

ABSTRACT

Bidirectional control of a DC motor is achieved with standard power transistors and a simple transistorized pre-amplifier. A permanent magnet, DC motor is used as a test vehicle to illustrate the feasibility of control without an amplidyne or mechanical relay. The "bang-bang" capability of the controller to operate as a near-ideal "relay" is emphasized. The inherent flexibility allowed in selecting the switching characteristics is also demonstrated. The discussion points toward practical application and stresses the analysis of the switching characteristics and system performance. The feasibility of using this controller to operate any other type of standard DC motor is

Library
U. S. Naval Postgraduate School
Monterey, California

TABLE OF CONTENTS

Chapter	Title	Page
	Introduction	9
I.	The two transistor "relay"	13
	1. The experimental system	13
	2. Observation of switching characteristics	18
	3. The describing function	39
	4. Open loop frequency response	46
	5. Closed loop frequency response	51
	6. Phase trajectories	54
	7. Transient responses	61
II.	The four transistor "relay"	69
	1. The experimental system	69
	2. Observation of switching characteristics	74
	3. The describing function	85
	4. Open loop frequency response	87
	5. Closed loop frequency response	90
	6. Phase trajectories	92
	7. Transient responses	95
III.	"Bang-bang" control of any DC motor with a four transistor "relay"	98
	Conclusions	103
	Recommendations and Acknowledgements	105
	Bibliography	107

LIST OF ILLUSTRATIONS

Figure Page

I-1-1 Block Diagram of Experimental System 16

I-1-2 Motor Characteristics 17

I-2-1 $-e_{in}$ vs e_R . Resistive Load 21

I-2-2 $-e_{in}$ vs e_m. Locked Rotor 23

I-2-3 $-e_{in}$ vs e_m. Motor Running 26

I-2-4 $-e_{in}$ vs e_m. Motor Running 29

I-2-5 $-e_{in}$ vs e_m. Motor Running 29

I-2-6 $-e_{in}$ vs collector voltage. Motor Running 29

I-3-1 Describing Function, Taken Open Loop 40

I-4-1 Open Loop Relative Gain and Phase Shift vs Frequency 48

I-4-2 Open Loop Relative Gain and Phase Shift vs Frequency 49

I-4-3 Open Loop Step Response 50

I-5-1 Closed Loop Frequency Response 52

I-5-2 Jump Resonance 53

I-6-1 Dead Zone Circuit 54

I-6-2 Phase Plan Plot Showing Effect of Dead Zone 56

I-6-3 Phase Plane Plots, Various Gains 56

I-6-4 Phase Plane Plots, Various Values of Tachometer Feedback 58

I-6-5 Phase Plane Plot 60

I-6-6 Phase Plane Plot 60

Figure Page

I-7-1 Closed Loop System Step Response 63

I-7-2 Open Loop Collector Voltage Step Response 64

I-7-3 Closed Loop Step Response 65

I-7-4 Closed Loop Step Response With Lead Compensation 67

I-7-5 Motor Voltage With Triangular Input, Open Loop 67

I-7-6 Error Signal With Triangular Input 68

II-1-1 Circuit Diagram of Four Transistor "Relay" Experimental System 73

System

II-2-1 Input vs Output, Four Transistor "Relay" 77

II-2-2 Input vs Output, Four Transistor "Relay" 79

II-2-3 Input vs Output, Four Transistor "Relay" 82

II-2-4 Input vs Output, Four Transistor "Relay" 84

II-3-1 Describing Function, Four Transistor "Relay" 86

II-4-1 Open Loop Frequency Response, Four Transistor "Relay" 88

II-4-2 Open Loop Step Response, Four Transistor "Relay" 89

II-5-1 Closed Loop Frequency Response, Four Transistor "Relay" 91

II-6-1 Phase Trajectory, Four Transistor "Relay" 93

II-6-2 Phase Trajectory, Four Transistor "Relay" 93

II-6-3 Phase Trajectory, Four Transistor "Relay" 93

II-6-4 Phase Trajectory, Four Transistor "Relay" 93

Figure Page

II-6-5 Phase Trajectory, Four Transistor "Relay" 94

II-7-1 Time Responses, Four Transistor "Relay" 96

II-7-2 Error Signal With Triangular Input, Four Transistor "Relay" 97

III-1 "Bang-Bang" Control of DC Motors With a Transistor "Relay" 101

III-2 Step Response of a Split-Field Series Motor 102

INTRODUCTION

Recent trends in modern automatic control theory have been toward some form, or mode, of optimum control of a plant or system. During the past several years the need for better controls in industrial, military, and space applications has stimulated a great deal of interest in problems of optimal control and system optimization. This requirement, together with the evolution of the digital computer, has given rise to a design and synthesis concept based upon state-space definition of a system and involving, most fundamentally, the determination of an extremum of a functional. An example of a modern automatic control system is digital control with time varying gains for optimum performance of a sampled data system. This is the so-called adjoint control scheme. Another spectacular instance of an optimum control problem is the rendezvous of manned space vehicles and space flight in general. [1]

Modern control philosophy, on the other hand, is the same as classical control philosophy except that some of the terms have been updated to correlate more closely with the more recent theories of modern automatic control. The current philosophy is that:

> "Control, even though it functions in a "perfect" fashion, can accomplish only so much in a given time. It is necessary to have sufficient energy for the system to accomplish the

> desired performance. With certain acceleration or velocity limits, considerably more time is required than if these limiting values were higher. "Bang-bang", or other full-forward full-reverse systems tending to operate at the maximum allowable acceleration can yield significantly shorter times to accomplish a given energy-limited type of task than can a linear control using the same maximum acceleration limit. The increases in energy and/or power to improve the response time capabilities of a controlled system appear to be of the order of the square or cube of the proportional decrease in time involved. Depending on the energy capabilities of a control system relative to its control capabilities, one can provide the greatest improvement in response of the system by reducing the time required by the control portion or the energy portion, depending on which tends to provide the greatest limitation on the system performance. In effect this means that the greatest improvement in the response of the system may be obtained by improving the limiting item, be it energy or control." [2]

This philosophy points directly to the subject of this thesis.

The standard DC motor has long been established as a prime mover in a wide variety of servo systems. Navy usage includes antenna drives, gun drives, and director drives, to cite a few common examples. For any given motor, if the system has acceleration or velocity limits, the "optimum" bidirectional performance is achieved by "bang-bang," or relay, control. Hence for this case, a "perfect" controller is an ideal relay. In practice a linear saturating control mode may be needed.

The major objective of this thesis was to transistor synthesize an ideal relay; the very essence of "optimum" control. The transistors have the obvious advantage of being small and light. An ideal relay for control of a DC motor will eliminate dead zone, hysteresis, and contact arcing. If power transistors are used then there is the possibility that this transistor "relay" will have sufficient gain to replace the conventional amplidyne, or at least to provide an alternate means of providing armature current. This latter consideration prompted the selection of a permanent magnet, DC motor, as a test vehicle.

The test circuit eventually selected was the Darlington configuration and complementary symmetry. It appeared that this circuit could control any standard DC motor. It was simple and cheap, because the transistors were readily available from any distributor and they had no special switching features.

In view of the primary objective, great attention and emphasis was focused on the switching characteristics because system performance will be optimum in the same sense that the switching characteristics are perfect. However, all of the usual performance observations were made to provide a point of departure for practical applications with this type of motor.

Another leading objective was to provide flexibility in selecting the switching characteristics. Control of dead zone, and gain control from linear operation up to an ideal relay, were sought. Hence considerable effort was expended to determine what parameters could be adjusted to provide this flexibility and to otherwise analyze the causes of the switching characteristics, whatever they might turn out to be. It was anticipated that these features would be extremely desirable for a multi-purpose, modular type of "relay" that could be used interchangeably throughout a given installation in a wide variety of switching modes. And it was also assumed that such a flexible "relay" might find wide application as a classroom demonstrator and/or an education and research aid in servo laboratories. It was felt that if the final production model could fulfill *any* of the various objectives then this thesis would be a significant contribution to the art and science of DC motor control, especially if ideal relay characteristics could be realized.

I

THE TWO TRANSISTOR "RELAY"

1. The experimental system

The experimental system is shown in block diagram form in Fig. I-1-1. The basic two transistor "relay" consists of a complementary symmetry pair with the armature circuit of a permanent magnet, DC motor as their load. The 75 ohm and 50 ohm resistors serve to balance the voltage gains of the two transistors and to increase the input impedance of the circuit so that the preceding power amplifier has a satisfactory impedance match. The current gains of the two transistors are about 35 when operated at six volts supply voltage. Since the starting current of the motor at six volts is 2.5 amperes, the power amplifier must be capable of delivering about 75 milliamperes into a load of less than 100 ohms. The transistors are rated at 150 watts with a maximum collector current of 10 amperes and a maximum collector to emitter voltage of 65 volts. The base to emitter input resistance is nominally 10 ohms and the maximum base current is two amperes. [3] The transistors were mounted on a common heat sink.

The "relay" driver was a Hewlett-Packard 467A DC power amplifier rated at 20 volts and 10 watts. This amplifier was not considered part of the "relay" because of its high cost and poor saturation characteristics.

Since the HP467A power amplifier does not have a summing junction and has a maximum gain of 10, a Philbrick, chopper stabilized, DC amplifier was used for tachometer and position feedback. This amplifier performed quite satisfactorily when not allowed to saturate. An additional Philbrick amplifier was used to enable recording proper polarity of signals.

The DC, permanent magnet, servo motor manufactured by Electrocraft Corp., was used because of its low cost, lack of cogging and built-in tachometer. Motor characteristics are shown in Fig. I-1-2. Unfortunately, it was not feasible to use the built-in tachometer because of excessive noise on its output at the high shaft speeds involved. An inertial mass of 100 grams was placed directly on the motor shaft. This gave an inertial load of 0.2 lb. in.^{2}. A shunt resistor (diodes) was inserted in parallel with the armature to limit transient effects.

The gear train was made up from Mark 1A analog computer surplus parts and had a 29.62 reduction factor to the potentiometer. The gear ratio from the potentiometer to the tachometer was reduced by 51 to 33. The gears were hand picked to minimize backlash.

The external tachometer was an Elinco DC permanent magnet generator which generated three volts per 100 rpm. Therefore, the intrinsic tachometer gain, K_t, is (3x33)/51 volts per 100 revolutions per minute of the output shaft (potentiometer).

Both the Brush Recorder and the oscilloscope were used to record data. Because of the noise introduced by the high speed transistor switching, it was necessary to use a 200/(s+200) RC filter on the inputs to the oscilloscope. For uniformity, a similar filter was used on the Brush Recorder.

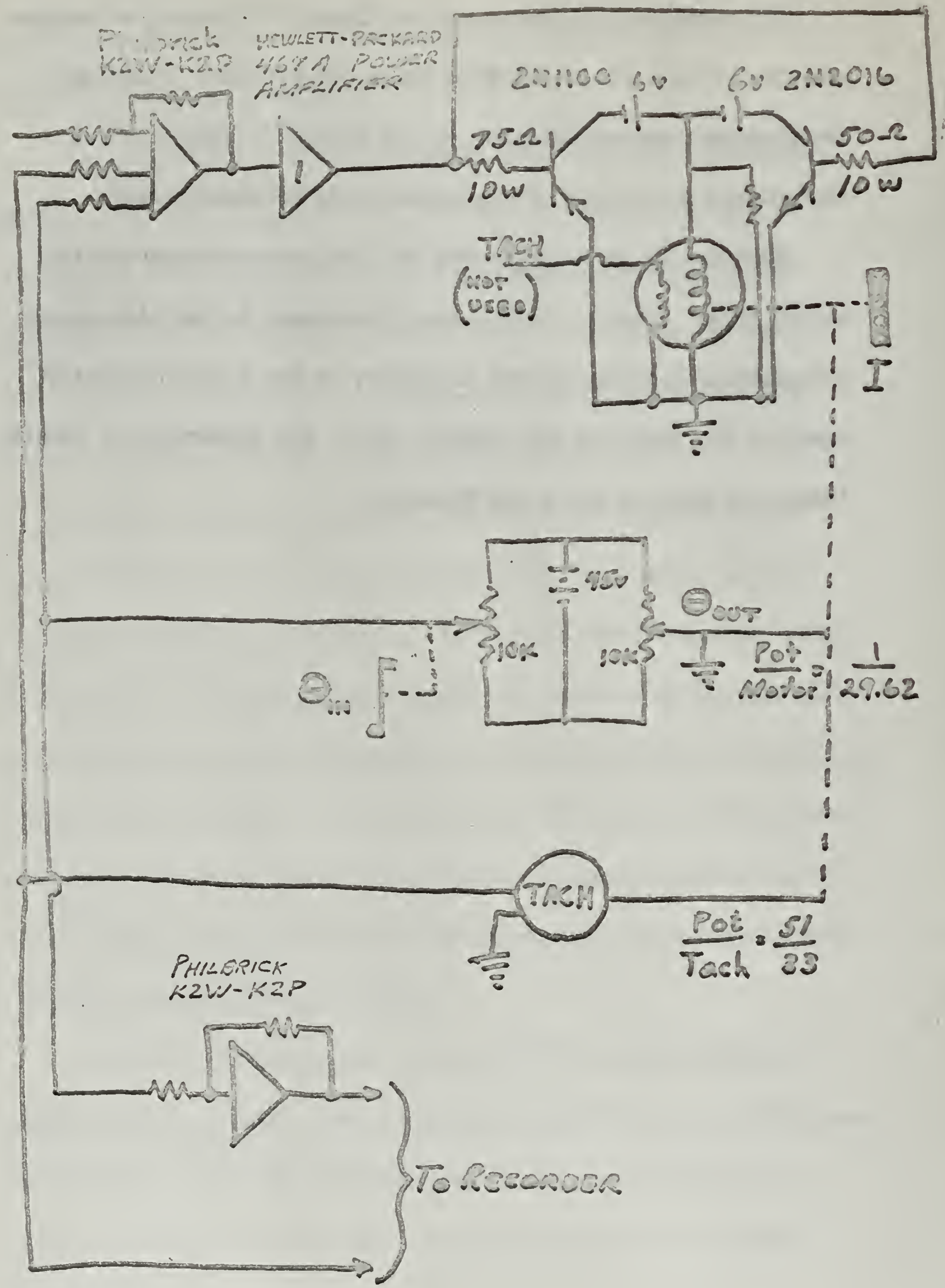
Philbrick
K2W-K2P
HEWLETT-PACKARD
467A POWER
AMPLIFIER
1
2N1100
6v
6v
2N2016
75Ω
10W
50Ω
10W
TACH
(NOT
USED)
I
45v
Θ OUT
10K
10K
Θ IN
Pot / Motor = 1 / 29.62
TACH
Pot / Tach = 51 / 83
PHILBRICK
K2W-K2P
To RECORDER

FIG. I-1-1 Block diagram of experimental system.

]

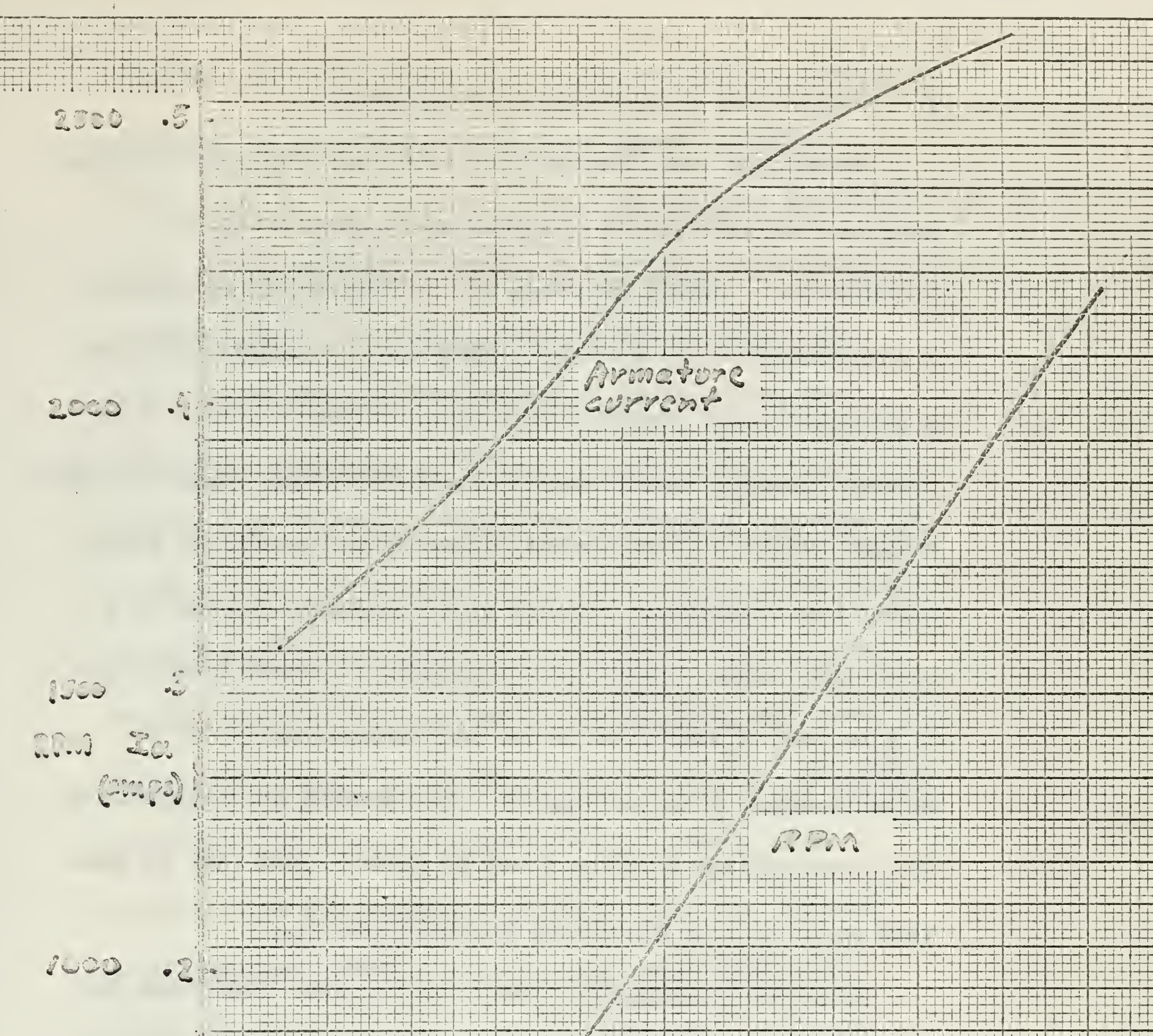

FIG. I-1-2 Motor characteristics. Armature current and RPM vs armature voltage

2. Observation of switching characteristics

The system was operated open loop with a triangular driving function and performance was principally observed on the oscilloscope. Within the range of low frequencies of interest, it was found that the Philbrick operational amplifier introduced some phase shift, when driven into saturation, because of an inherent time lag in returning to linear operation. There was also a phase shift from the Hewlett Packard power amplifier, when driven into saturation, because of its spurious response to a saturating signal. Hence care was taken to select combinations of gain, and of amplitude of the input signal, so as not to saturate either of the amplifiers. This limited the magnitude of the output voltage from the power amplifer to less than 20 volts. This upper limit is henceforth referred to as E_{PA}.

Being thus assured that there was no phase shift from the amplifiers, E_{in} at the base resistors versus e_{out} at the motor terminals was observed, henceforth referred to as e_i vs e_m. A phase shift phenomenon was observed having the typical shape of a hysteresis loop. To help locate the source of this hysteresis effect, a slide wire rheostat was substituted for the motor and adjusted to draw approximately the same magnitude of current as the motor. Then e_i vs e_R was observed with e_i ranging in magnitude up to E_{PA}, and in frequency up to 100 Hz. No phase shift was detected, hence the hysteresis effect could be attributed to neither the unregulated power supplies (batteries) nor the the time required for the transistors to come out of saturation. Fig. I-2-1(a) is a time exposure of a typical trace. The faint second image is caused by a mirror in the Polaroid camera mount. Since a negative e_i causes a positive e_R, and vice versa, the figure is correctly depicted as $-e_i$ vs e_R. Hence the right half is the PNP side of the circuit. It contributes a smaller portion of the dead zone because it is a germanium transistor with a typically smaller value of Vbe required to initiate conduction than its silicon counterpart in the left half of the figure. Neglecting the effect of the base resistors for the moment, it is apparent that this value of Vbe is analogous to "pull-in" and "drop-out" voltage in mechanical relay vernacular. Although there is no phase shift, it should be noted that the unregulated power supplies (batteries) do cause the load lines on the transistor characteristics to curve in direct proportion to the degree of the lack of regulation, thus contributing to the non-linear slopes of the gain characteristics of the transistors, henceforth referred to, collectively or individually, as k_x. The dead zone is seen to be about one volt wide, and the non-linear gain zones are each about 1.5 volts wide, up to Vce_{sat}.

Fig. I-2-1(b) is a time exposure of e_i vs e_R where R has been increased to about 25 ohms. This is roughly ten times the armature resistance. This increase causes a flatter load line on the transistor characteristics and a corresponding direct increase in k_x, up to Vce_{sat}. This graphically illustrates that one way to more nearly approximate a relay is simply to add resistance in series with the armature and accept the reduction in efficiency. Motor speed can be held constant by an increase in the supply voltage proportionate to the resistance thus inserted. The limit, as always, is the maximum power capability of the transistors (or possibly the power supplies).

Since reactive loads introduce phase shifts as a function of frequency, the motor was reinserted into the circuit and locked rotor observations of e_i vs e_m were made to ascertain any possible phase shifts that could be attributed to the inductive load. As in the resistive load tests, e_i ranged in frequency up to 100 Hz. But E_i was held constant at about .2 E_{PA}. Fig. I-2-2 is a series of time exposures of the traces obtained. A phase shift first appears at about two Hz and increases with frequency thereafter. The phase shift on the NPN side is consistently slightly greater than

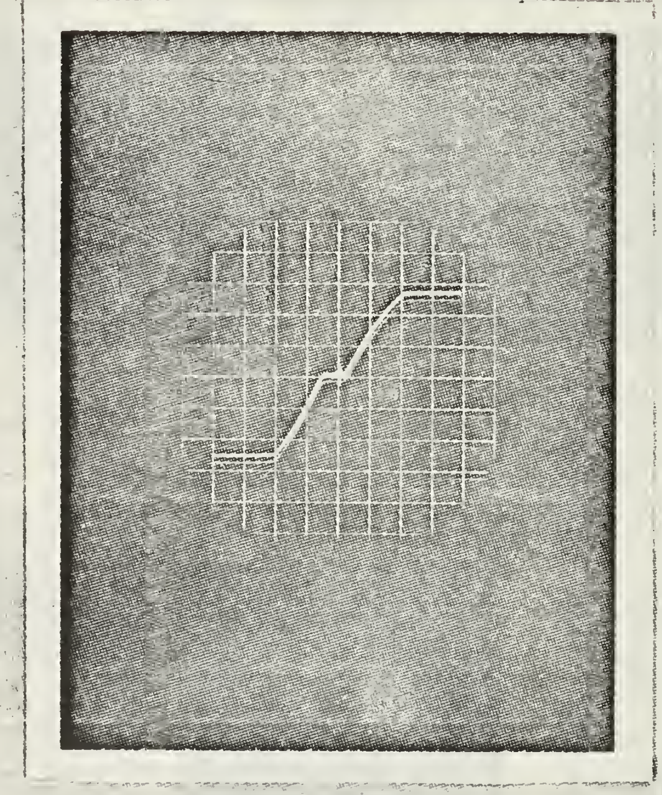

Fig. I-2-1(a) $-e_{in}$ vs e_R. Resistive load.
$e_{in} = .2\ e_{PA}$, $R = 2.5\Omega$, $f = .6\,Hz$
Abscissa: $-e_{in}$, 1 v/cm
Ordinate: e_R, 2 v/cm

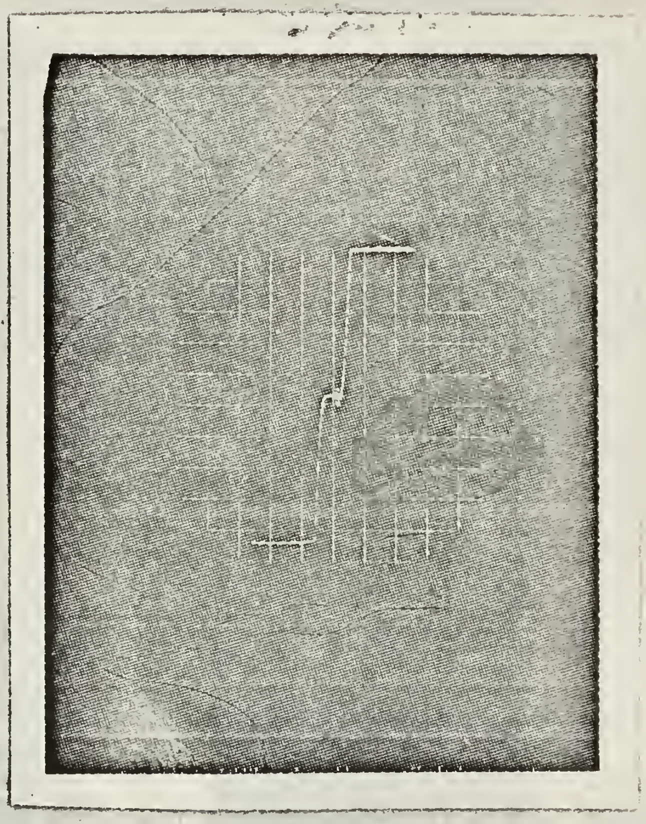

Fig. I-2-1 (b) $-e_{in}$ vs e_R. Resistive load.
$e_{in} = .2\ E_{PA}$, $R = 25\Omega$, $f = .2\,Hz$
Abscissa: $-e_{in}$, 2 v/cm
Ordinate: e_R, 1 v/cm

on the PNP side because of the greater Vce_{sat} of the silicon NPN transistor. The magnitude of the inductive transients increases until, at 100 Hz, it is larger than E_m and thereafter is effectively clipped by the shunt resistor (diodes). Also, in accordance with transistor theory, the width of the hysteresis loop is virtually uniform at each frequency, and k_x increases with frequency.

Now, with the rotor free, if the hyseresis loop is different than with the rotor locked, then there has to be a back emf effect causing changes in the collector voltages during portions of the cycle, which translate into shifting load lines and a hysteresis effect somewhat analogous to reactive loading. Fig. I-2-3 is a series of time exposures of the traces obtained for the various amplitudes and frequencies of e_i indicated. The hysteresis loop is indeed very much different. First, observe that k_x, and dead zone, remain, fundamentally, functions only of the transistor characteristics and the unregulated power supplies. The width of the hysteresis loop, a variable hereafter referred to as h, at frequencies of e_i up to two Hz (wherein it has been established that there is no phase shift from inductive loading) is slightly less on the NPN side. Since the back emf is a function of the motor speed, and hence proportional to

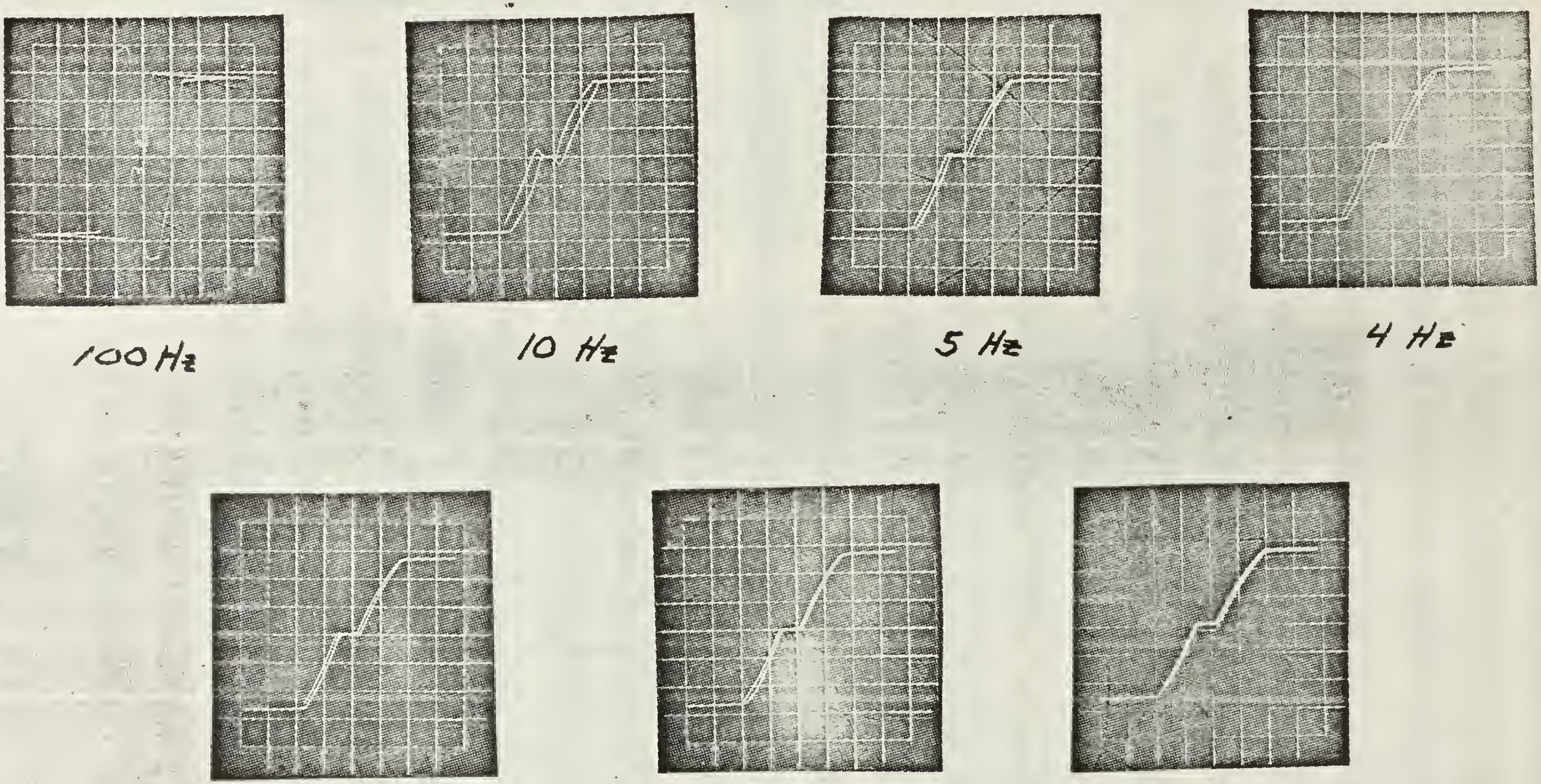

100 Hz 10 Hz 5 Hz 4 Hz

3 Hz 2 Hz .6 Hz

Fig. I-2-2 $-e_{in}$ vs e_M. Locked rotor.
$e_{in} = .2\,E_{pA}$
Abscissa: $-e_{in}$, 1 v/cm
Ordinate: e_m, 2v/cm

conduction time and voltage gain, then the NPN transistor either conducts for a shorter period of time, or has a smaller voltage gain, or both. The shorter conduction time has already been established because of the asymmetrical dead zone. It was determined from steady state speed observations that the motor always turned faster when operated from the PNP side. This is because the PNP transistor has both a higher current gain and a smaller Vce_{sat} . Therefore the voltage gain on the NPN side is the lower of the two and thus the speed here is reduced because of *both* conduction time and voltage gain disparities. One obvious way to match performance is to insert a resistance in the PNP collector circuit. But this detracts from both efficiency and performance of this half of the circuit, so a better way to match performance is to change the NPN transistor so as to improve performance on *this* half of the circuit. Substituting an NPN transistor with enough current gain to offset the disparities in conduction time and Vce_{sat} will match the maximum speeds attained on each half of the cycle, but unless the substitute is a germanium transistor with exactly the same value of Vbe required for conduction and precisely the same Vce_{sat} as the PNP transistor, then k_x for the NPN can not have the same shape as k_x for the PNP, and the distance traversed during each half of the cycle cannot be matched. So a prerequisite to having a "perfectly matched pair" is to use a germanium NPN transistor. An extensive search of most major manufacturer's catalogs and price lists, and several informal inquiries of both retail and wholesale distributors, failed to locate a germanium NPN transistor with more than a fraction of the desired power rating. Since a "perfectly matched pair" is a purely theoretical possibility, it was decided to continue to use the original silicon NPN transistor, in spite of the imbalance, and attempt to reduce any unacceptably deterious side effects to a tolerable level by modifications in the supporting circuits, if possible.

Returning to the observations that may be made in Fig. I-2-3, h was reduced on the NPN side as a result of both shorter conduction time and less voltage gain. At 10 Hz there is essentially no back emf effect because the hysteresis loop here is practically identical to the hysteresis loop at 10 Hz for the locked rotor (Fig. I-2-2). Of course this must be true because as $f \rightarrow \infty$, the motor responds less and less until eventually there is no movement at all, and the locked rotor condition has thus been reestablished.

Continuing with Fig. I-2-3, throughout the range of f_i, h increases with E_i and, up to 2 Hz, varies inversely with f_i.

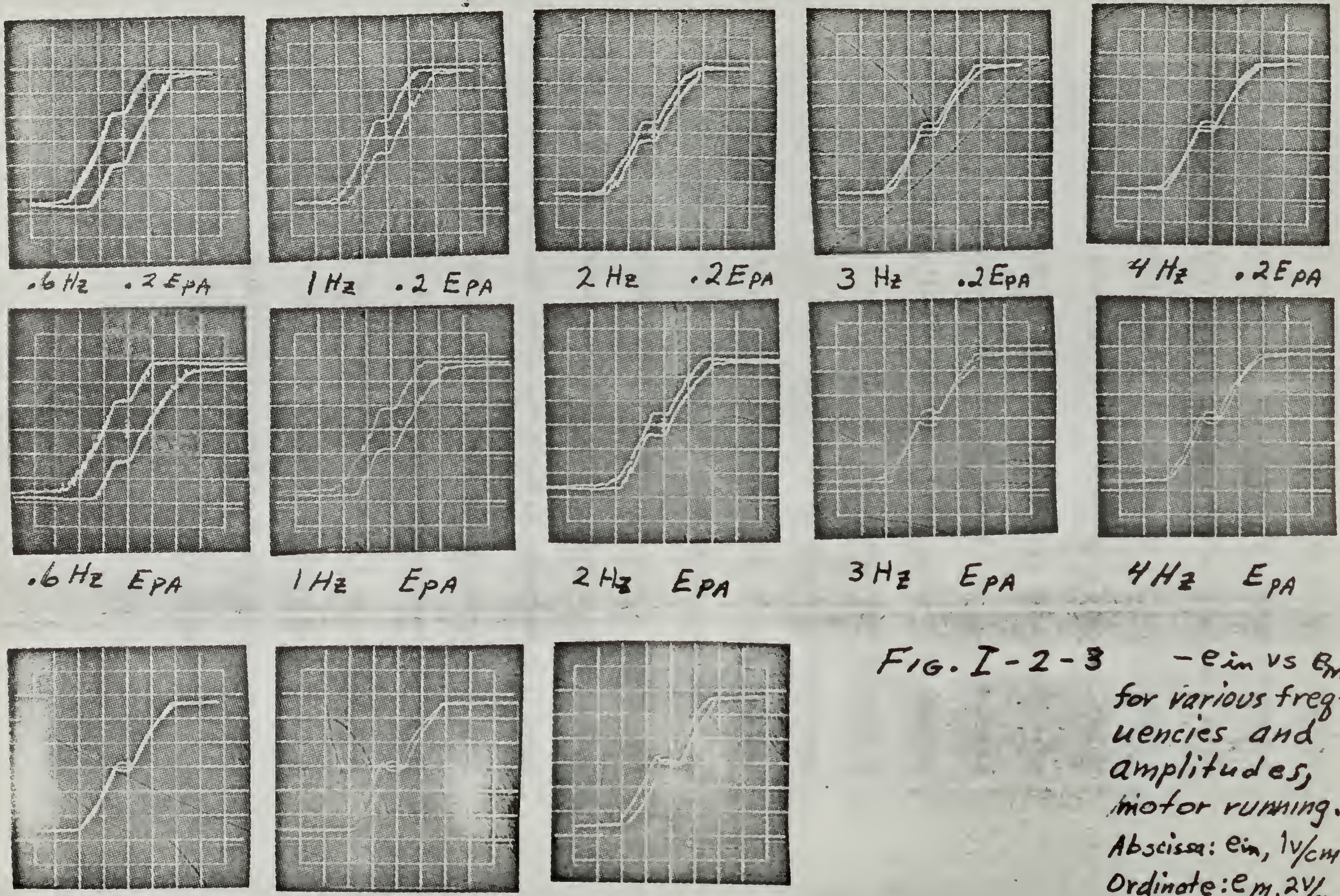

.6 Hz .2 EPA
1 Hz .2 EPA
2 Hz .2 EPA
3 Hz .2 EPA
4 Hz .2 EPA
.6 Hz EPA
1 Hz EPA
2 Hz EPA
3 Hz EPA
4 Hz EPA
5 Hz .2 EPA
5 Hz EPA
10 Hz .2 EPA

FIG. I-2-3 $-e_{in}$ vs e_m for various frequencies and amplitudes, motor running.
Abscissa: e_{in}, 1V/cm
Ordinate: e_m, 2V/cm

Hence, in general, the back emf effect on h increases with amplitude and decreases with frequency of the input signal. At frequencies greater than two Hz, but less than 10 Hz, h is a composite of the back emf effect and the inductive loading effect. At 4 and 5 Hz, the hysteresis loop crosses itself. Hence, at these frequencies the back emf effect has the opposite polarity of the inductive loading effect such that the net phase shift is practically zero. It is concluded that the location on the hysteresis loop where the back emf applies, can change, such that at about 4 Hz and higher, although h continues to steadily decrease with frequency, the back emf effect can produce phase shifts in the opposite sense to those at lower frequencies, at least during part of the cycle, if not throughout. Hence the hysteresis loop can cross on itself or, perhaps, even invert completely and produce a phase shift of an opposite sense to that at lower frequencies, throughout the cycle. At lower frequencies, say .6 Hz, it is also noted that the slope of the hysteresis loop across the dead zone is steeper than at higher frequencies, thus showing that the slope here varies inversely with frequency. And, finally, noise appears for the first time on e_m, being most apparent at the lower frequencies. It was concluded that this was typical brush noise.

Fig. I-2-4 illustrates that at very low frequencies, the width h no longer varies inversely with frequency. Indeed, the converse appears to be true. However, this is deceiving because, in reality, at this extremely low frequency the motor does not reverse direction cleanly but tends to have a stop and go, creeping motion. This allows stiction effects to persist, thus invalidating any practical analysis because a nearly constant dynamic friction load throughout most of the cycle must be assumed at the onset of any practical analysis. Hence the observations made from Fig. I-2-3 are valid only for $f_i > f_o$, where f_o is the minimum frequency at which a clean motor reversal will occur. It was found experimentally that f_o was about .02 Hz. Note also from Fig. I-2-4, the characteristic small hitch in e_m caused by the motor physically reversing on each side of the dead zone. This reversal is seen to occur very nearly in phase with e_i.

Next refer to Fig. I-2-5. Note that the slope of the hysteresis loop across the dead zone is inversely proportional to E_i. Observe that the characteristic small hitch in e_m, which occurs when the motor physically reverses, now appears later in the cycle, very near the saturation point. Indeed, it is now obvious that this small hitch also occurs at the higher frequencies shown in Fig. I-2-3, but is not visible because

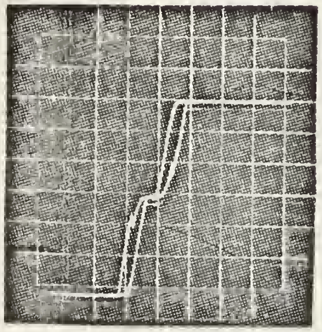

Fig.I-2-4

-e_{in} vs e_m, motor running, $f = .01$ Hz

$e_{in} = .2\,E_{PA}$

Abscissa: e_{in}, 1V/cm

Ordinate: e_m, 2V/cm

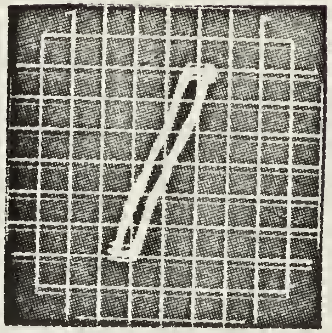

$e_{in} < V_{BEO}$

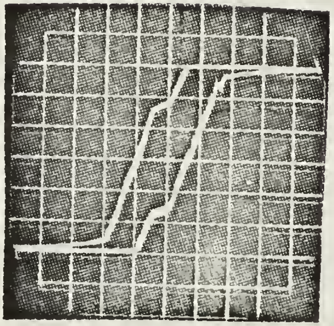

$e_{in} = E_{PA}$

Fig.I-2-5 — e_{in} vs e_m, motor running, $f = .1$ Hz

Abscissa: e_{in}, 1V/cm

Ordinate: e_m, 2V/cm

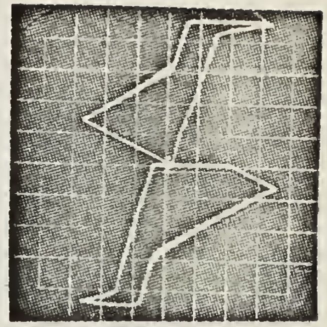

Fig.I-2-6 -e_{in} vs collector voltage.
This double exposure shows PNP on top, NPN on bottom.
$f = .2$ Hz $e_{in} = .2E_{PA}$
Abscissa: e_{in}, 1V/cm
Ordinate: V_c, 2V/cm

it has moved into the saturation part of the cycle. This small hitch is caused by the composite action of the host of non-linearities affecting, mainly, the load torque at this crucial time. Some examples of the non-linearities are stiction, friction and backlash. Fig. I-2-6 is a double exposure showing the performance of each transistor acting alone. The greater motor speed on the PNP side is apparent. Also the back emf is seen to decay almost linearly. It is apparent that the slope of the hysteresis loop across the dead zone is directly related to this back emf decay characteristic.

To better understand why the back emf influences the shape and magnitude of the hysteresis loop, it is necessary to examine the interaction of the many parameters involved.

The back emf, being a function of the motor speed attained, depends mainly on conduction time and voltage gain. Due to the inertial load the motor coasts after being switched and acts as a generator. This back emf will have a polarity such that, in accordance with Lenz's law, it will attempt to induce current to flow in the armature to prevent the armature current from decreasing. Hence the polarity of the back emf will always be such as to keep the polarity of the voltage drop across the motor constant. As long as the back emf persists, the collector voltage on the side coming out of conduction will be the difference between the battery voltage and the back emf, whereas the collector voltage on the side coming into conduction will be the sum of the two. On this opposite side the back emf attempts to induce current flow in the armature to oppose the increasing i_c. But here, on the underside of the hysteresis loop, due to the decay of the back emf from friction and windage, and the counter torque produced by the reversal of the armature current, the magnitude of the back emf effect on h will be typically much less than on the side coming out of conduction. Hence outside of the dead zone, the back emf affects the collector voltages directly, causing variations in i_c, and forcing the load lines to shift in response to the instantaneous collector voltage, e_c. This shifting of the load lines causes the loci of the operating point to describe a curvilinear path while there is a back emf. But during part of the cycle the motor is speeding up and then the operating point follows either a resistive or an inductive load line, depending on the frequency. It is easy to visualize that the closed path of the operating point will contain some distinctive area because the load line for e_i increasing is different from that for e_i decreasing. The shape and magnitude of this enclosed area is reflected directly in the shape and area of the hysteresis loop.

As long as e_i remains clear of the dead zone, the back emf will have some limited success in its efforts to induce armature current. But when e_i enters the dead zone, i_c must stop flowing, regardless of what e_c is doing, and the voltage on the motor is then equal to the back emf.

Now it is apparent why the back emf affects the hysteresis loop. But voltage gain is nearly constant, hence h is affected mainly by conduction time. This explains why h increases with e_i and varies inversely with frequency. The slope of the hysteresis loop across the dead zone depends on the back emf decay and must, therefore, increase directly with the length of time e_i spends in the dead zone. Hence the slope here varies inversely with both amplitude and frequency of e_i.

A further refinement in the manner in which h varies with e_i can be made as follows. Each increase in e_i will not produce a proportionate increase in h because the slope of e_i increases less and less as e_i approaches E_{PA}. Also, at some critical low frequency, the motor will just barely reach the maximum speed possible at $e_i \doteq E_{PA}$. At lower frequencies the motor will reach its maximum possible speed when $e_i < E_{PA}$ because now the conduction time required to reach maximum speed can be exceeded at, say, $e_i = E_{PA}$. So the most precise way to describe the effect of e_i on h is to say that when h increases with e_i, the increase becomes ever less with either increasing e_i or frequency, and, depending on some low critical frequency, h can cease increasing with e_i altogether, and become constant thereafter; this effect increasing with lower frequencies.

For second, and higher, order systems the velocity lag increases with frequency, hence the physical reversal of this motor, which is dominantly second order, can lag by as much 90 degrees at low frequencies. Although the magnitude of the back emf effect on h must continue to decrease with increasing frequency because of the conduction time effects, the portion of the hysteresis loop where the effect applies will change. As frequency increases the velocity lag increases and more of the back emf effect is applied to the transistor coming into conduction. The rate of this change to the opposite side will depend on the order of the system and the location of the poles. At any rate, the net effect of this shifting of the portion of the hysteresis loop to which the back emf applies will be to alter the resulting phase shift because the back emf affects the opposite side transistor differently than the transistor coming out of conduction, as explained earlier. Indeed, the velocity lag does not have to be very large before this opposite side shifting effect on the hysteresis loop shape will become appreciable. One can theorize that somewhere above 45 degrees phase shift, the shift will be great enough to cause a pronounced change in the hysteresis loop because now the back emf effect acts, every more dominantly, on the underside of the hysteresis loop instead of on the top side. If k_x is affected so that h is not uniform, then this opposite side shifting effect will cause phase shifts in both directions on either half of the cycle such that the hysteresis loop can cross on itself. Further velocity lags would cause all of the back emf effect to be applied to the underside of the hysteresis loop and then the phase shift, although necessarily much less because of the counter torque, would be entirely in the other sense and the crossing over of the hysteresis loop would cease. One can predict that for a fifth order system this phenomenon would be reenacted as the hysteresis loop returned to its original sense, and shape, with a 360 degree shift in velocity lag. However, by this time the frequency would probably be so high that the back emf effect would be lost.

To complete the analysis of how the back emf effect is reflected in the hysteresis loop, the effect of back emf on k_x must be considered. Since the load lines shift differently for increasing and decreasing e_i, the loci of the operating point cannot describe symmetrical paths. Since the transistor curves are nonlinear, k_x on the underside of the hysteresis loop will be different than k_x on the top side. The opposite side shifting effect accents this feature because the rate of decay of the back emf at the opposite side transistor is quite rapid, comparatively, thus causing the operating point loci to curve more rapidly here than when the transistor is coming out of conduction. Since the opposite side shifting effect increases with frequency, the lack of uniformity in h will also increase very slightly with frequency. Inductive loading will subtract on the underside of the hysteresis loop, and add on the top side, to further increase and compound this lack of uniformity and the resulting crossover/cancelling phenomenon.

An attempt to write the analytical equations for the hysteresis loop would lead to a set of nonlinear differential equations with many variables and much interdependence, or cross coupling. Some variables, such as the effect of temperature changes on the transistor characteristics, could safely be ignored, and others could be approximated; but it appears that even then the only practical way to solve such a set of difficult relationships would be with a digital computer. In view of the work involved, and since the hysteresis loop can be interpreted without the analytical expression, no attempt was made at writing this set of equations.

Throughout the observations of the switching characteristics it was observed that whenever either the frequency or the amplitude of the triangular driving function was appreciably changed, the DC balance of the generator would change slightly. Hence the asymmetrical distribution of the dead zone appears to wander from picture to picture in Fig. I-2-1 through Fig. I-2-6. The dead zone is, in fact, fixed. Besides being a function of the transistor characteristics, the dead zone is increased by the base resistors.

If the base resistor, R_b, is small, then there will be essentially no voltage drop across it until the transistor starts to conduct at its turn-on voltage. Hence for R_b small its effect on dead zone is negligible and both pull-in and drop-out voltages are dictated by the turn-on voltage. However, there is some small amount of base current flowing in the dead zone. So, as R_b becomes large (greater than 1000 ohms) there will be a small increase in the critical value of external turn-on voltage, thus expanding the dead zone.

When the transistor conducts, both base current and collector current increase. So, depending on the magnitude of the base current, there will be a voltage drop of some magnitude across R_b and the voltage gain up to Vce_{sat} must decrease. A theoretical approximation of voltage gain, using h parameters, has R_b in both the numerator and the denominator in such a fashion that increasing R_b increases the denominator slightly more than the numerator. This prediction was verified experimentally. As with the dead zone expansion, R_b has to be more than 1000 ohms to appreciably change k_x, up to Vce_{sat}. More than a few thousand ohms will appreciably flatten k_x and unless the gain of the amplifier in increased, the transistors will not saturate and operation will be quasi-linear.

These R_b features can be used to vary both dead zone and voltage gain. With variable resistors in each base circuit, separate adjustments could be made to both sides of the circuit. With a single variable resistor inserted ahead of the base junction, both sides could be affected simultaneously. Hence a wide variety of switching characteristics could be synthesized. But even if there were no hysteresis effect, the great drawback to this scheme is that dead zone increases as voltage gain decreases. It may be possible to design a circuit to circumvent this dual action, but this circuit will be more complicated than the original. The practical value of such a circuit is questionable, especially because R_b detracts from the relay action.

It is obvious that if this basic two transistor test circuit were modified to remove the dead zone, then a variable R_b might hold more promise as a vehicle for adding flexibility to the switching characteristics in the control loop. Removing the dead zone would also eliminate much of the hysteresis effect.

3. The describing function [4, 5]

The describing function, G_D, for this system was sought, primarily, to determine if there was any intrinsic property of transistor "relays" that would prohibit either the collection of data to compute a describing function (if desired), or the interpretation (and use) thereof, once it was found. If the required measurements can be made, and G_D reflects the composite nonlinearities of the system, then the normal use of G_D can be assumed. It was hoped that such an attempt at interpretation would provide a deeper insight into the relative importance of system parameters, thus assisting with the synthesis of an improved production model. Also, if G_D corresponded with the composite nonlinearities, it was anticipated that application of the established describing function techniques for interpretation of frequency responses and, possibly, transient performance, might also help with this ultimate synthesis objective.

This system has the common property of all type one control loops in that the open loop output voltage, either at the motor shaft or at the potentionmeter, cannot easily be determined directly due to position drift. Since noise prohibits the employment of the internal tachometer for measurement purposes, the external tachometer at the output of the gear

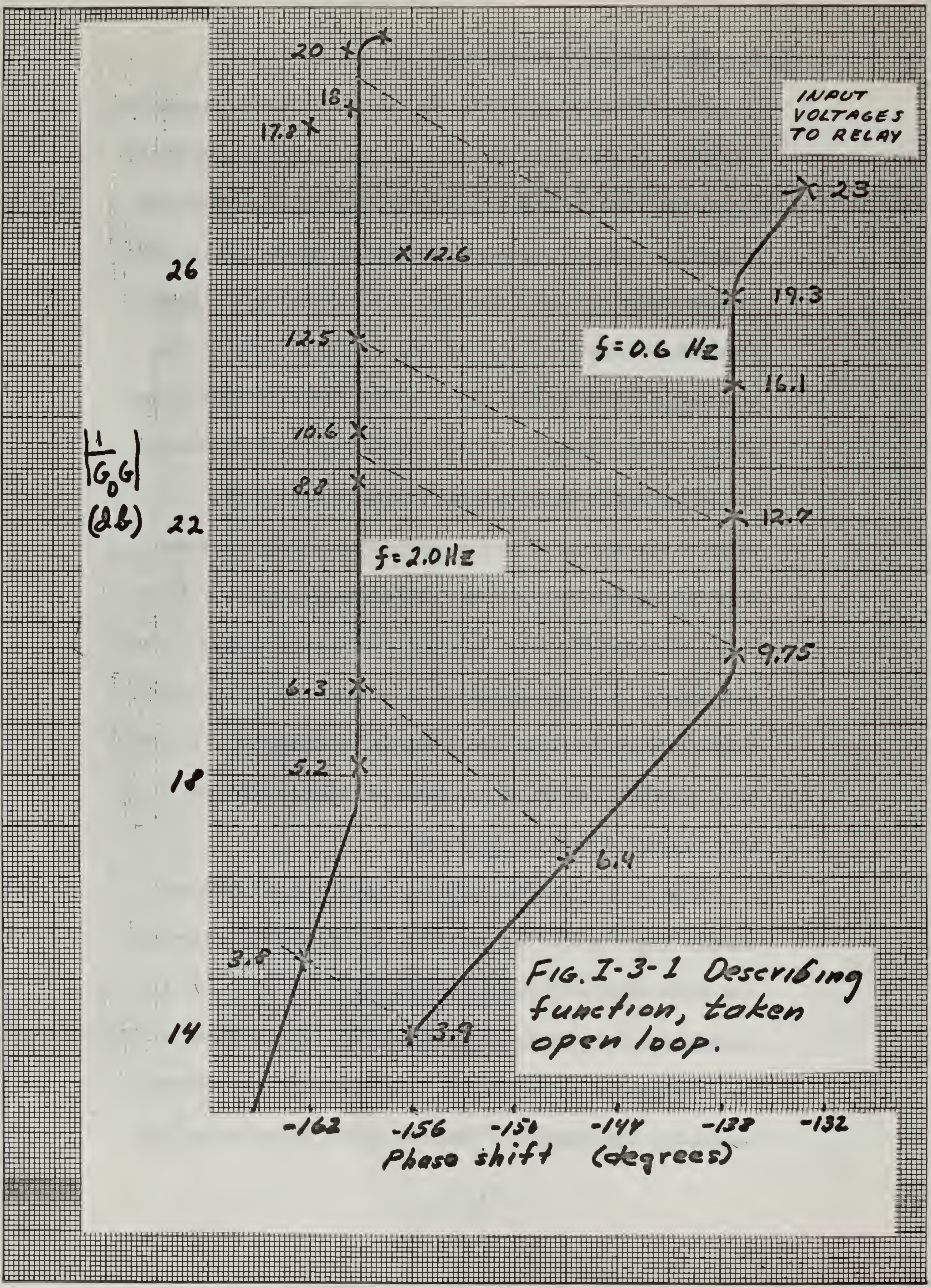

FIG. I-3-1 Describing function, taken open loop.

train was used. Open loop data at frequencies of .6 and 2 Hz was collected using the Brush Recorder, and the usual computations were made. Fig. I-3-1 is a plot of these describing functions on a Nichols chart. The phase angle ϕ includes a -90 degree shift to correct for the tachometer. $\frac{1}{G_D G}$ has been shown, as usual, so that the effect of gain changes on the forward transfer function may be correlated directly.

The closed loop method for determining the describing functions, utilizing the M and N contours, was also attempted, but the results were inconclusive. This is normally the case with low order systems because poor filtering allows harmonics to distort the error signal.

In order to ascertain if G_D correctly depicts the composite nonlinearities of the system, the effect of the hysteresis loop, $-e_i$ vs. e_m, of the preceding section, must be determined at the potentiometer. The difficulty, as before, is that the switching characteristics are a function of the load, both electrical and mechanical. Hence the nonlinearity cannot be isolated from the linear portion of the forward transfer function, and tested separately. So e_i vs. e_{shaft} must be deduced from $-e_i$ vs. e_m. Then any nonlinearity between the shaft and the potentiometer must be added to this new hysteresis loop, and if E_{PA} is exceeded, this nonlinearity too must be taken into account in order to eventually find e_{in} vs. e_{out}, the net hysteresis loop. The behavior of this net hysteresis loop must be correctly reflected in G_D.

Because of the motor dynamics, e_i vs. e_s will have a variable width h' which varies in the same manner as h, and for the same reasons. The shape will be contorted, and the degree of contortion variable, again in a manner analogous to e_i vs. e_m. The characteristic area and the overall form will, of course, be quite different. This new hysteresis loop will vary in height and it will have an overall changing tilt. But whatever its shape, between the shaft and the potentiometer the backlash, b, will simply increase the width of e_i vs. e_s on each side by an amount b/2. Care was taken to eliminate binding and reduce friction to a minimum, so the major nonlinearity between shaft and potentiometer is backlash. This too was minimized as much as possible for a simple, crude gear train. So bounce may be safely neglected. Also neglecting the elasticity of gears and shafts, motor bearing and brush friction, armature reaction, and other similar minor effects such as temperature effects on transistor characteristics, a fair estimate of the width of the net hysteresis loop has to be: h' + b, where b is a constant and h' is directly proportional to amplitude of input signal and inversely proportional to frequency, in the same sense as h. For $E_i > E_{PA}$, another refinement to this general character must be added.

For a theoretical describing function, the only cause of a relative phase shift is some kind of hysteresis effect. This relative phase shift always contains the ratio of hysteresis width to input magnitude in such a fashion that in the limit, as the amplitude of input approaches infinity, the relative phase shift approaches zero. The magnitude of the describing function usually contains this ratio also, in such a fashion as to change with hysteresis width and shape.

Returning to Fig. I-3-1, the hook in the describing functions at high amplitude is caused from the power amplifier being saturated. But the nonlinearity from the saturating power amplifier was observed to be time varying, and thus the describing function here has no meaning because a fundamental restriction of describing function theory is that the nature of the nonlinearity be time invariant.

For $E_i < E_{PA}$, the relative phase shift should be dominated by the ratio $\frac{h' + b}{E_i}$. At .6 Hz h' is greater than at 2 Hz (for any common E_i) so there is more relative phase shift at the lower frequency. At either .6 or 2 Hz, E_i contributes to h' in a graduated, decreasing matter. So for E_i small, there is more increase in h' with increasing E_i, than for E_i large, and the effect will be most pronounced at the lower frequency. Hence the phase shift at .6 Hz is quite rapid at small E_i. At 2 Hz the frequency effect makes h' so small that there is, comparatively, a minor phase shift in the range of allowed gain, in spite of the E_i contribution to h'. At .6 Hz, as h' becomes nearly constant for increasing E_i, the ratio $\frac{h' + b}{E_i}$ decreases ever faster in the same graduated matter, thus making the relative phase angle change rather abruptly toward zero.

For a hysteresis loop of this complexity, G_D is almost certain to have h' + b in the magnitude expression somewhere. And G_D should contain terms to account for the lack of uniformity in the width h', caused by the variations in k_x. The dashed straight lines in Fig. I-3-1 connect points of equal E_{in}. The top two lines are in the region of zero relative phase shift. They are not parallel, and hence G_D does indeed reflect the effects of frequency changes.

Further speculation over the causes of the various effects appearing in Fig. I-3-1 is prohibited because of the general inaccuracy of the phase data, an intrinsic property of all but the very simplest describing functions. However, it is submitted that the general observations are sufficient to conclude that the describing function does correctly reflect the composite non-linearities of the system. The usefulness of the describing function technique is limited, however, mainly because of its frequency dependence.

The large range of amplitude available wherein there is practically no relative phase shift is particularly encouraging. This shows that the hysteresis effect on relative phase shift can be small, at least in the range of frequencies from somewhere less than .6 Hz up to where inductive loading becomes an important factor. The hysteresis effect on magnitude, however, emphasizes the general desirability of eliminating the hysteresis effect altogether.

4. Open loop frequency response [4, 5]

The open loop frequency response of the system was taken by driving the input with a sine wave and by measuring the output at the external tachometer. Fig. I-4-1 shows the results with the "relay", and Fig. I-4-2 from driving the motor directly.

An examination of the data reveals that the 3 db bandwidth with the "relay" is about 0.53 cycles per second greater than that for the motor driven directly. The two bandwidths are, respectively, 0.83 cycles per second and 0.3 cycles per second. The "relay" system gives greater bandwidth because more volt-seconds per cycle are fed to the motor, allowing the motor to reach higher speeds for the same peak input voltage.

Upon further examination of the data, it is found that the phase curves do not correlate with the relative response curves. The midfrequency data becomes very rough indicating the possibility of a zero created by torsional forces, which in turn can be accounted for by having an inertial load on each end of the motor. Also, it is seen that generally the phase lag is about 10 degrees more than it should be. This could be due largely to the backlash of the gear train.

Referring to Fig. I-4-2, the data suggests that $\frac{K}{S[S + .3\ (2\pi)]}$ is a good approximation to fit the response curve. If the phase curve is used, the transfer function would be more nearly

$$\frac{K}{s\ [s + .5\ (2\pi)]}$$

In any event, except for the backlash, the open loop system is predominantly second order. Referring to Fig. I-4-3, the open loop speed response to a step input to the motor, it is seen that one time constant is approximately 1/3 second. This substantiates use of the $\frac{K}{s\ [s + .3\ (2\pi)]}$ transfer function for the motor and gear train.

While observing the open loop frequency responses, it was discovered that the major source of noise on the internal tachometer was due to transformer coupling with the armature. The effective turns ratio is about 6 to 1. Hence for every 6 volts appearing at the motor terminals there is roughly 1 volt of inductive feedover to the tachometer side. All transient effects, and noice in general, from the armature circuit appear on the tachometer side, plus the tachometer's intrinsic noise. The adverse effect on both magnitude and phase prohibits using the internal tachometer for any measurements, and seriously detracts from closed loop performance with the internal tachometer.

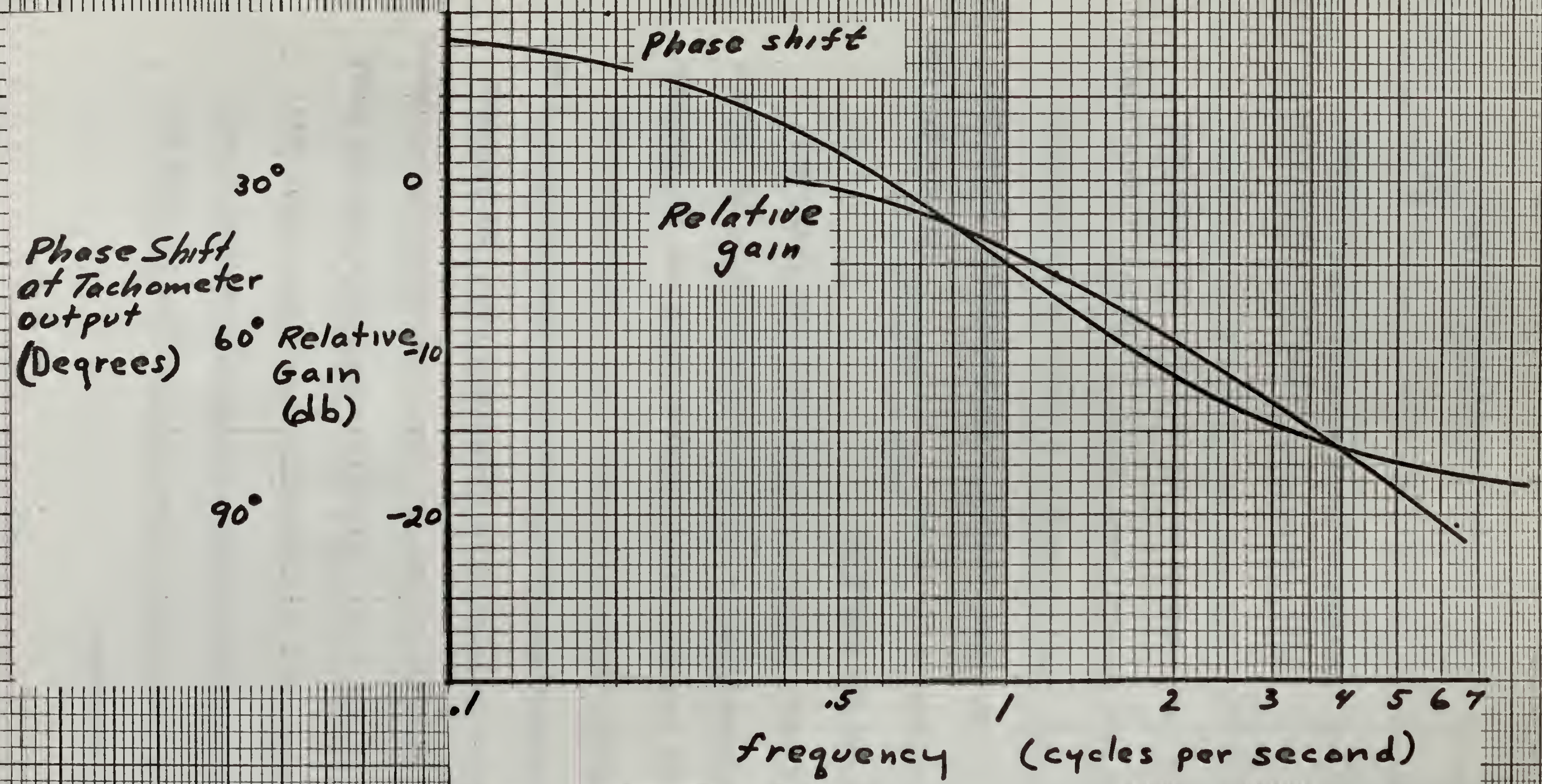

FIG. I-4-1 Open loop relative gain and phase shift vs frequency. Output is from the tachometer.

K+E SEMI-LOGARITHMIC 358-71
KEUFFEL & ESSER CO. MADE IN U.S.A.
3 CYCLES X 70 DIVISIONS

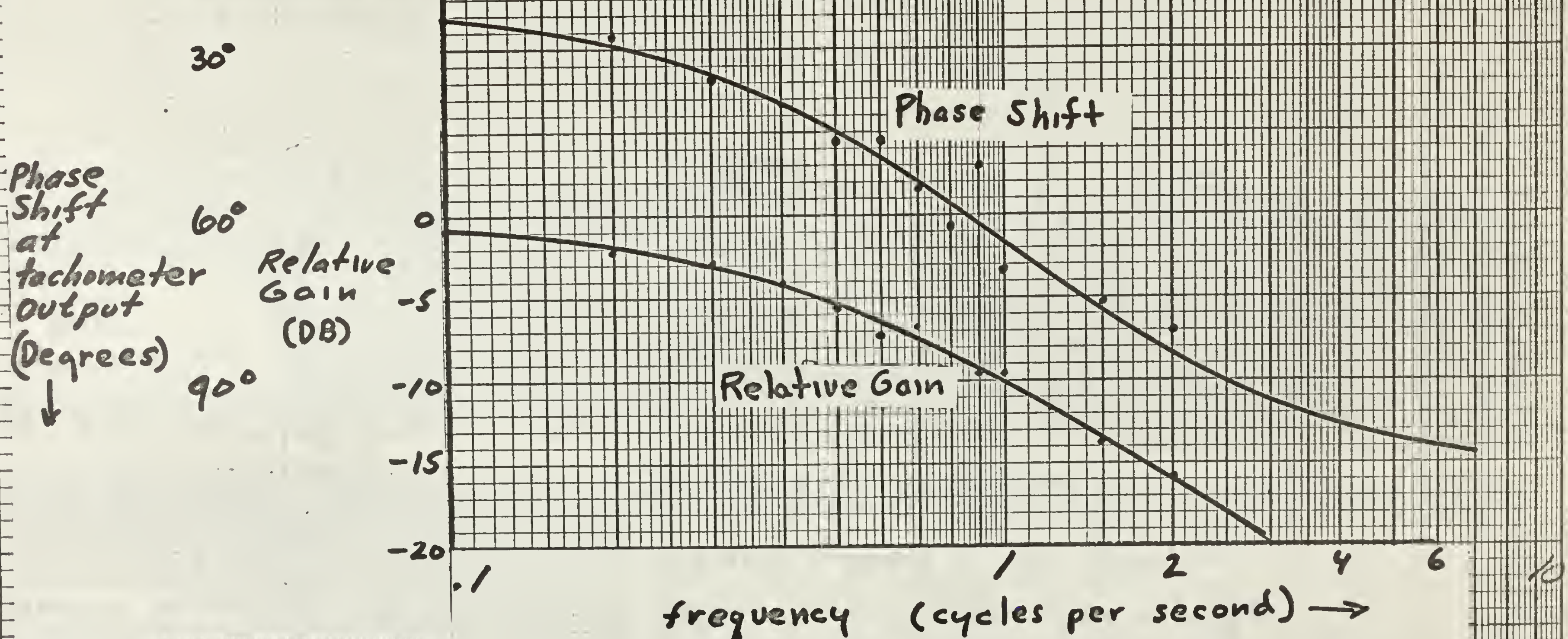

FIG. I-4-2 Open loop relative gain and phase shift vs frequency. Input is directly to the motor, output is from tachometer.

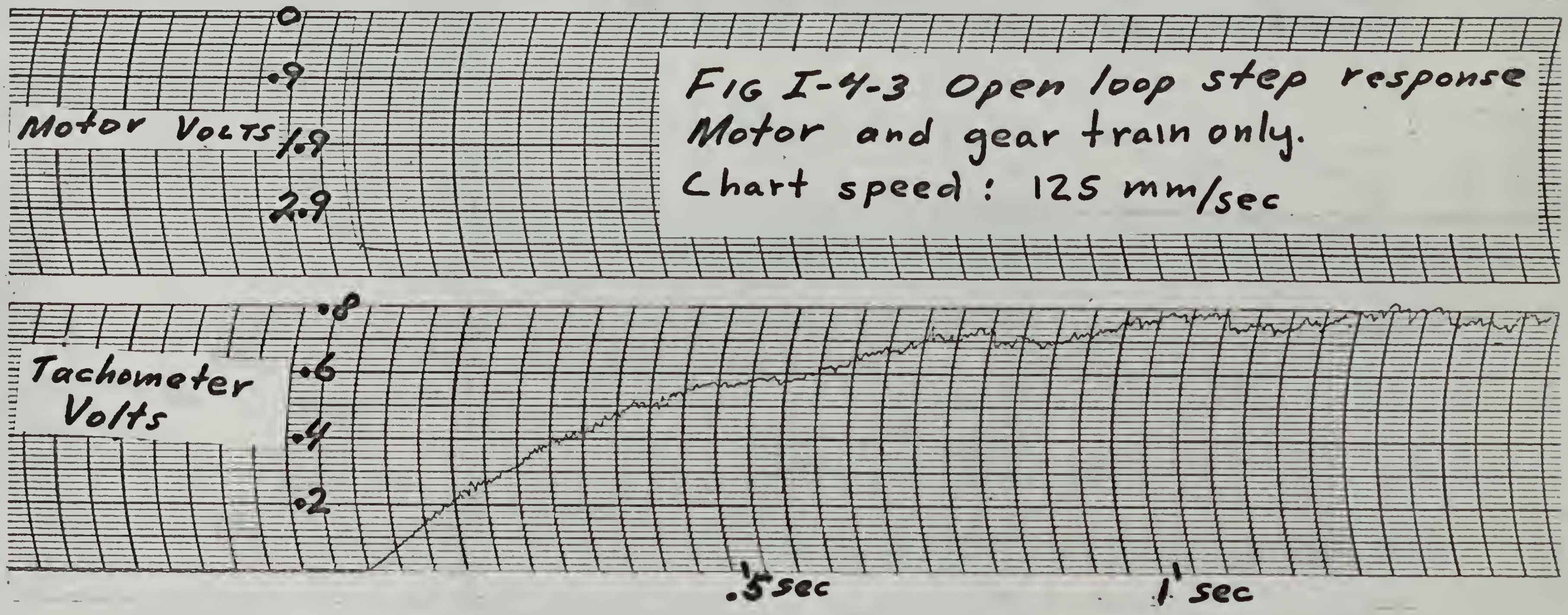

Fig I-4-3 Open loop step response
Motor and gear train only.
Chart speed : 125 mm/sec

5. Closed loop frequency response [4, 5]

Closed loop frequency response data was taken using the circuit configuration shown earlier in Fig. I-1-1.

The value of 20 for the linear gain was chosen because it is less than the limit cycle gain but enough to clearly illustrate underdamping.

From Fig. I-5-1, it can be seen that the closed loop 3 db bandwidth is about 1.5 cycles per second, and 1.3 times greater than the open loop bandwidth, as can be anticipated.

An interesting phenomenon known as jump resonance (soft-spring type) is a characteristic of this lightly damped system. Fig. I-5-2 is an expanded plot of closely taken data to show the details of the jumps. This is a commonly encountered property with non-linear systems.

KEUFFEL & ESSER CO. MADE IN U.S.A.
3 CYCLES X 70 DIVISIONS

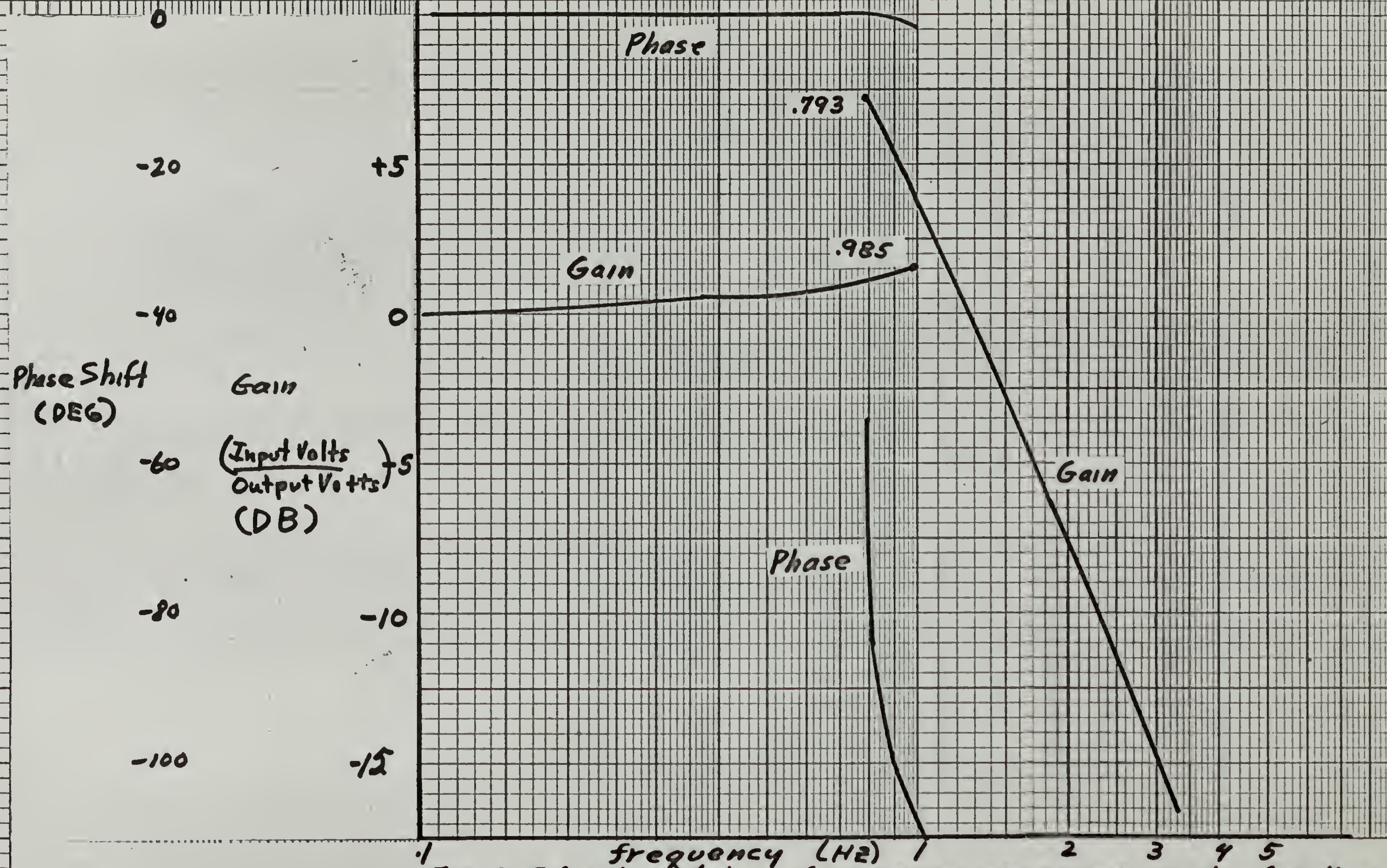

FIG. I-5-1 Closed loop frequency response, unity feedback
Kp = 20

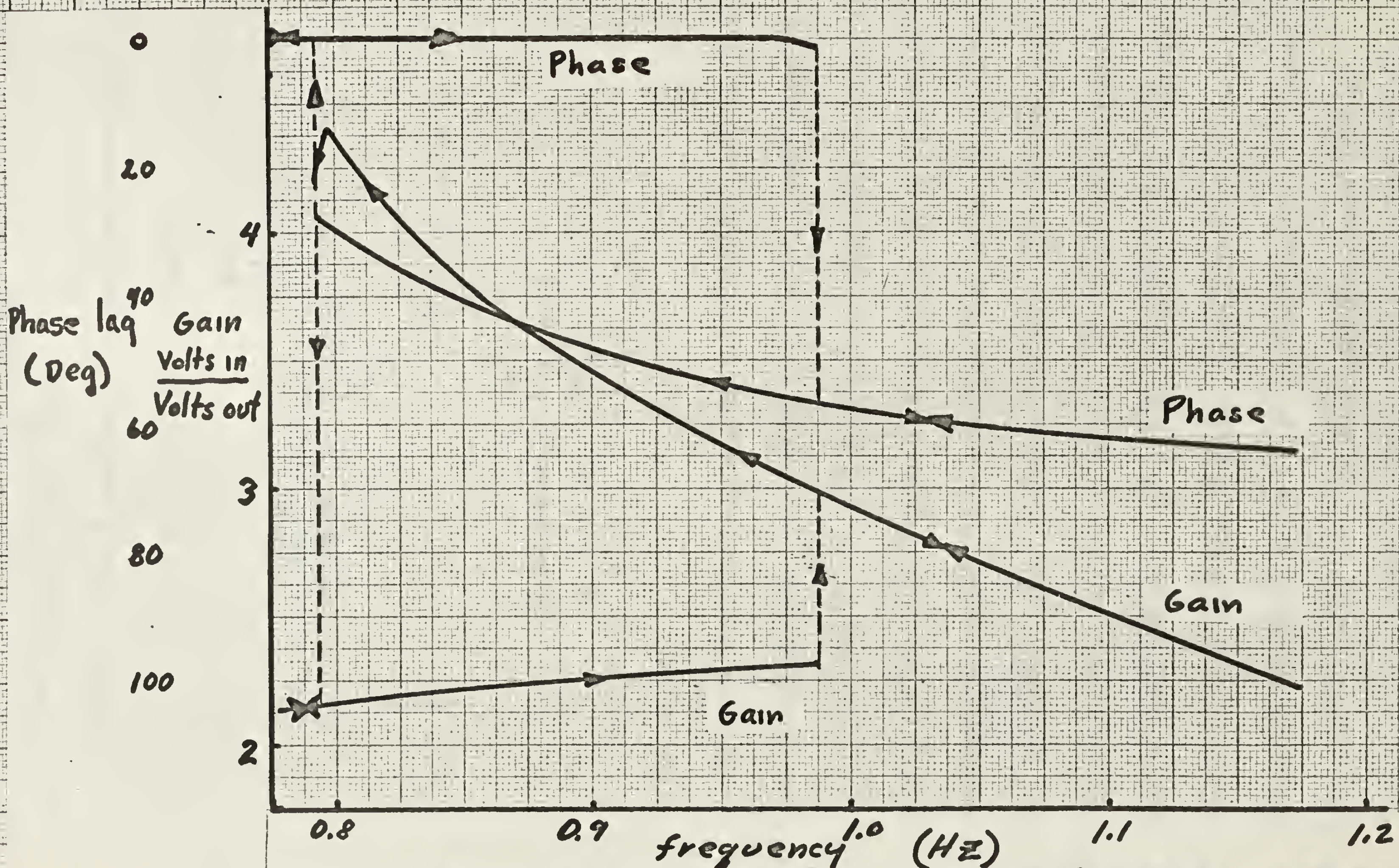

FIG. I-5-2 Jump resonance. Closed loop frequency response with unit position feedback. Kp = 20

6. Phase Trajectories [4, 5]

Several phase trajectories were recorded at various gain settings, both with and without tachometer feedback. In these photographs e is taken at the potentiometer and e dot is taken at the external tachometer. Refer again to Fig. I-1-1 for the block diagram. Since the oscilloscope is a wide band recorder, a low pass RC filter, 200/(s + 200), was inserted in the vertical circuit to reduce clutter due to noise from the external tachometer. It was verified that the Brush Recorder could also be used to obtain a hand-drawn phase trajectory.

In Fig. I-6-1, the use of diodes to increase the dead zone is illustrated. The number which may be used depends on the error voltage available and on the forward voltage drop of the diodes.

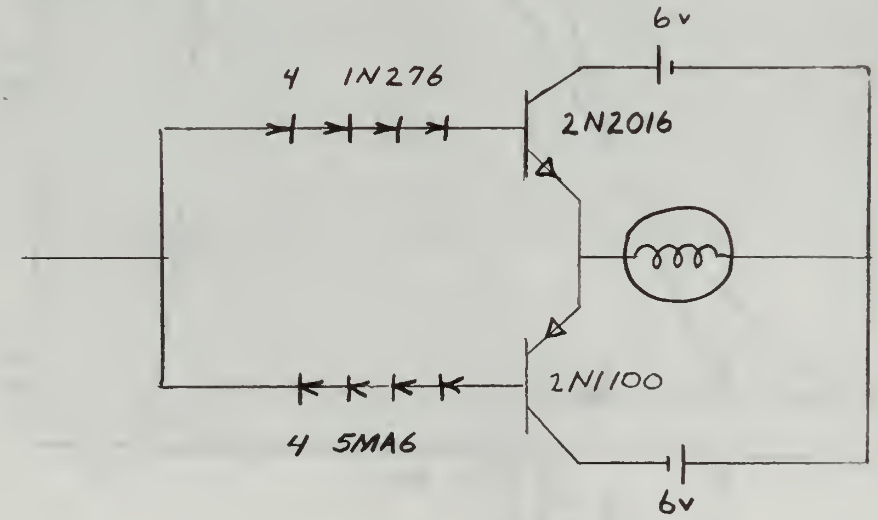

Fig. I-6-1. Dead zone circuit

The phase plane photograph depicting the diode effect on dead zone is shown in Fig. I-6-2.

For the case of position feedback only, Fig. I-6-3 shows the effect of different values of forward gain. Fig. I-6-3(a) is for $K_p=2$, a value so low that linear operation is maintained. Fig. I-6-3(b) and Fig. I-6-3(c) depict "relay" operation.

Figures I-6-4 through I-6-6 show how position and rate feedback, applied together, shape the system response. Note the "bang-bang" control shown by Fig. I-6-4(c) and the tilting of the dividing lines shown so well by Figures I-6-5 and I-6-6.

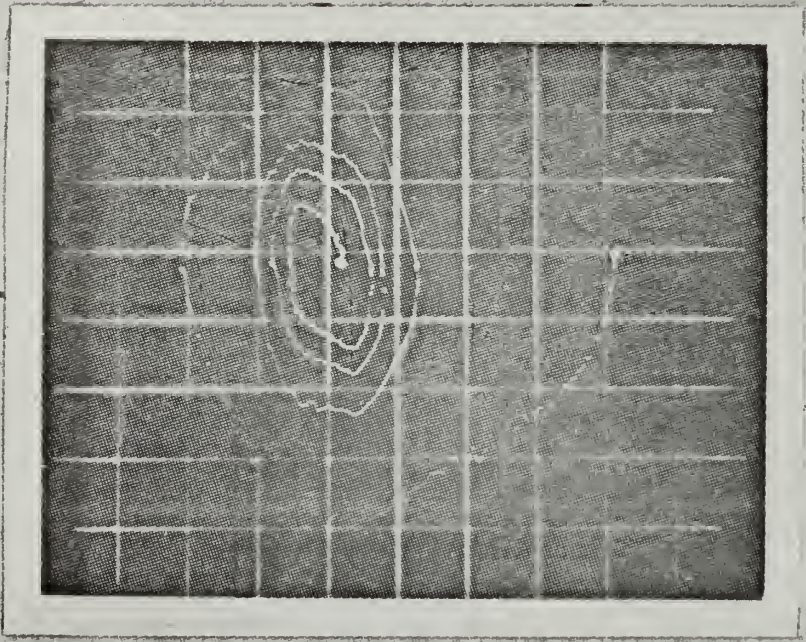

Fig. I-6-2 Phase plane plot showing effect of inserting diodes in error channel to increase the effect of dead zone. Ka = 20
Abscissa : error, .33 v/cm
Ordinate : error dot, .64 v/cm

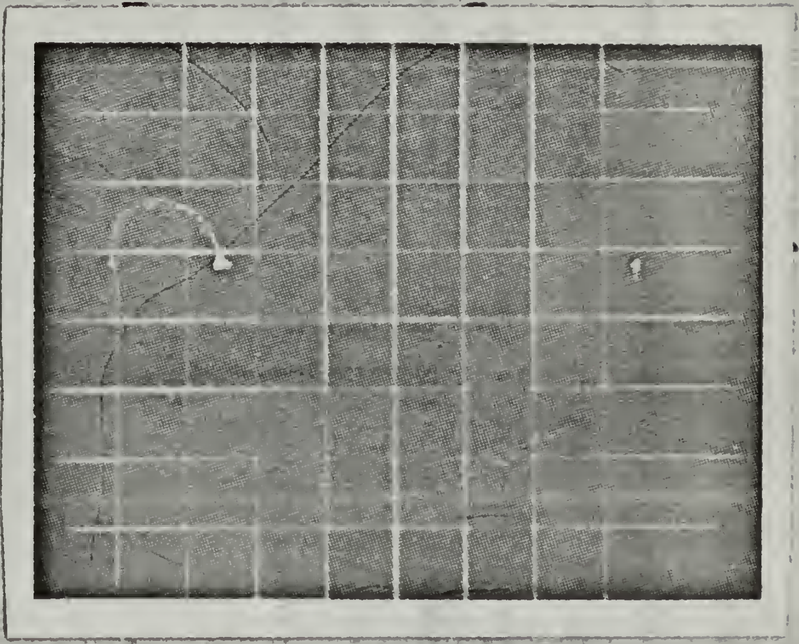

Fig. I-6-3(a) Phase plane plot showing effect of low gain, hence linear operation. Ka = 2.
Abcissa : error, .2 v/cm
Ordinate : error dot, .43 v/cm

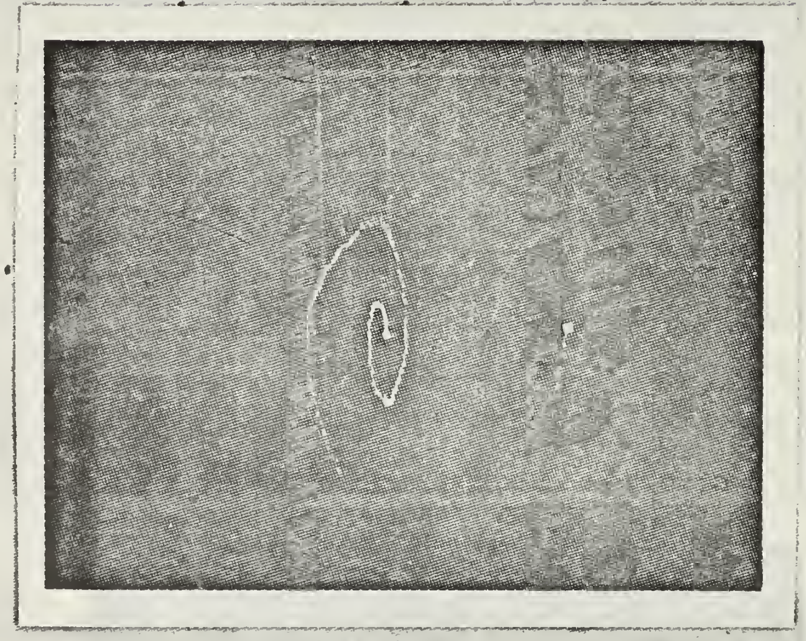

Fig. I-6-3(b) Phase plane plot, medium gain. Ka = 10
Abscissa : error, 10v/cm
Ordinate : error dot .1v/cm

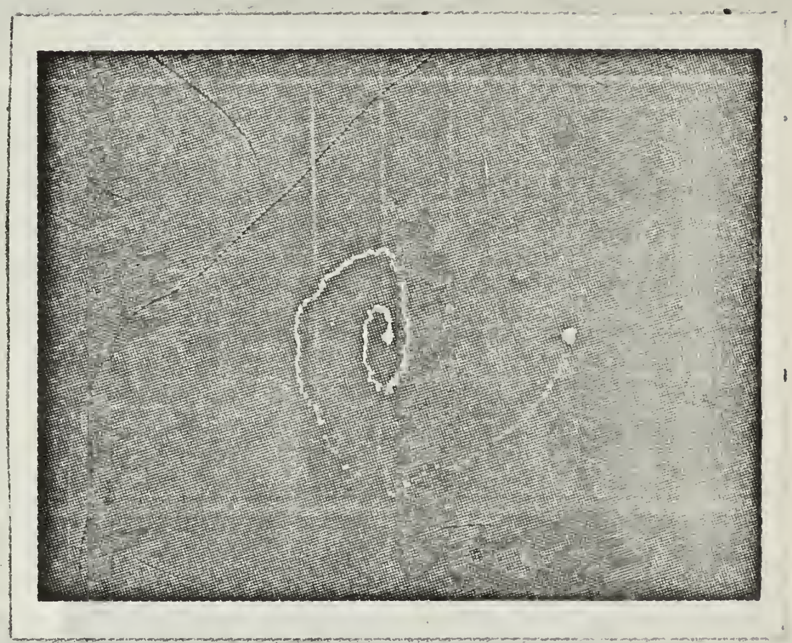

Fig I-6-3(c) Phase plane plot, gain set just below that required for a limit cycle. Ka = 20
Abscissa : error, 10v/cm
Ordinate : error dot, .1v/cm

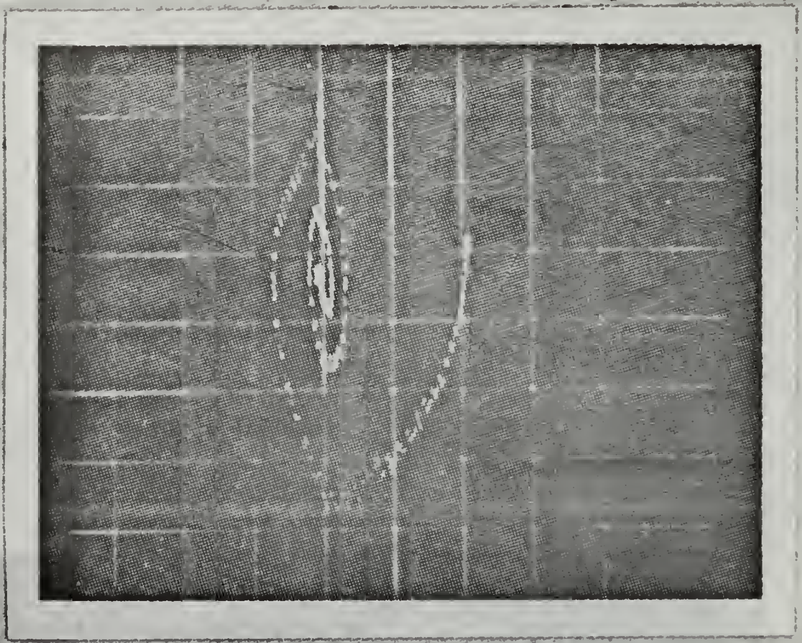

Fig. I-6-4(a) Phase plane plot showing effect of small amount of tachometer feedback.
$K_a = 10$, $K_t' = .5 K_t$
Abscissa: error, 1v/cm
Ordinate, error dot, 50mv/cm

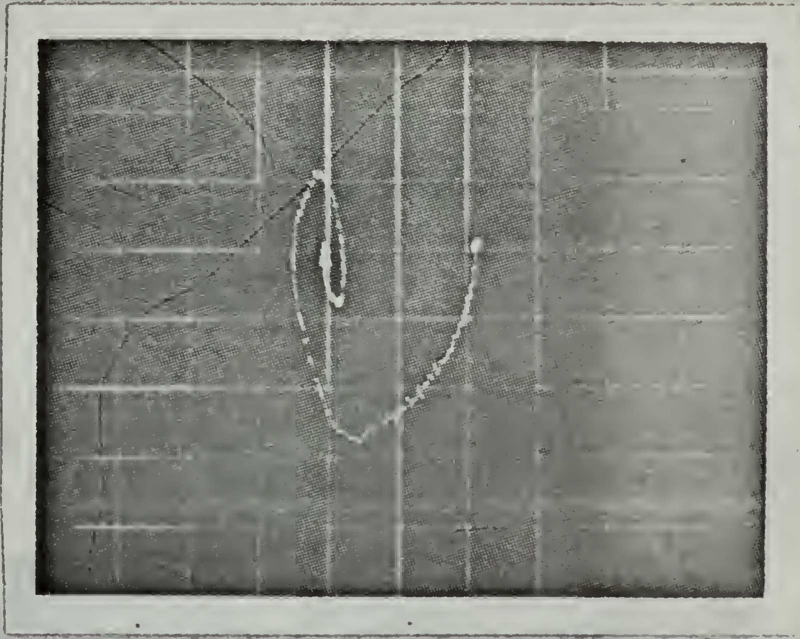

Fig. I-6-4(b) Phase plane plot showing effect of medium tachometer feedback. Note the substantial tilt of the dividing lines.
$K_a = 10$, $K_t' = 1.0 K_t$
Abscissa: error 1v/cm
Ordinate: error dot, 100$\frac{mv}{cm}$

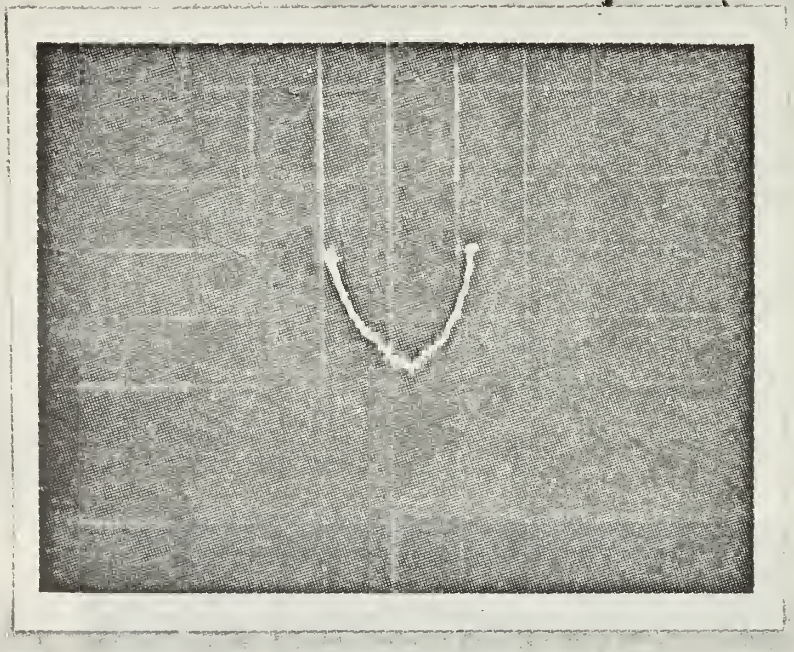

Fig. I-6-4(c) Phaseplane plot showing effect of tachometer feedback. This is close to minimum time.
$K_a = 10$, $K_t' = 5\,K_t$
Abscissa : error 1V/cm
Ordinate : errordot $500\frac{mv}{cm}$

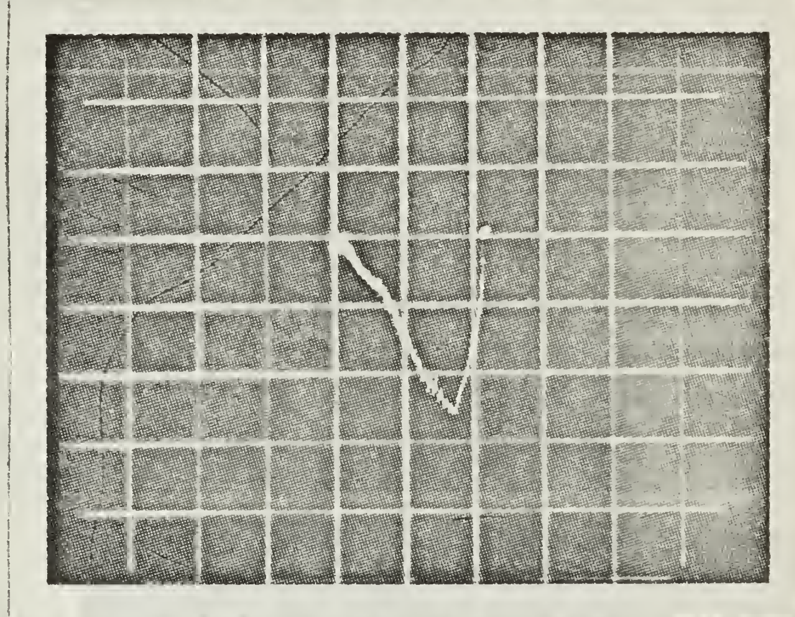

Fig. I-6-4(d) Phase plane plot showing effect of excessive tachometer feedback.
$K_a = 10$, $K_t' = 10\,K_t$
Abscissa : error , 1V/cm
Ordinate : error dot, $500\frac{mv}{cm}$

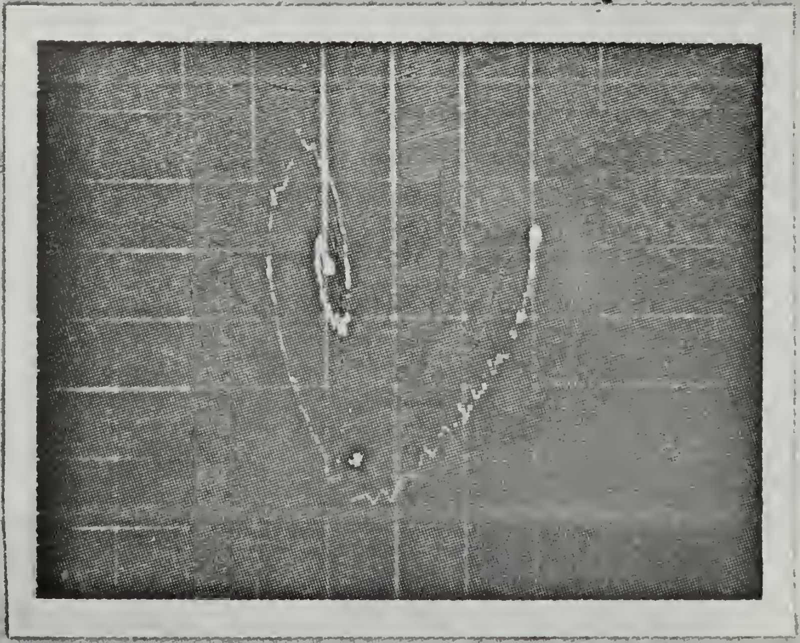

Fig. I-6-5 Phase plane plot showing effect of tachometer feedback. $K_a = 20$, $K_t' = K_t$.
Abscissa; error, 200 $\frac{mv}{cm}$
Ordinate: error dot, 50 $\frac{mv}{cm}$

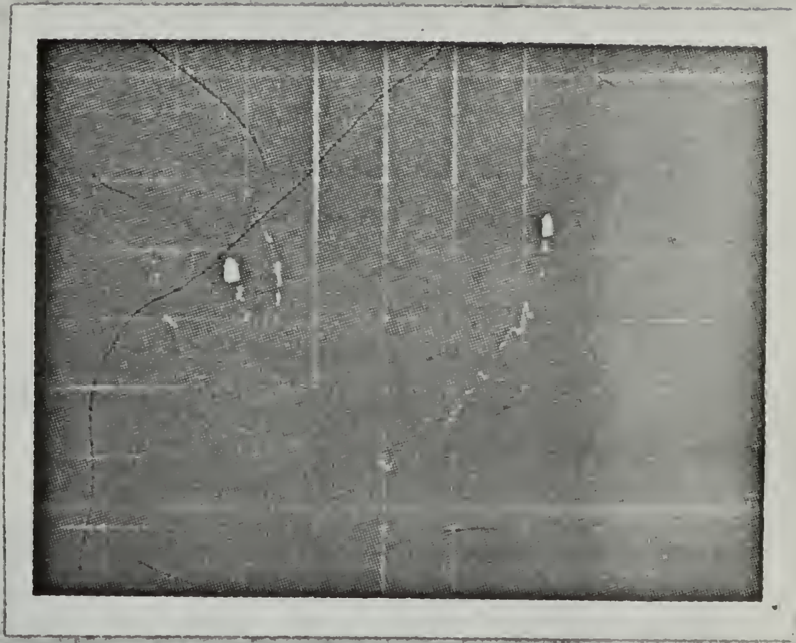

Fig. I-6-6 Phase plane plot showing effect of tachometer feedback with high position feedback gain.
$K_a = 50$, $K_t' = K_t$
Abscissa: error, 100 mv/cm
Ordinate: error dot, 50 mv/cm

7. Transient responses [4, 5]

To add credance and substance to the observations and deductions made in earlier sections, time responses to various input signals were observed on the Brush Recorder. The broad effects of tachometer feedback and cascade compensation were also investigated.

Fig. I-7-1(a) is the closed loop system step response with unit position feedback for the NPN half of the cycle, and Fig. I-7-1(b) is for the PNP half. The system is slightly underdamped. The greater voltage gain on the PNP side is immediately apparent.

Fig. I-7-2 is the open loop step response of the individual transistors. Dead zone and hysteresis effects on the collector voltage slopes are obvious.

Fig. I-7-3 shows the overall effect on the closed loop system step response of increasing the amount of tachometer feedback. System response to increasing feedback gain on the tachometer channel appears to be entirely conventional. The nominal forward gain was held constant at $k_a = 20$.

Fig. I-7-4 illustrates that the effect of cascade compensation is very similar to that of tachometer feedback, and that this system may be compensated in the usual manner. The lead compensator was inserted between the Philbrick amplifier and the power amplifier. Filter components were purely arbitrary. The filter transfer function was $\frac{5(S+.1)}{3(S+.6)}$.

Fig. I-7-5 shows the open loop triangular response at the motor terminals. Dead zone and hysteresis effects on the slopes are again obvious. The hitch caused by the motor reversal is plainly visible. Note that the frequency is .02 Hz, the approximate lower limit on frequency for a clean motor reversal.

Fig. I-7-6 shows the error signal with a triangular input. Dead zone is again apparent. The appearance of harmonics on the error channel is plain. Note that noise increases directly with tachometer feedback as would be expected.

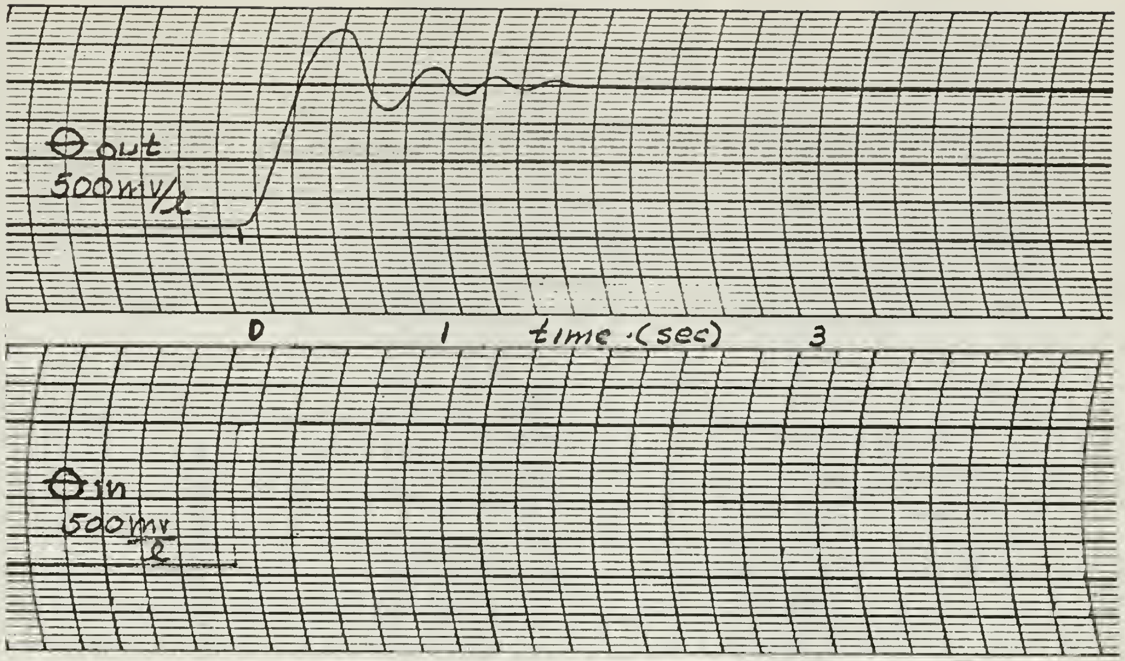

a. NPN Side

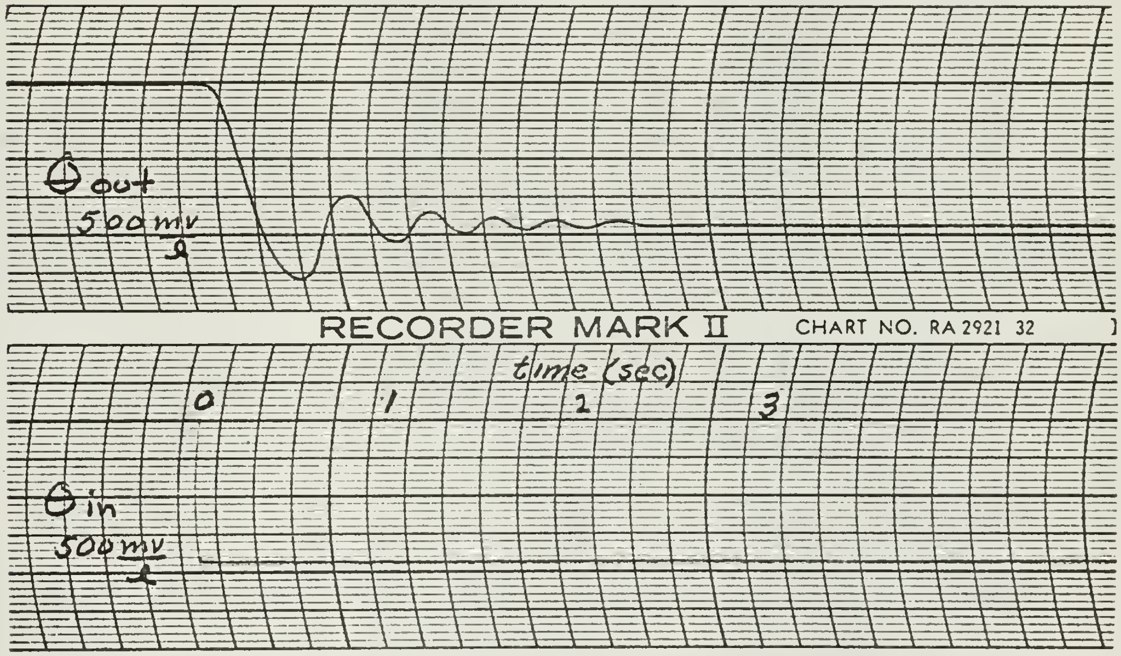

b. PNP Side

Fig. I-7-1 Closed loop system step response, Θin and Θout, unity position feedback only $K_p = 20$.

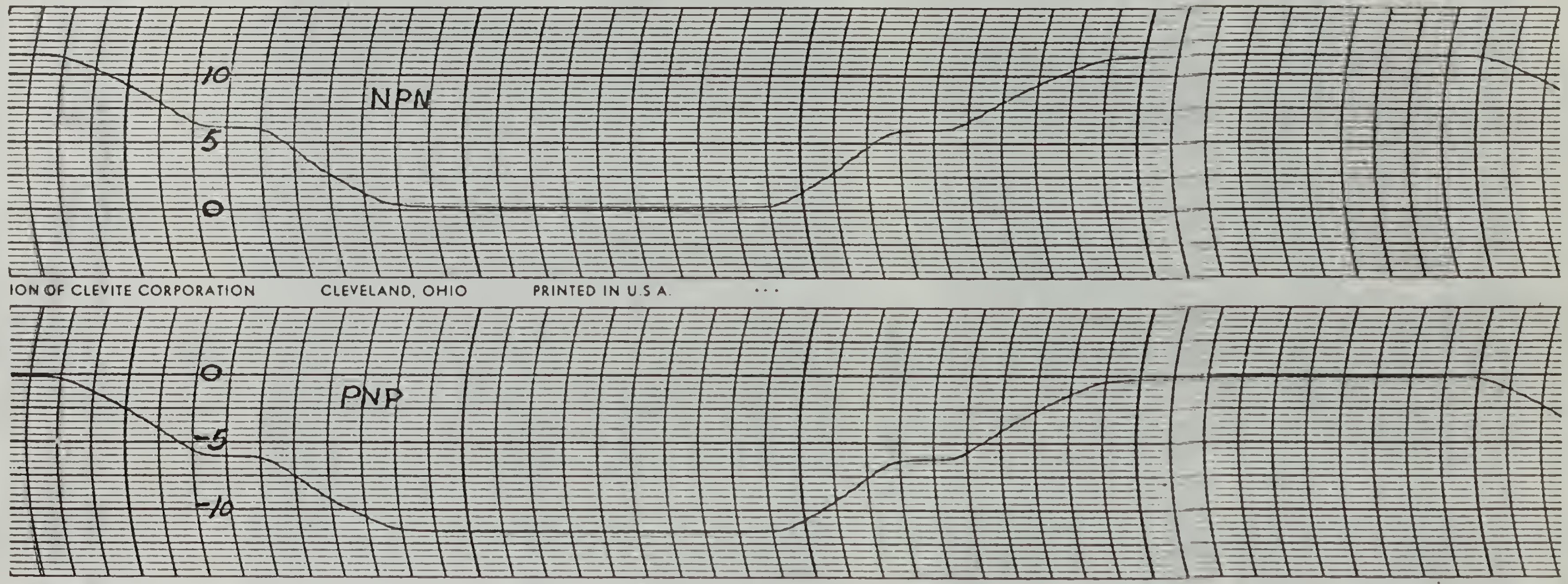

Fig. I-7-2 Open loop collector voltage step responses.

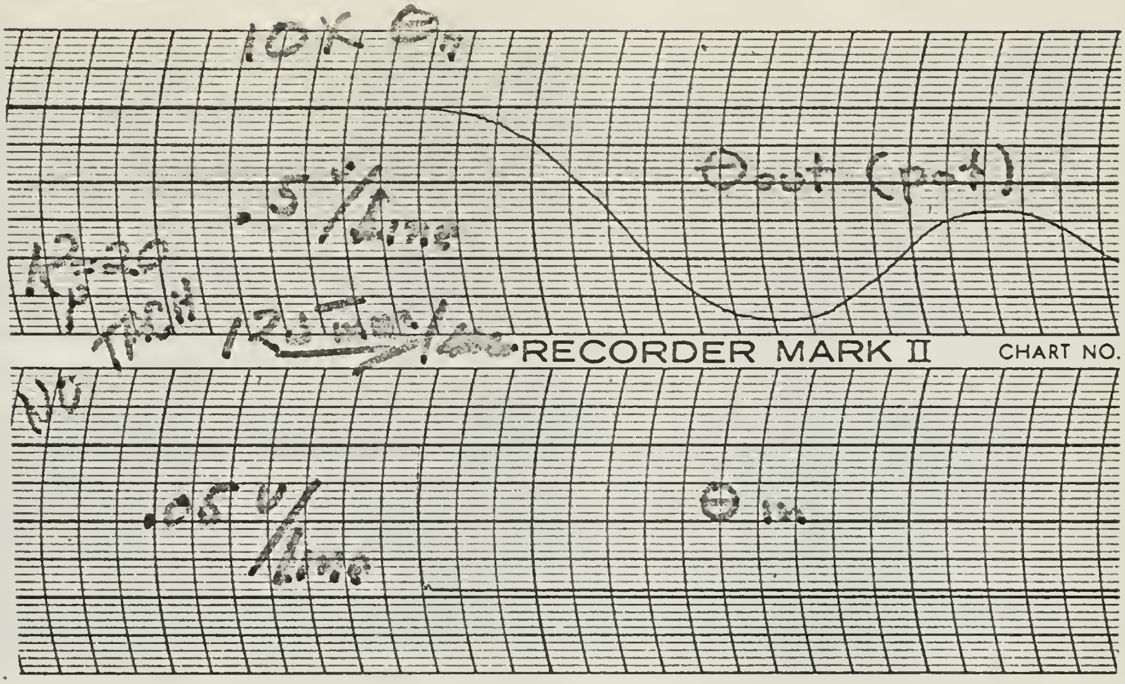

Fig. I-7-3(a) Closed loop step response. $K_p = 20$
$K'_t = 0$

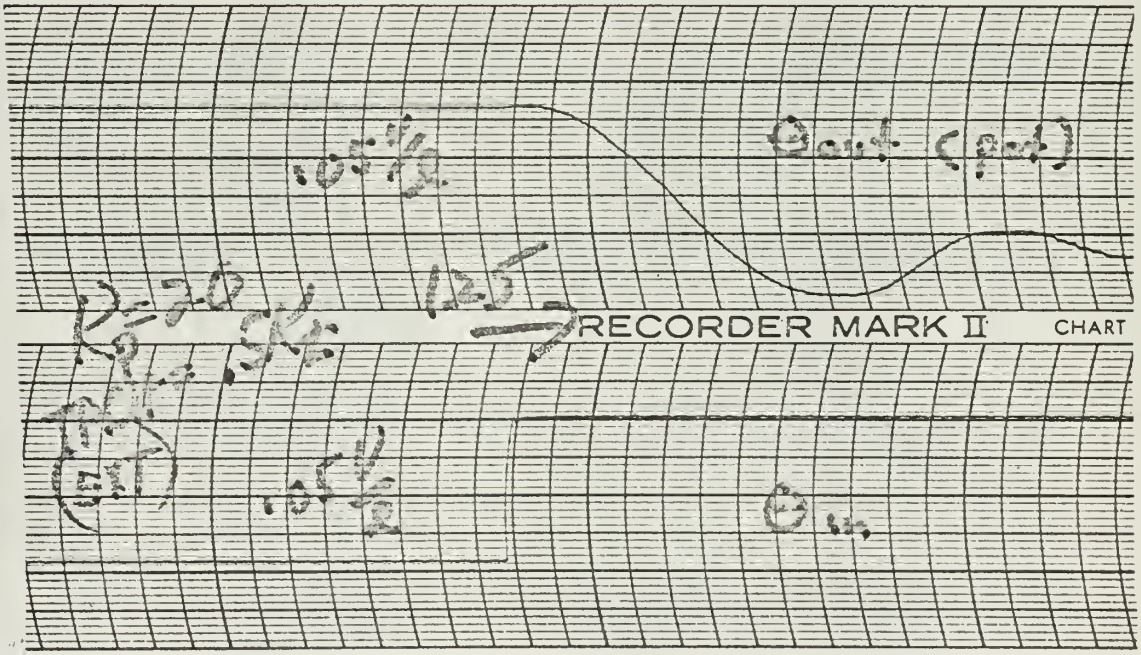

Fig. I-7-3(b) Closed loop step response. $K_p = 20$
$K'_t = .5\ K_t$

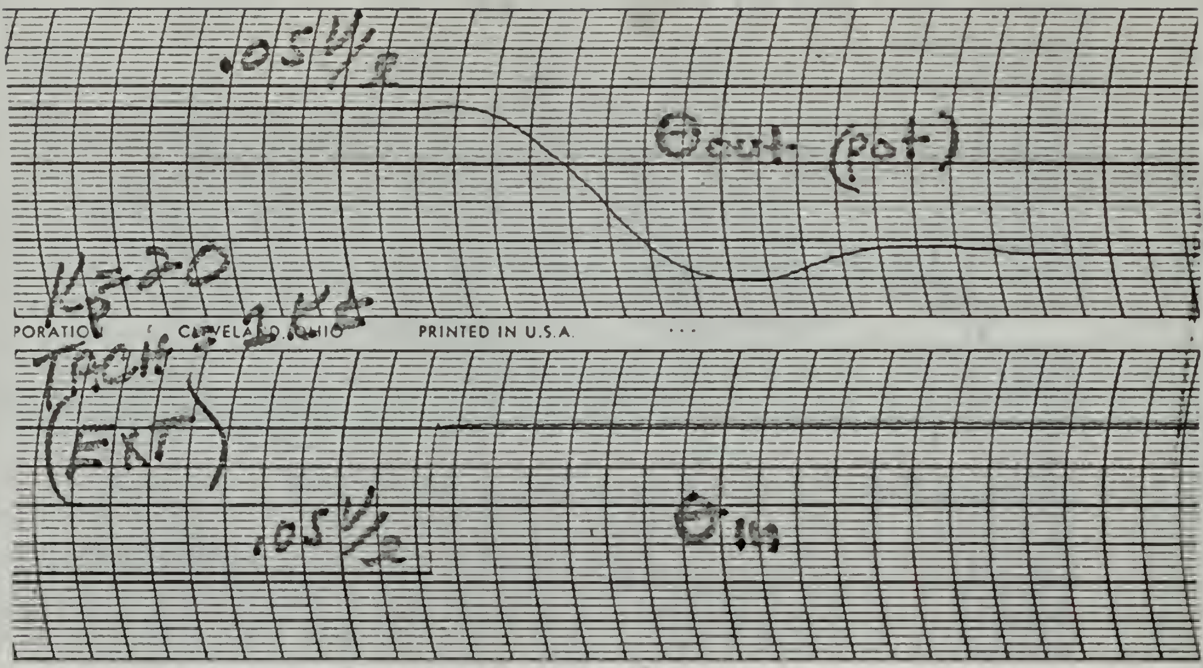

Fig. I -7-3 (c) Closed loop step response. $K_p = 20$
$K'_t = K_t$

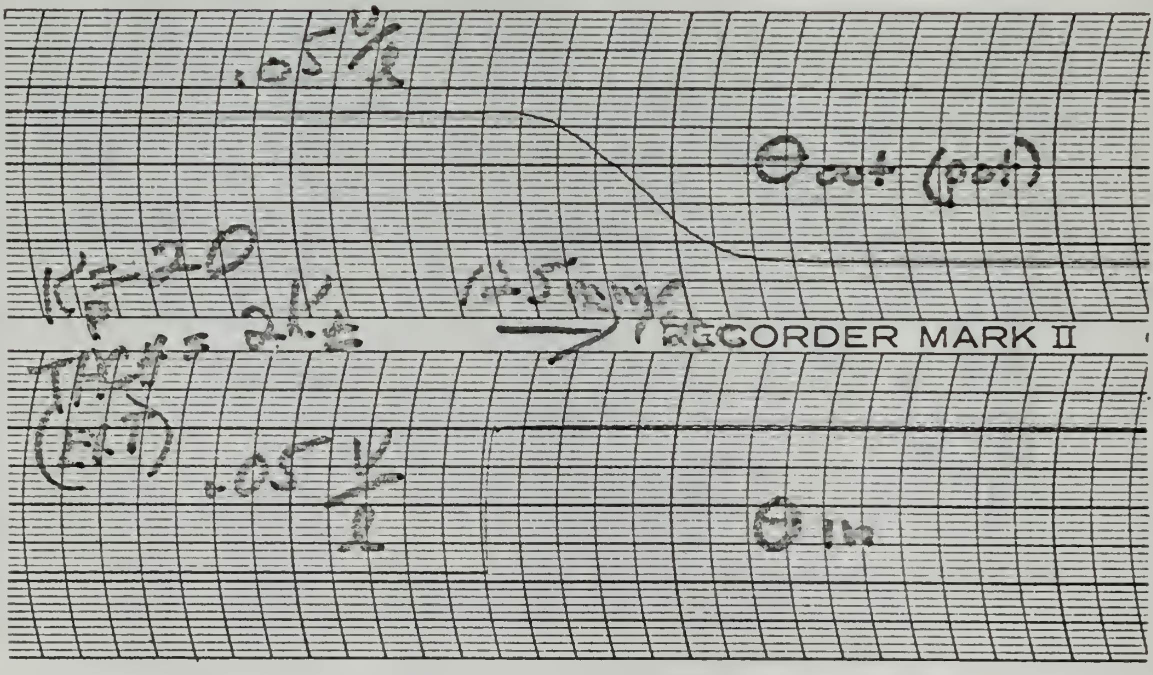

Fig. I -7-3 (d) Closed loop step response. $K_p = 20$
$K'_t = 2K_t$

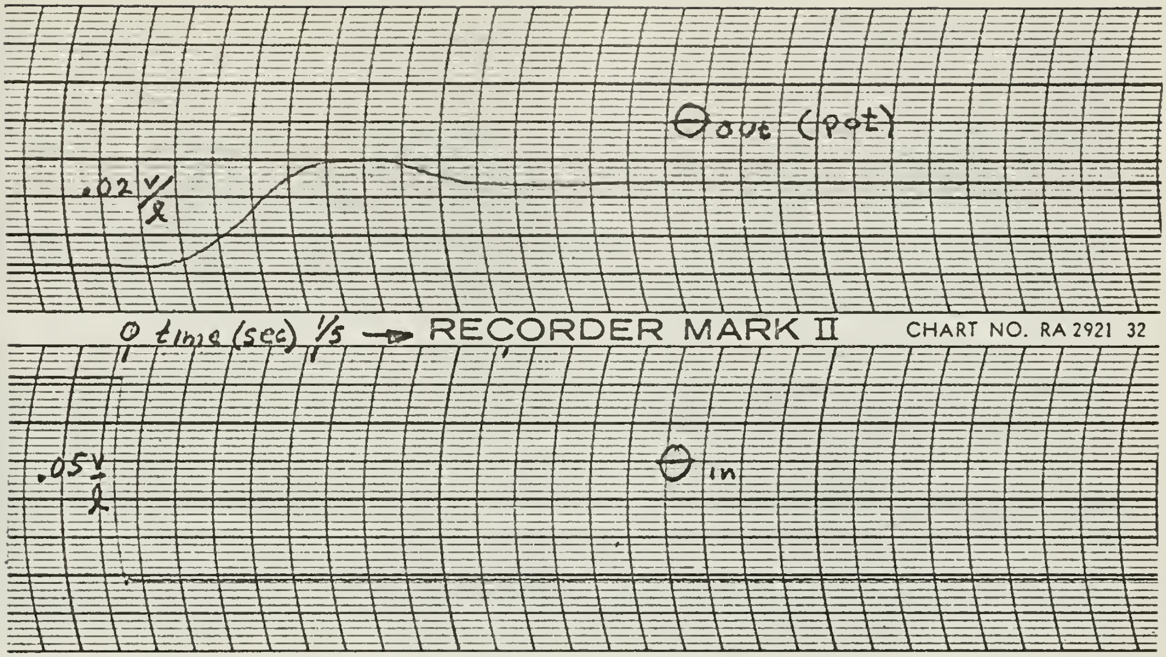

Fig. I-7-4 Closed loop system step response with lead compensation. $K_p = 20$

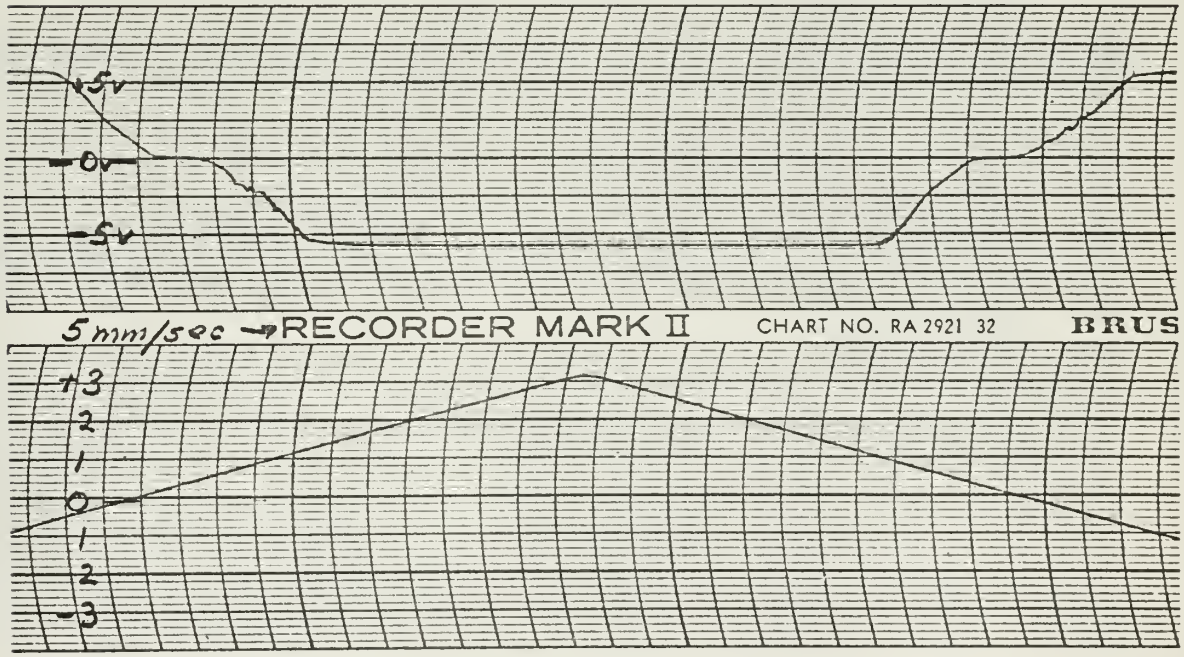

Fig. I-7-5 Motor voltage with triangular input, open loop

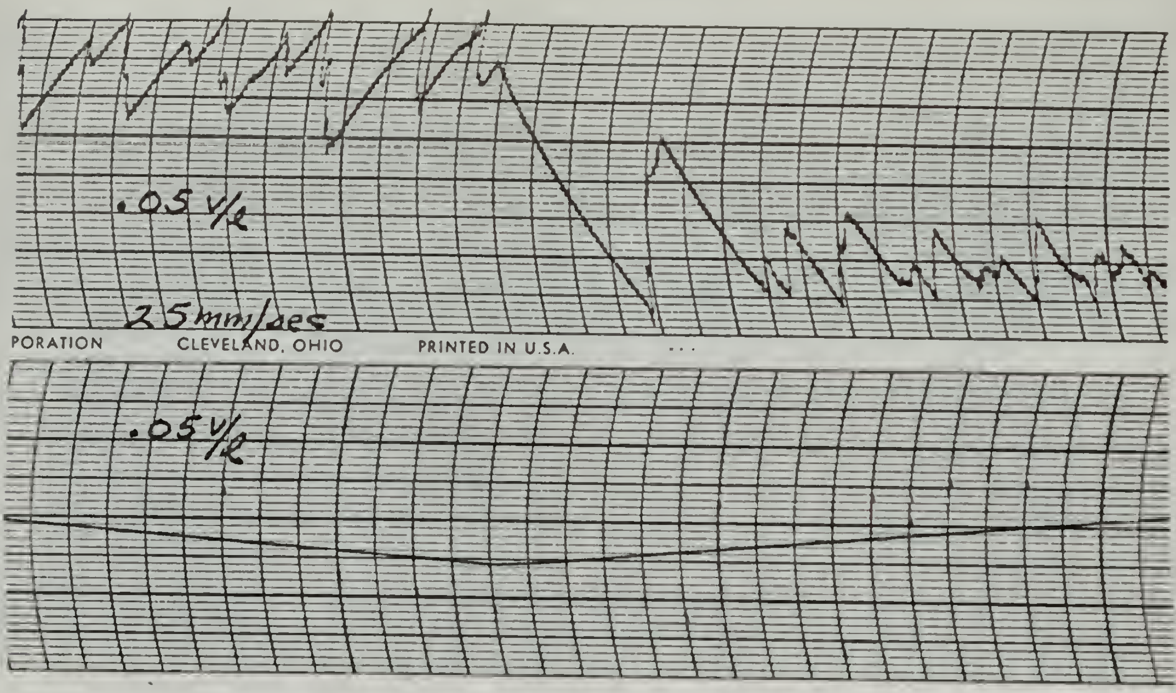

Fig. I-7-6 (a) Error signal with triangular input.
Unit position feedback, Kp = 20, f = .05 Hz

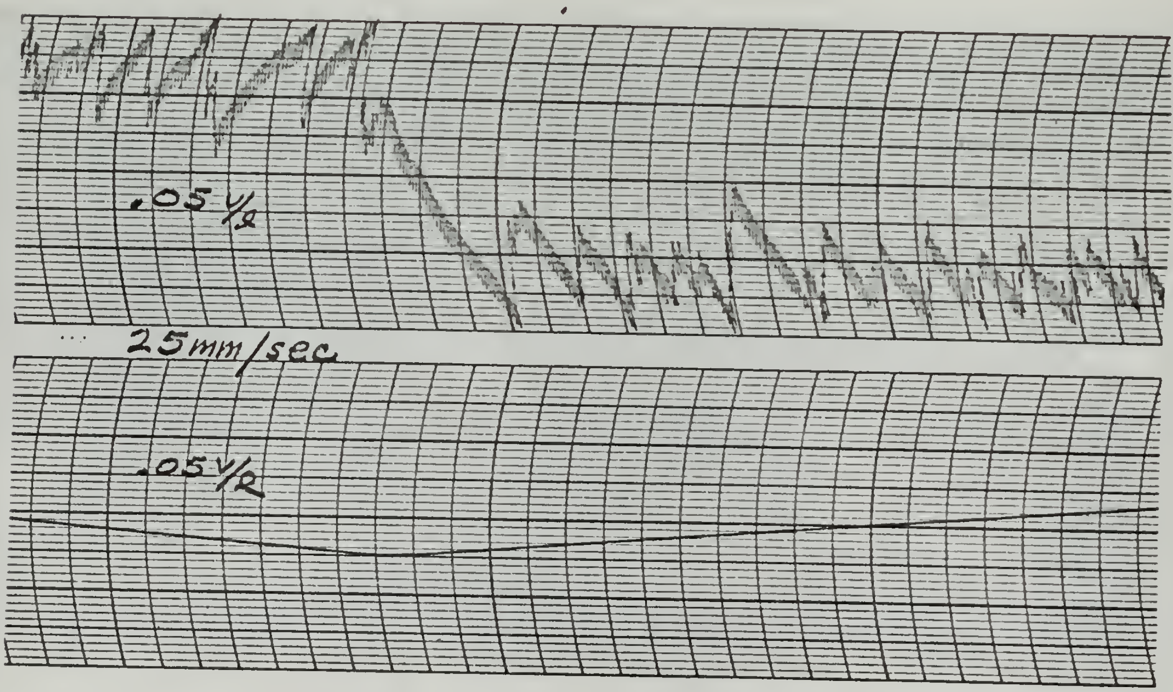

Fig. I-7-6 (b) Error signal with triangular input.
Kp = 20 $K'_t = .2 K_t$ f = .05 Hz

II. THE FOUR TRANSISTOR "RELAY"

1. The experimental system

The experimental system is shown in Fig. II-1-1. The two main power transistors, the motor with gear train and inertial load, the potentiometer, and the external tachometer were retained from the simpler circuit used in Chapter I. The 2N1306 and the 2N1307 transistors were cascaded with the main power transistors to form a Darlington, complementary symmetry amplifier. These were added to increase the current gain from about 35 at six volts to about 2500-3000 at 12 volts. The gain disparity continued to favor the PNP side. Transient armature current at 12 volts was about 3.25 amperes, hence the main power transistors were operated up to roughly 1/3 to 1/2 their rated power. This was sufficient to cause some heating, but temperature effects remained negligible except when operated continually with tachometer feedback for more than about 30 minutes. The cascaded transistors were also mounted on a heat sink. The five ampere fuze was added for transistor protection. The indicator lights were incorporated for no-load testing, quick visual identification of which side was conducting, and other demonstrative purposes. They proved to be a valuable visual aid in seeing the lag of the output shaft. The 12 volt supply was used because higher voltages were required to reduce mechanical effects and to increase the steady state speed. A higher voltage power supply was not available at the required current level of about four amperes.

The potentiometer voltage was nearly doubled to 80 volts to increase sensitivity and to reduce the amplifier gain requirements. The common base resistor, $R_b = 220$ ohms, was inserted for impedance matching with the driving amplifier. This was adjudged to be the minimum value feasible without exceeding a tolerable level of distortion. The shunting diodes were superseded by a 10 ohm resistor to cope with the increased transient effects. This too was an engineering compromise between performance and efficiency. Approximately 20% of the available power was thus dissipated as heat. A $200/(s + 200)$ RC filter was used for recording the tachometer signal as before.

The principal purpose of using the full Darlington configuration was to eliminate the need for a power amplifier. With this four transistor "relay", current gain was sufficient to operate the system closed loop with no driving amplifier. But performance under these conditions was very sluggish. The system was also driven using only the Philbrick amplifier of Chapter I, but again the time delay coming out of saturation was a disadvantage because the way to eliminate or significantly reduce dead zone is to saturate the driving amplifier and consider _it_ as part of the "relay". Then the length of time the error signal can linger in the dead zone is reduced to nearly zero and the typical "bang-bang" performance of a near-ideal relay can be realized.

As an interesting sidelight, a Sensistor* stabilized, four stage, transistor differential amplifier was built and tested. This too was found to be more than capable of driving the system. But temperature drift was excessive, perhaps due to a lack of component balancing. It was discovered that when this amplifier was operated with position feedback only, in cascade with the power amplifier, and on the verge of a limit cycle, the system would act as a crystal receiver. Circuit leads acted as the antenna and the many intrinsic nonlinearities served to detect the signal which was then amplified and fed to the armature winding which acted as a speaker. The broadcast from the local radio station then emanated from the motor with sufficient volume to be audible and intelligible to a distance of several feet. This intriguing phenomenon was a source of much entertainment to fellow students and faculty members alike.

*Trademark, Texas Instruments

It was decided that a small, simple, transistorized preamplifier with excellent saturation characteristics (no phase shift) and good temperature stability would be the most desirable driver. Accordingly, the amplifier depicted in Fig. II-1-1 was built. The design is similar to Liu's but has better frequency response and saturation characteristics. [6] The 22K ohm resistor is critical for good saturation characteristics. The 2N1719 was mounted on a large heat sink. The amplifier was operated for short durations at ± 30 volts but the ± 24 volts is the recommended maximum for normal use. The saturation characteristics are excellent up to a nominal gain of 100. That there is negligible temperature drift is quite remarkable since there is no temperature control other than the heat sink. Current requirements are between 100 and 150 milliamperes at full load. The output is more than sufficient to supply the input power for the Darlington amplifiers.

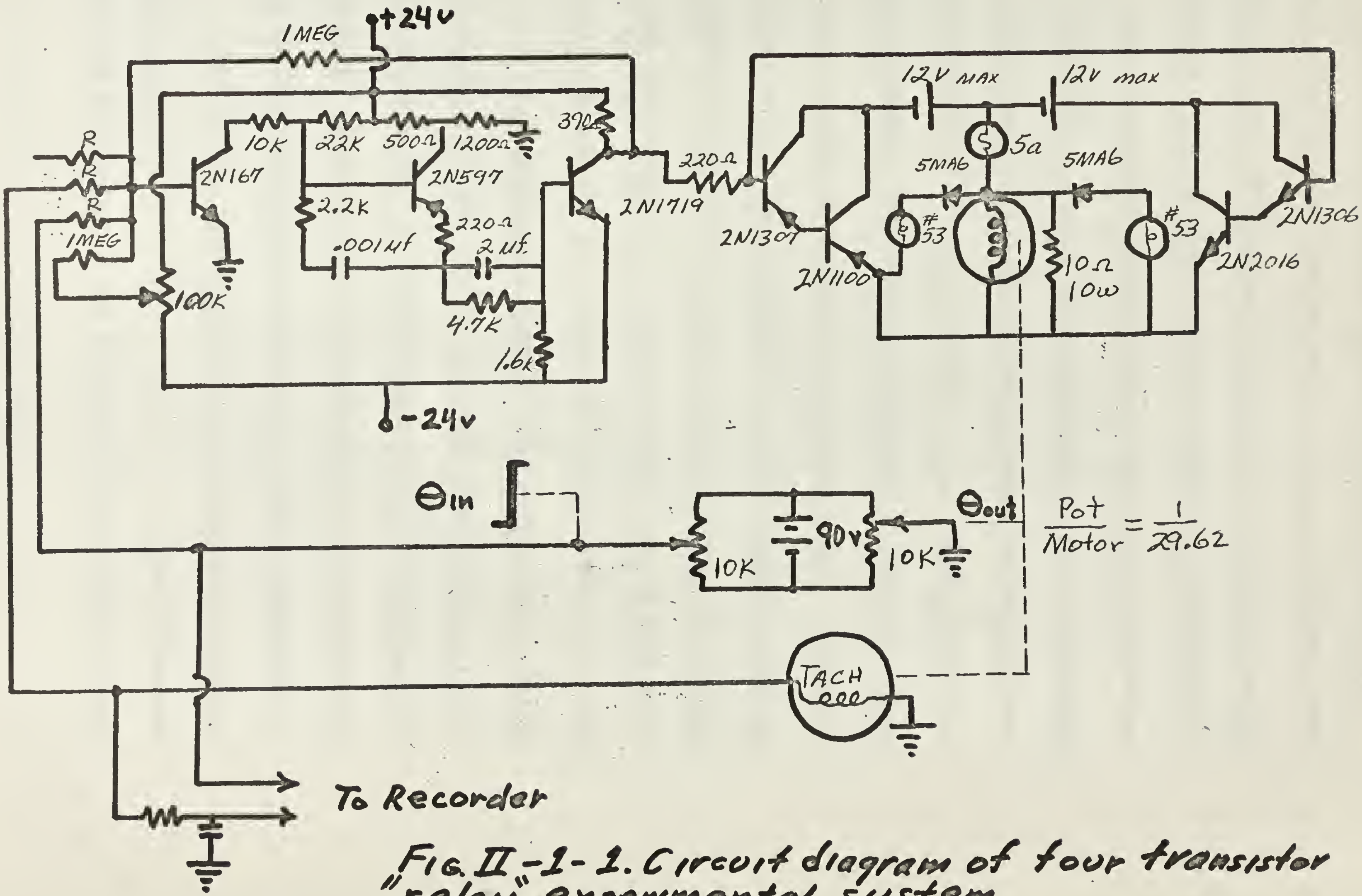
+24v
1MEG
R
R
R
1MEG
10K
2N167
100K
22K
500Ω
1200Ω
2.2K
2N597
.001uf
220Ω
2 uf.
4.7K
1.6k
390Ω
2N1719
-24v
220Ω
2N1307
2N1100
12V MAX
12V max
5a
5MA6
5MA6
#53
#53
10Ω
10w
2N1306
2N2016
Θin
Θout
10K
90v
10K
Pot/Motor = 1/29.62
TACH
To Recorder

Fig. II-1-1. Circuit diagram of four transistor "relay" experimental system.

2. Observation of switching characteristics.

The two cascaded transistors on each side of the full Darlington configuration can be conveniently treated as one equivalent transistor with lumped parameters. The transistor characteristics for these equivalent transistors are essentially the same as for the second stage power transistors taken separately, i.e., the two transistor "relay". The major exception is that these equivalent transistors each have a current gain which is the product of the two cascaded transistors, an order of magnitude of 2500-3000. Hence the four transistor "relay" has the same intrinsic dead zone and k_x as the two transistor "relay" of Chapter I, but a current gain approaching that of a conventional amplidyne. The effect of adding resistance to the collector circuits, or in series with the armature, is identical to the effect with the two transistor "relay". The same is true regarding resistors in the base circuits, or diodes in the base circuit. And this system can be compensated in an analogous manner. The hysteresis effect is unchanged and varies with E_i and f_i as before. Hence the four transistor "relay" has the same flexibility, and the same intrinsic problems with hysteresis effects, as the two transistor "relay". If the dead zone is increased with diodes, or if the dead zone is increased and k_x reduced by increasing

R_b, then there is a direct increase in the hysteresis effect. Therefore, the extreme flexibility in the choice of switching characteristics has little application outside of the classroom unless space and weight are at a premium. Then even the worst possible case of a quasi-linear amplifer with dead zone and hysteresis might well become an attractive vehicle for some approximate linear control scheme because in spite of all the inherent drawbacks, system performance is, in general, still "good", and the motor responds "sharply". The difficulty arises in attempting to predict the phase shift and reducing dead zone. However, for more normal applications, the complementary symmetry of the Darlington configuration is fundamentally a switching circuit and not a strong competitor in the field of linear control.

The four transistor "relay" was operated open loop with a triangular driving function and observations were again made on the oscilloscope. Fig. II-2-1 is a series of time exposures of the traces obtained with a nominal gain of $K_a = 1$. Fig. II-2-1(a) illustrates that the driving amplifier was operating linearly and that true gain was approximately .8 of the nominal gain.

With E_{in} = 4 volts and K_a = 1, E_i equals about 4 volts which is equivalent to the .2 E_{PA} used so extensively in section I-2 for the two transistor "relay." Also f_i = .6 Hz was chosen for the observation of all the switching characteristics so that further direct comparisons to Chapter I could be made. Fig. II-2-1(b) shows the now familiar hysteresis effect. The only improvement (or difference) is that k_x has been doubled by increasing the supply voltage from 6 to 12 volts. Since the driving amplifier changes the sign of the signal, figure II-2-1(b) is correctly depicted as $+e_{in}$ vs e_m and the right half is still the PNP side. The asymmetrical distribution of the normal 1 volt dead zone appears to be offset to the NPN side by more than the usual amount. This is because the driving amplifier, and/or the driving function generator, were not both precisely balanced. This is a common feature of all the observations of this section, hence no significance should be attached to the distribution of the dead zone relative to zero. The bulk of the dead zone remains on the NPN side, wherever the dead zone may be located relative to zero. This ability to relocate the dead zone by adjusting the driving amplifier balance is one more extremely desirable feature of the four transistor "relay". Fig. II-2-1(c) shows the net phase shift from e_{in}

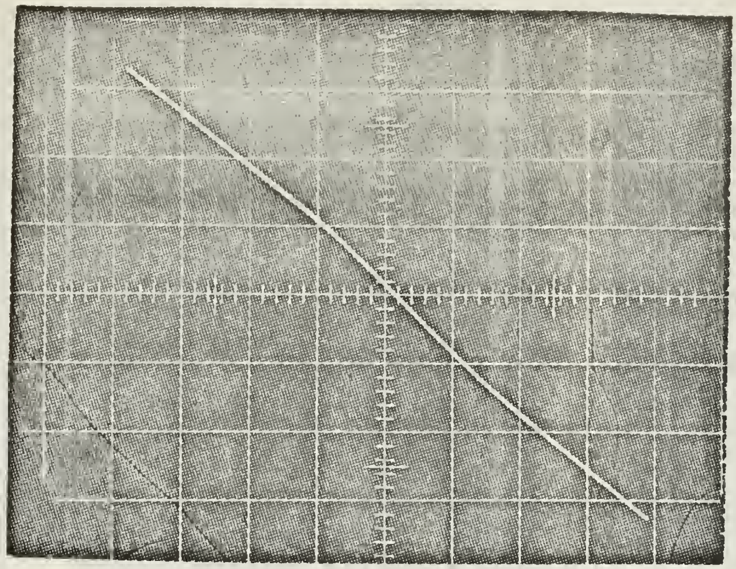

Fig II-2-1(a) ein vs eout

for summing amplifier, no load

$K_A = 1$ f = .6 Hz

Abscissa: ein, 1V/cm

Ordinate: eo, 1V/cm

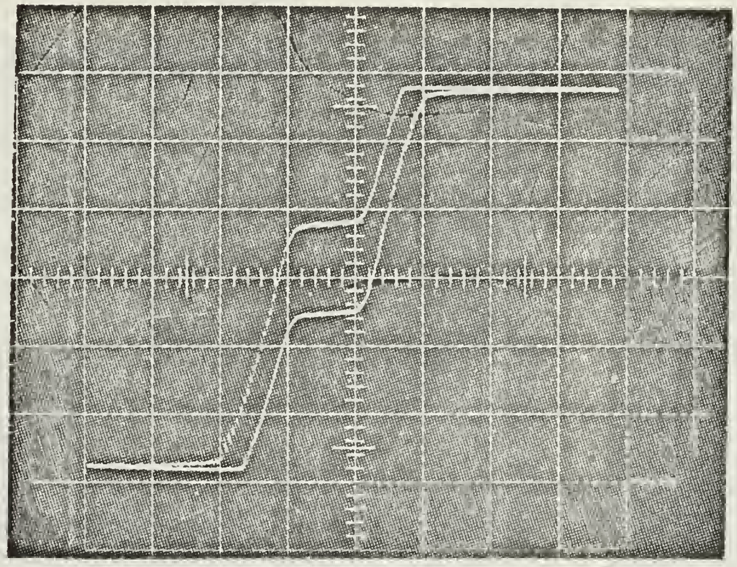

Fig. II-2-1 (b)

ein vs em for four transistor "relay". $K_A = 1$

f = .6 Hz

Abscissa: ein, 1V/cm

Ordinate: em, 4V/cm

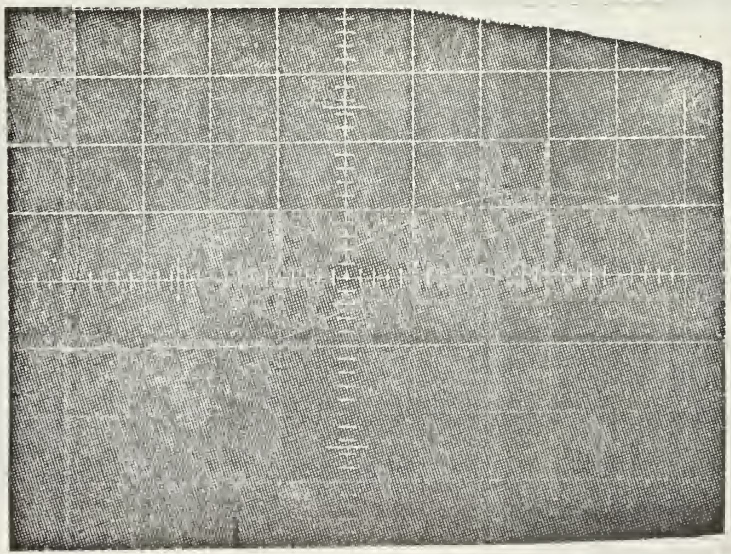

Fig. II-2-1(c)

ein vs eout for open loop four transistor "relay".

$K_A = 1$ f = .6 Hz

Abscissa: ein, 1V/cm

Ordinate: eout, 10V/cm

to the output at the potentiometer, e_{out}. This picture was obtained by purposely offsetting the amplifer balance and carefully adjusting the setting so as to stop position drift long enough to get a time exposure. The blank distance was caused by the oscilloscope triggering during the particular cycle being photographed. At this low gain setting the balance control is extremely sensitive and hence the observation of e_{in} vs e_{out} was both tedious and time consuming. However, at higher gains the balance control is increasingly less sensitive and it is not a significant chore to stop the position drift for short durations of time. For all observations of e_{in} vs e_{out} the procedure was to adjust the balance control to stop the drift and then to reset the vertical position of the oscilloscope to approximate center, and then to take the photograph as quickly as possible. Hence in all observations of e_{in} vs e_{out} no significance should be attached to the vertical offset relative to zero.

Fig. II-2-2 is a series of time exposures with the nominal gain increased to $K_a = 10$. Fig. II-2-2(a) shows that the driving amplifier was saturating slightly and that it introduced no phase shift. Fig. II-2-2(b) illustrates the effect of the inpedance mismatch, which was accepted to

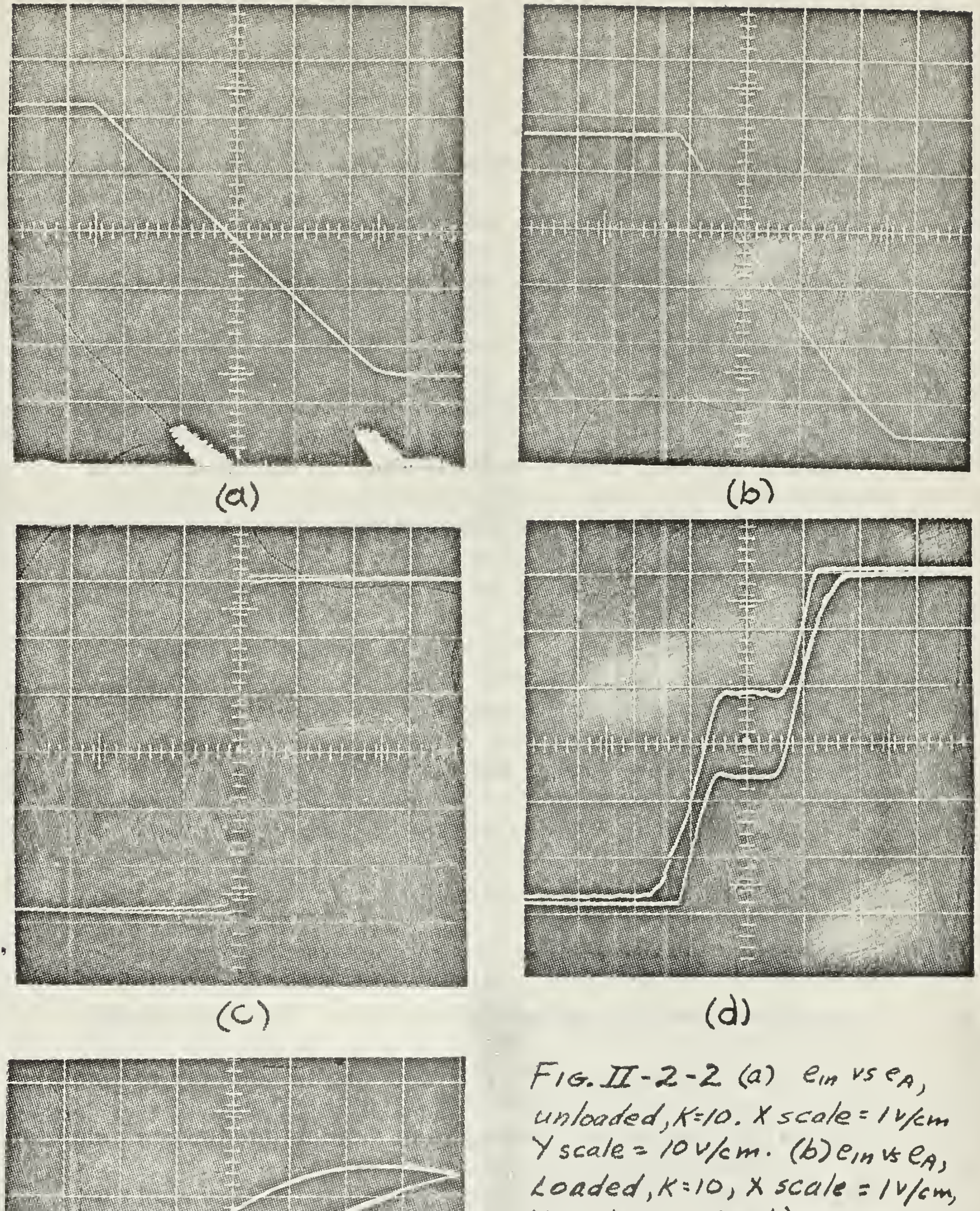

(a) (b)

(c) (d)

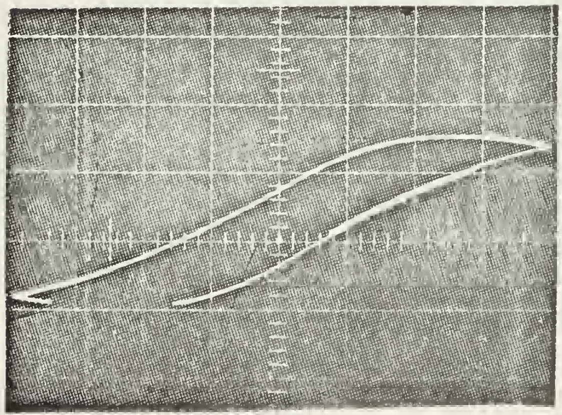

(e)

FIG. II-2-2 (a) e_{in} vs e_A,
unloaded, K=10. X scale = 1 v/cm
Y scale = 10 v/cm. (b) e_{in} vs e_A,
Loaded, K=10, X scale = 1 v/cm,
Y scale = 5 v/cm. (c) e_{in} vs e_m, K=10
X scale = 1 v/cm, Y scale = 4 v/cm
(d) e_{in} vs e_m, K=10
X scale = .1 v/cm, Y scale: 4 v/cm
(e) e_{in} vs e_{out}, K=10.
X scale = 1 v/cm, Y scale = 10 v/cm

keep Rb as small as possible. As always, it seems, the PNP side is favored. Indeed in view of dead zone, $V_{ce\ sat}$, current gain, and now the effect of impedance mismatch, the PNP side can be literally called the "strong" side. Fig.(s) II-2-2(c) and (d) illustrate the reduction in dead zone and hysteresis effect. The dead zone is now about .1 volt wide as opposed to the usual 1 volt with the two transistor "relay". Thus a convenient rule of thumb is established. The overall width of the dead zone in volts is equal to the reciprocal of the nominal gain of the driving amplifier. The blank distance in Fig. II-2-2(e) is caused by the potentiometer arm passing through its dead space. This can be avoided by simply applying an arbitrary θ_{in} manually and repeating the observation. The overlap illustrates the position drift.

Fig. II-2-3 is a series of time exposures with the nominal gain increased by another factor of 10 to $K_a = 100$. The saturating amplifier is now being driven hard into saturation, but still without phase shift. The slight phase shift when loaded is on the PNP side and is probably caused by the back emf effect feeding back through the "strong" side all the way to the preamplifier. Dead zone is now about .01 volts wide and the overall hysteresis effect has been virtually eliminated. It is submitted that for most practical applications, and quasi-theoretically too, this is an ideal relay.

Fig. II-2-4 is a series of time exposures with the nominal gain increased by yet another factor of 10 to $K_a = 1000$. This is beyond the capability of the driving amplifier, and hence the indicated imbalance is the minimum degree possible. The balance control was set all the way to its mechanical stops. The hysteresis effect on the PNP side when loaded also increases somewhat. The dead zone is now less than .01 volts wide but greater than .001 volts because the rule of thumb for determining dead zone does not apply unless the preamplifier can be balanced. Fig. II-2-4(d) indicates that the switching characteristics may overlap. However, it is difficult to be sure because e_m traverses the dead zone so rapidly that it is nearly impossible to record a time exposure of the switching characteristic.

The traces of e_{in} vs e_{out} are particularly revealing. They are all practically identical when the driving amplifier has a high enough gain to saturate. But this is exactly the same as operating the two transistor "relay" in the vicinity of E_{PA}. Hence e_{in} vs e_{out} shows the linear phase shift of the system together with backlash.

It is concluded that by making R_b small, and saturating the driving amplifier without a phase shift, dead zone and

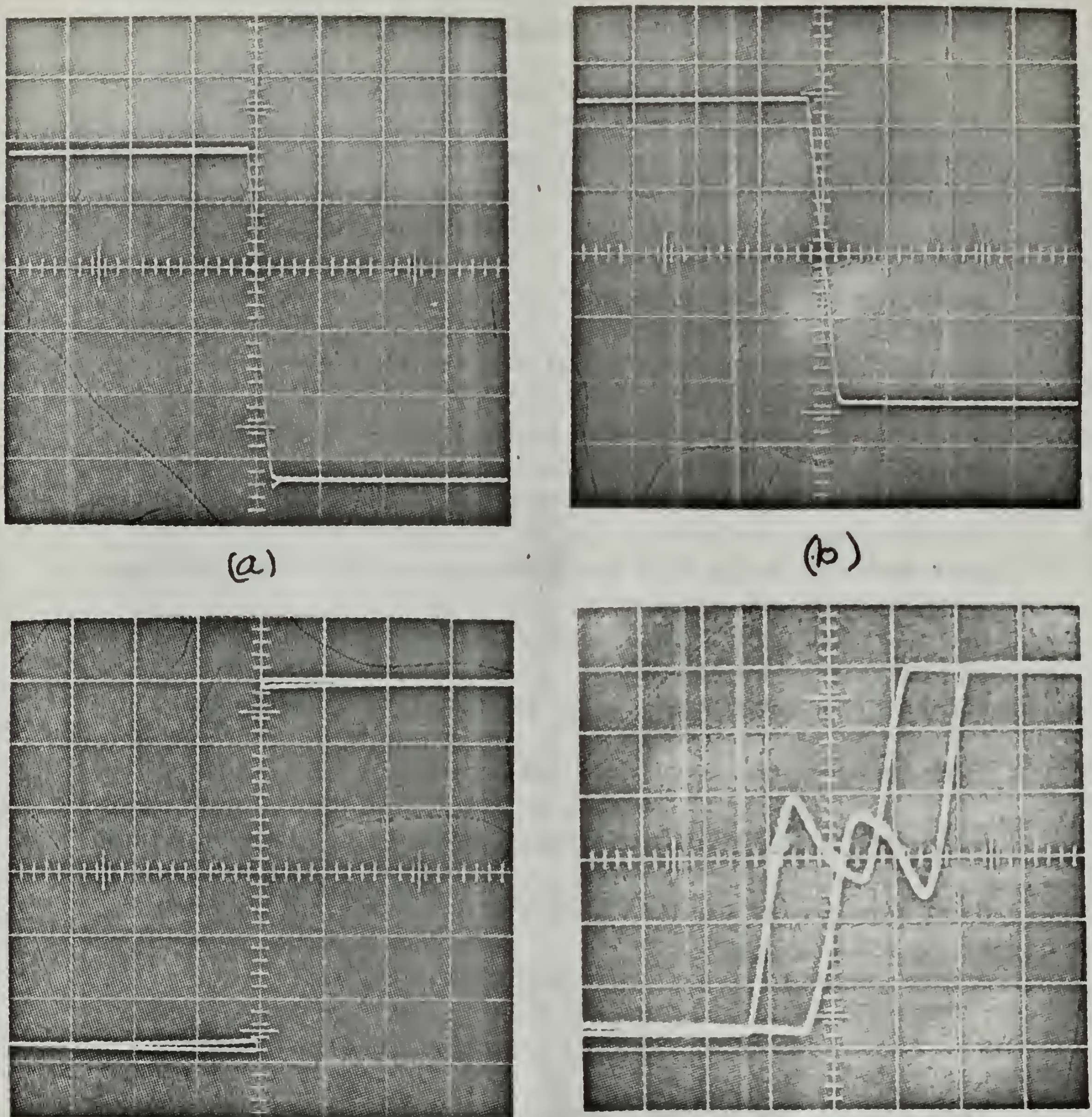

(a) (b) (c) (d)

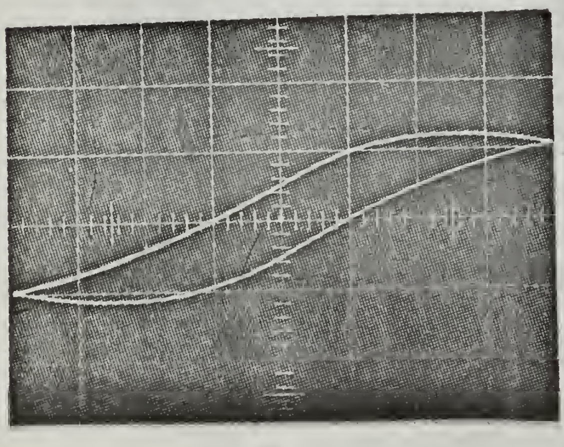

(e)

FIG. II-2-3 Input-output Characteristics, K=100

(a) Abscissa: e_{in}, 1V/cm, Ordinate; e_A unloaded, 10V/cm.

(b) Abscissa: e_{in}, 1V/cm. Ordinate: e_A, loaded, 5V/cm.

(c) Abscissa: e_{in}, 1V/cm. Ordinate: e_M, 4V/cm

(d) Abscissa: e_{in}, .01V/cm, ~~Ordinate: e_M, 4V/cm~~

(e) Abscissa: e_{in}, 1V/cm Ordinate: 10V/cm hysteresis effects can be virtually eliminated. The four transistor "relay" then has the properties of a highly idealized relay with practically no hysteresis, and a dead zone of an order of magnitude of 10 to 100 times less than a run-of-the-mill mechanical relay. And the four transistor "relay" has sufficient current gain to operate a rather substantial, permanent magnet, DC motor at a high performance level using only conventional unregulated power supplies, or even batteries, for that matter.

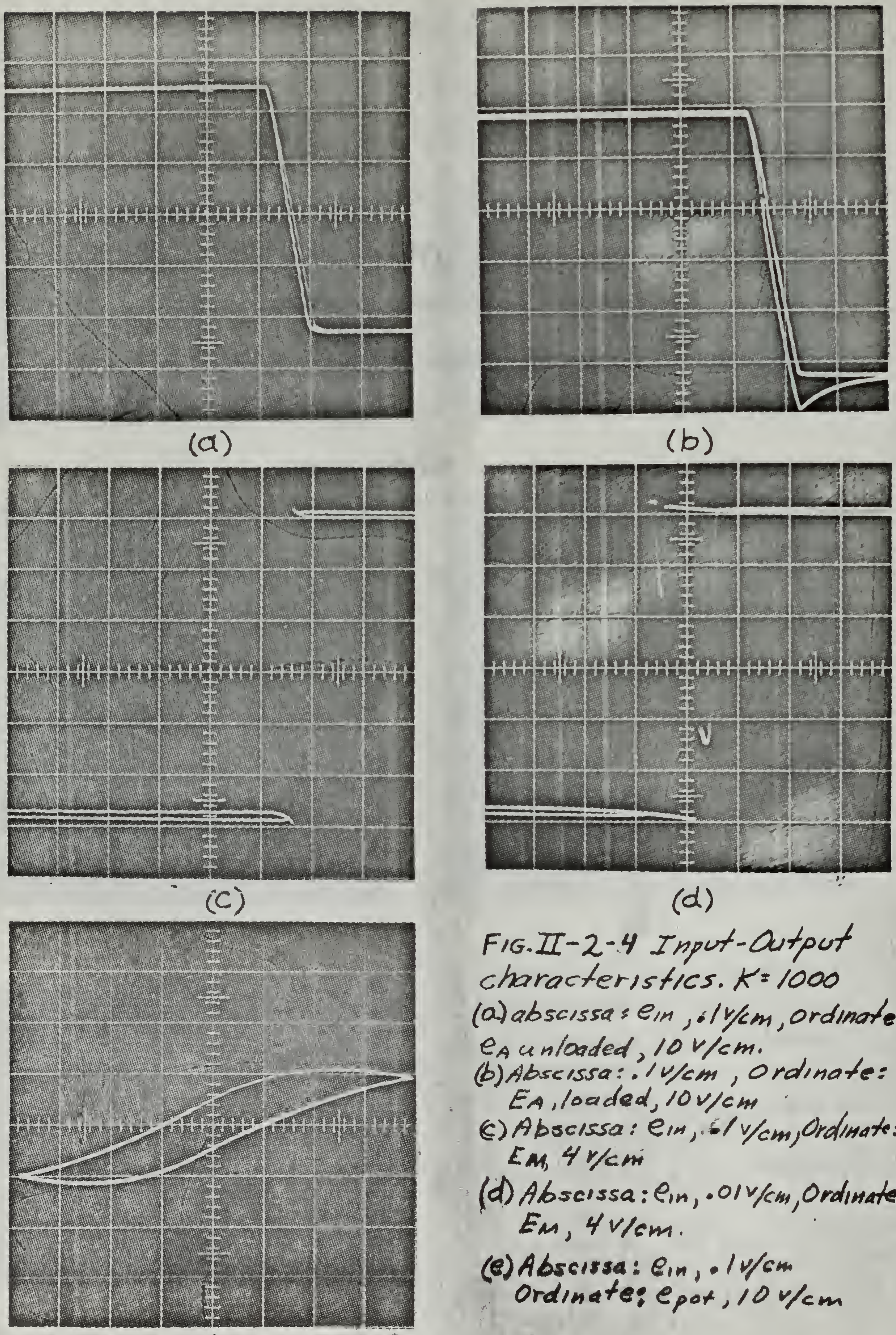

(a) (b) (c) (d) (e)

FIG. II-2-4 Input-Output characteristics. $K = 1000$

(a) abscissa: e_{in}, .1 V/cm, Ordinate: e_A unloaded, 10 V/cm.

(b) Abscissa: .1 V/cm, Ordinate: E_A, loaded, 10 V/cm

(c) Abscissa: e_{in}, .1 V/cm, Ordinate: E_M, 4 V/cm

(d) Abscissa: e_{in}, .01 V/cm, Ordinate: E_M, 4 V/cm.

(e) Abscissa: e_{in}, .1 V/cm Ordinate: e_{pot}, 10 V/cm

3. The describing function

The describing function for the four transistor "relay" was sought primarily to verify its performance as a near-ideal relay. The procedures of Chapter I were repeated, with $K_a = 100$. Fig. II-3-1 is a Nichols plot of the results at .6 Hz. Actual computations indicate a relative phase shift of about 2.5 degrees, as close to the theoretically perfect vertical as anyone is likely to encounter experimentally. Since G_D includes the system backlash, it is again concluded that for most practical applications, this is an ideal relay.

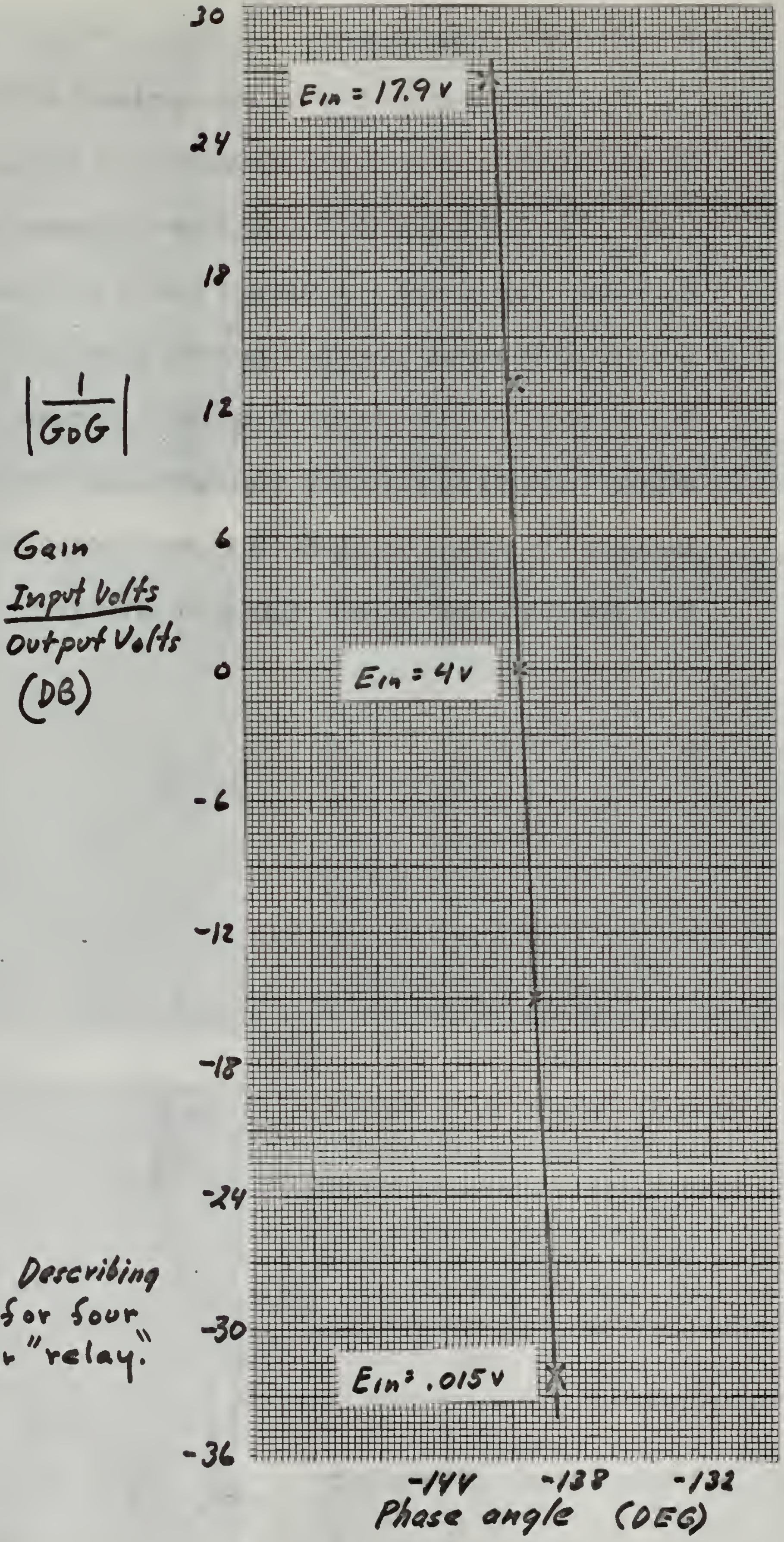

Fig II-3-1 Describing function for four transistor "relay."

4. Open loop frequency response

The open loop frequency response of the system was taken by driving the summing amplifier with a sine wave of four volts peak amplitude. Summing amplifier nominal gain was 100, which when multiplied by the final amplifier gain of about 2500, gave an overall gain of roughly 250,000 to a small signal input. Since the output voltage is limited to 12 volts, the minimum gain was three.

Analysis of the data plotted on Fig. II-4-1 reveals that the three db bandwidth is 0.4 cycles per second. The bandwidth of the two transistor "relay" was found to be 0.3 cycles per second. This increase in bandwidth is due to the longer time per cycle spent in saturation when using this near-ideal "relay." Again, the phase curve shows the additional phase lag due to backlash and other nonlinearities.

The open loop step response is shown in Fig. II-4-2. The time constant is seen to be 0.4 seconds which confirms the frequency response data. Using this value of 0.4 seconds, the open loop transfer function is found to be approximately

$$\frac{K}{s(s + 2.5)} .$$

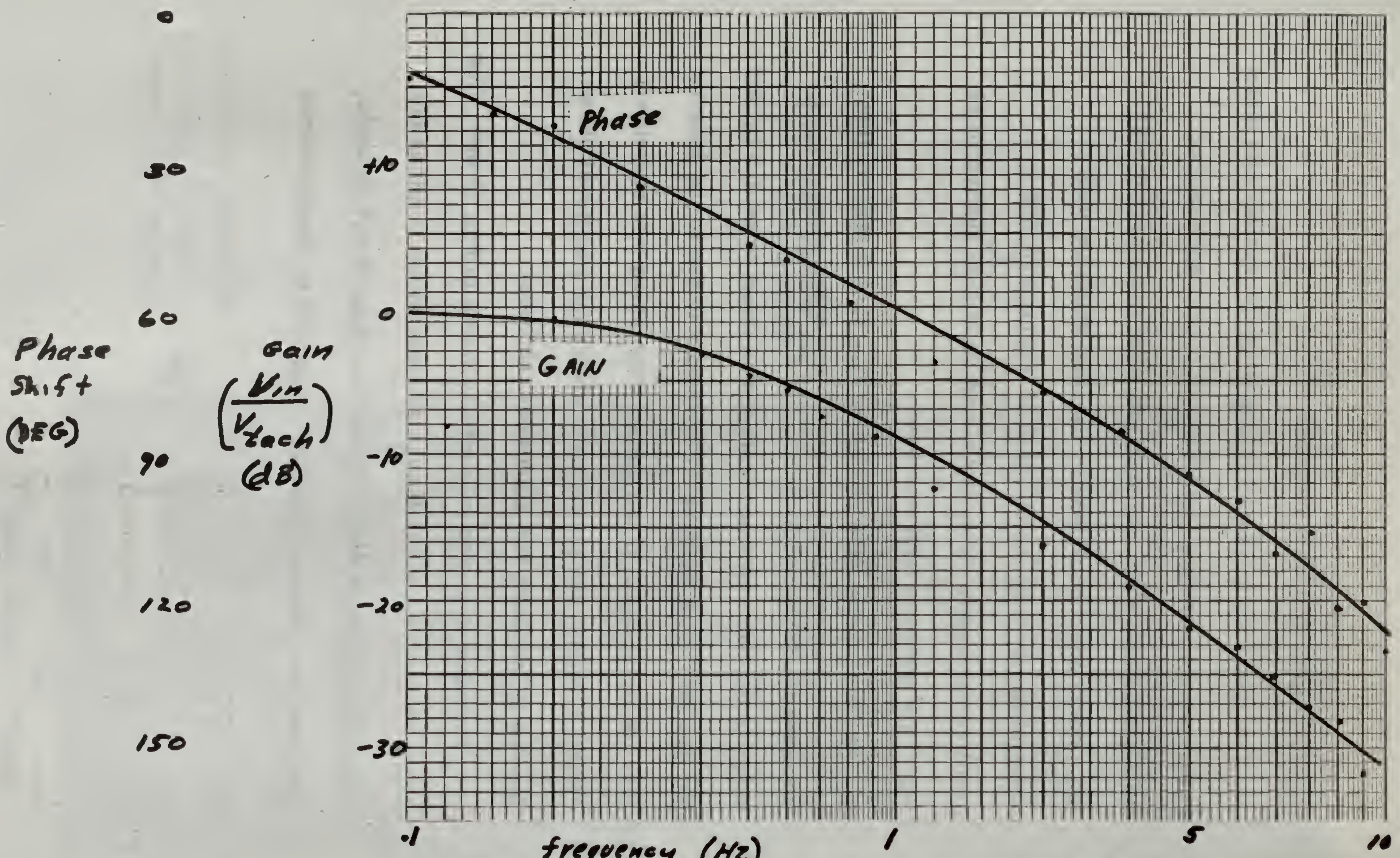

FIG II-4-3 Open loop frequency response, four transistor relay.

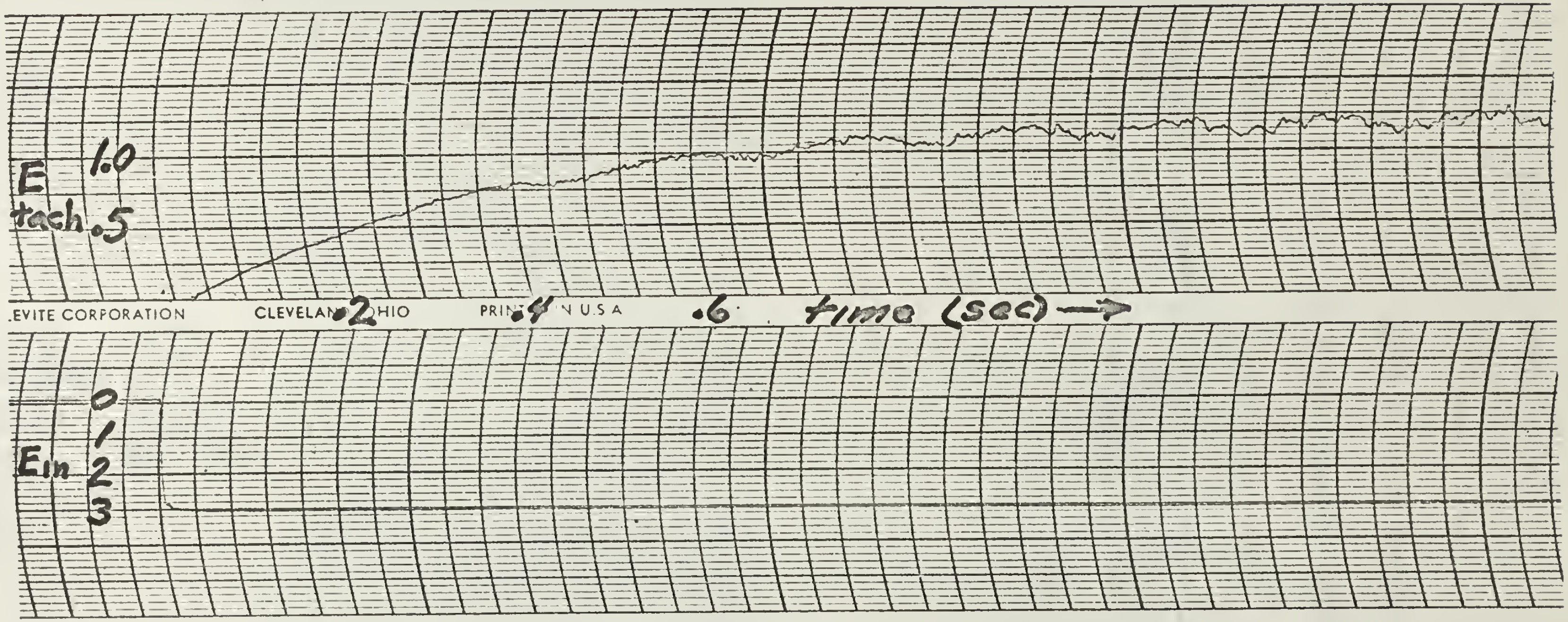

Fig. II-4-2 Open loop step response

5. Closed loop frequency response

Closed loop frequency response data were taken using the circuit configuration shown in Fig. II-1-1. The gain of the summing amplifier was set to four, to just avoid a limit cycle. The driving function was a sine wave of four volts peak amplitude. Under these conditions the three db bandwidth was found to be 1.3 cycles per second. The plot of the frequency response, including the jump resonance, is shown in Fig. II-5-1.

K·E SEMI-LOGARITHMIC 359-80
KEUFFEL & ESSER CO. MADE IN U.S.A.
4 CYCLES X 60 DIVISIONS

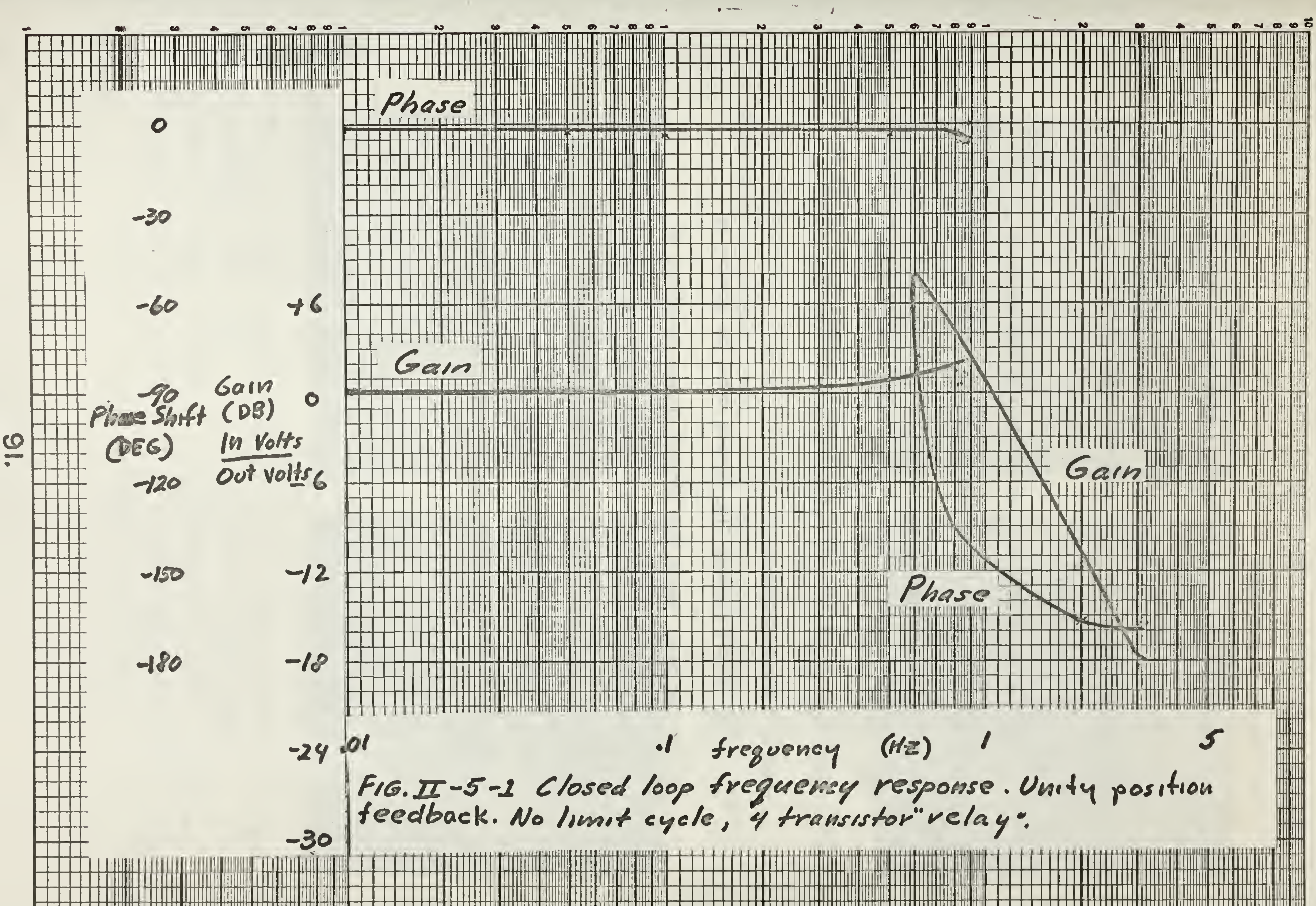

FIG. II-5-1 Closed loop frequency response. Unity position feedback. No limit cycle, "4 transistor" relay".

6. Phase trajectories

The phase trajectories for this near-ideal "relay" were taken in the same manner as previously done for Chapter I. The results, however, are much more typical of those expected for an ideal relay servo.

The value of 100 used for the gain of the summing amplifier was chosen over that of 1000 because the voltage at the summing junction is excessive at the latter gain value. The effect of this voltage is readily seen in Fig. II-6-4. (Note that negative error voltage is greater than the initial positive error voltage.)

Fig. II-6-1 through Fig. II-6-4 show the effects of increasing gain, while Fig. II-6-5 shows the effect of increasing tachometer feedback while holding position feedback constant at a summing amplifier nominal gain of 100. Note the more sharply defined switch points over those shown in Fig. I-6-1 through I-6-6 for the two transistor "relay."

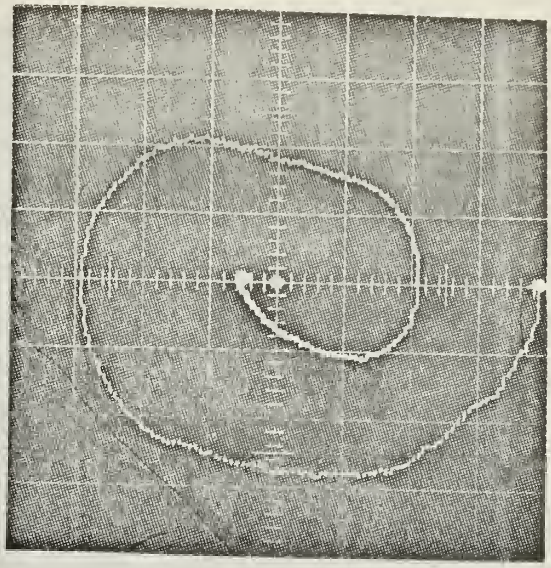

Fig. II-6-1 Phase trajectory. K=1
Abscissa: error, .5v/cm
Ordinate: error dot, .1v/cm

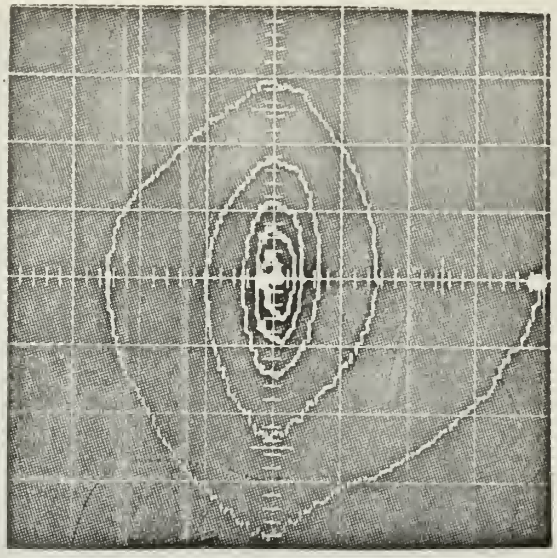

Fig. II-6-2 Phase trajectory. K=10.
Abscissa: error, .5v/cm
Ordinate: error dot, .1v/cm

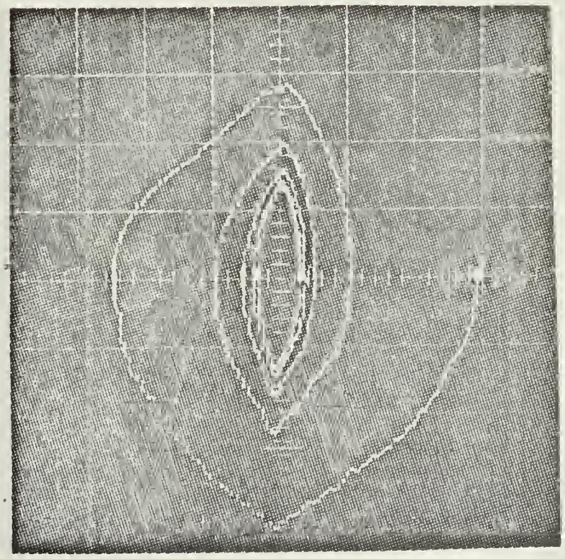

Fig. II-6-3 Phase trajectory. K=100.
Abscissa: error, .5v/cm.
Ordinate: error dot, .1v/cm

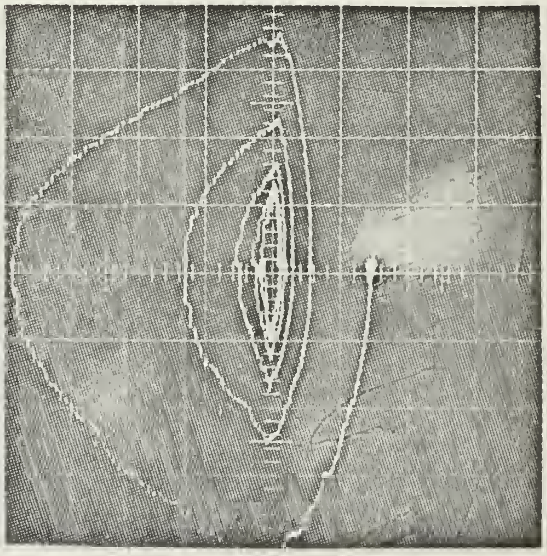

Fig. II-6-4 Phase trajectory. K=1000.
Abscissa: error, .5v/cm.
Ordinate: error dot, .1v/cm.

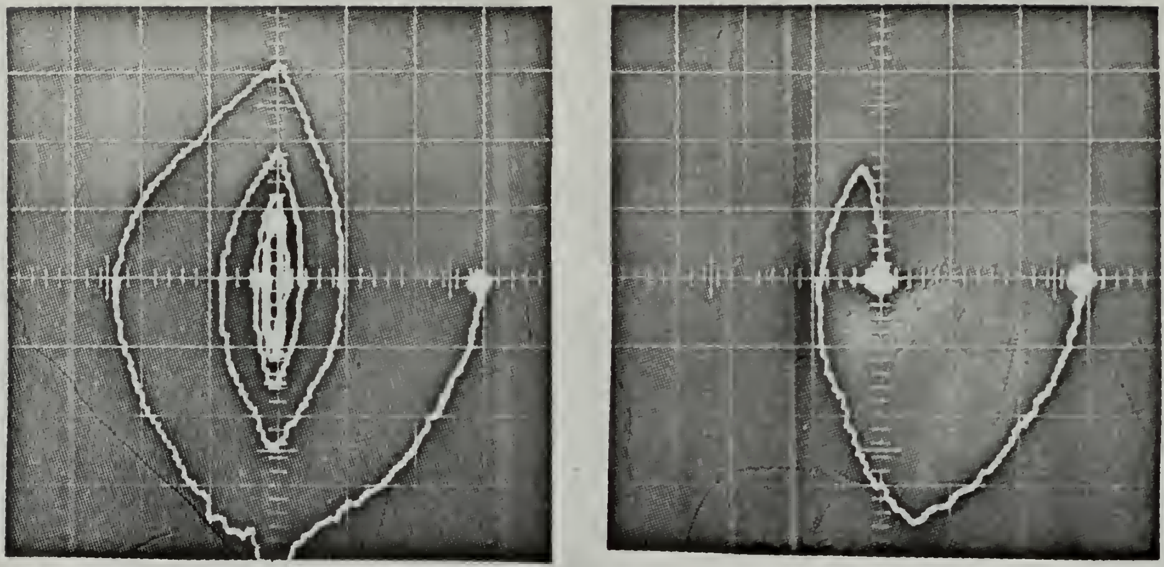

a) $K'_t = .133\,K_t$

(b) $K'_t = K_t$

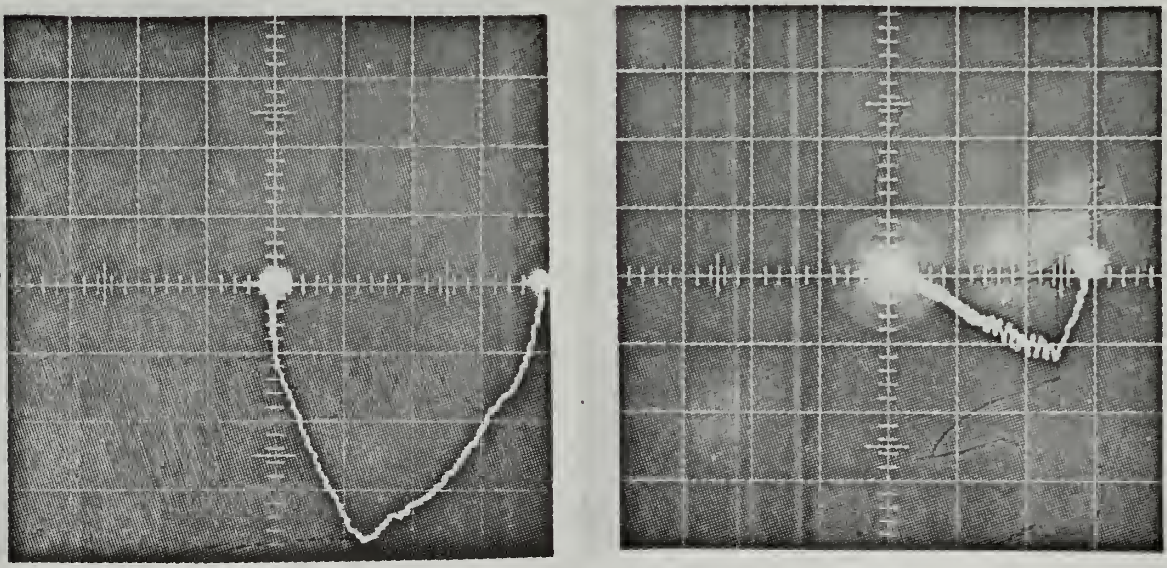

(c) $K'_t = 2\,K_t$

(d) $K'_t = 10\,K_t$

FIG. II-6-5. Phase trajectories, $K = 100$.
Abscissa: error, .1 v/cm
Ordinate: error dot, .5 v/cm

7. Transient responses

The employment of this near-ideal "relay" has resulted primarily in better servo performance. It must be noted that the more ideal a relay is made to be, the higher the frequency and the lower the amplitude of the limit cycle. For this section, an amplifier nominal gain of 100 was used for position feedback. Fig. II-7-1 shows the step response using two different amounts of tachometer feedback. Fig. II-7-2 shows the error signal at the output of the summing amplifier while a triangular wave is applied as the control signal. The high frequency noise is a result of the more ideal "relay" and the relatively noisy tachometer output.

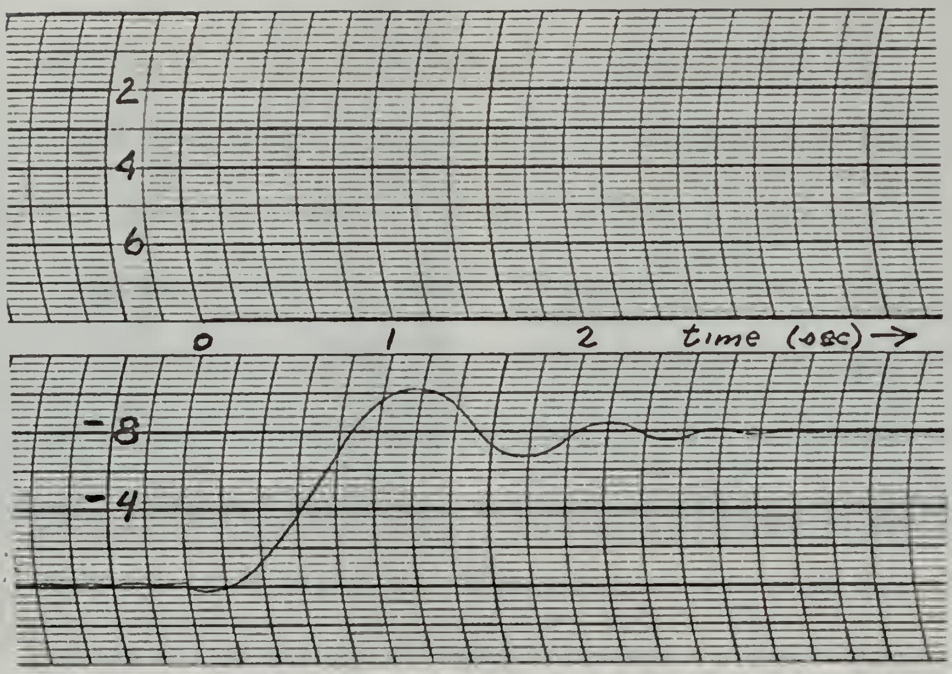

(a) No tachometer feedback

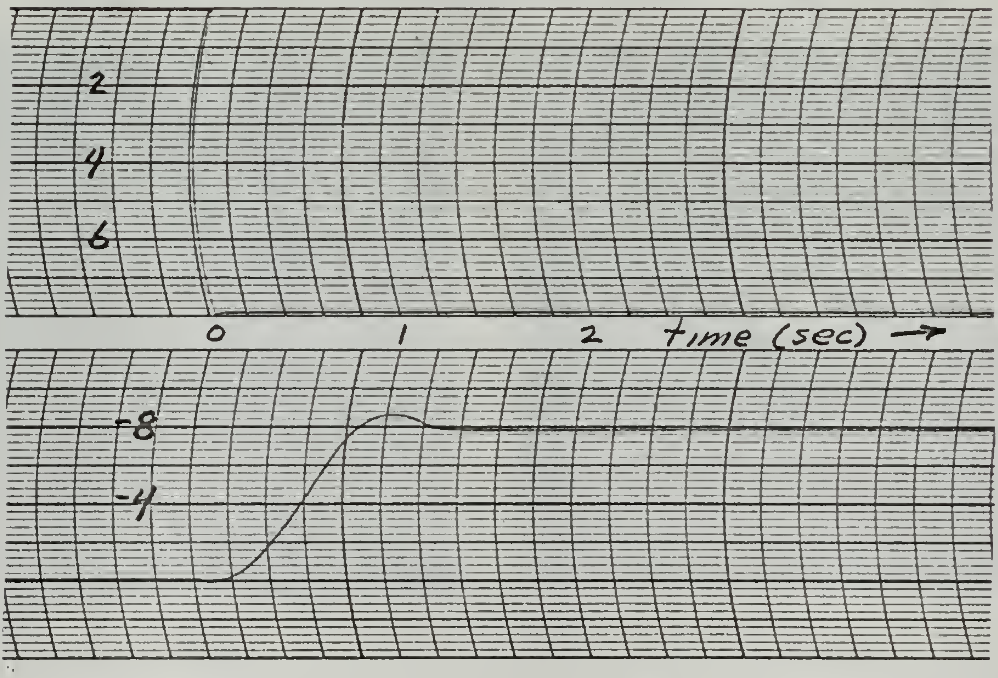

(b) $K'_t = 3K_t$

Fig. II-7-1 Time response, $K_p = 42$

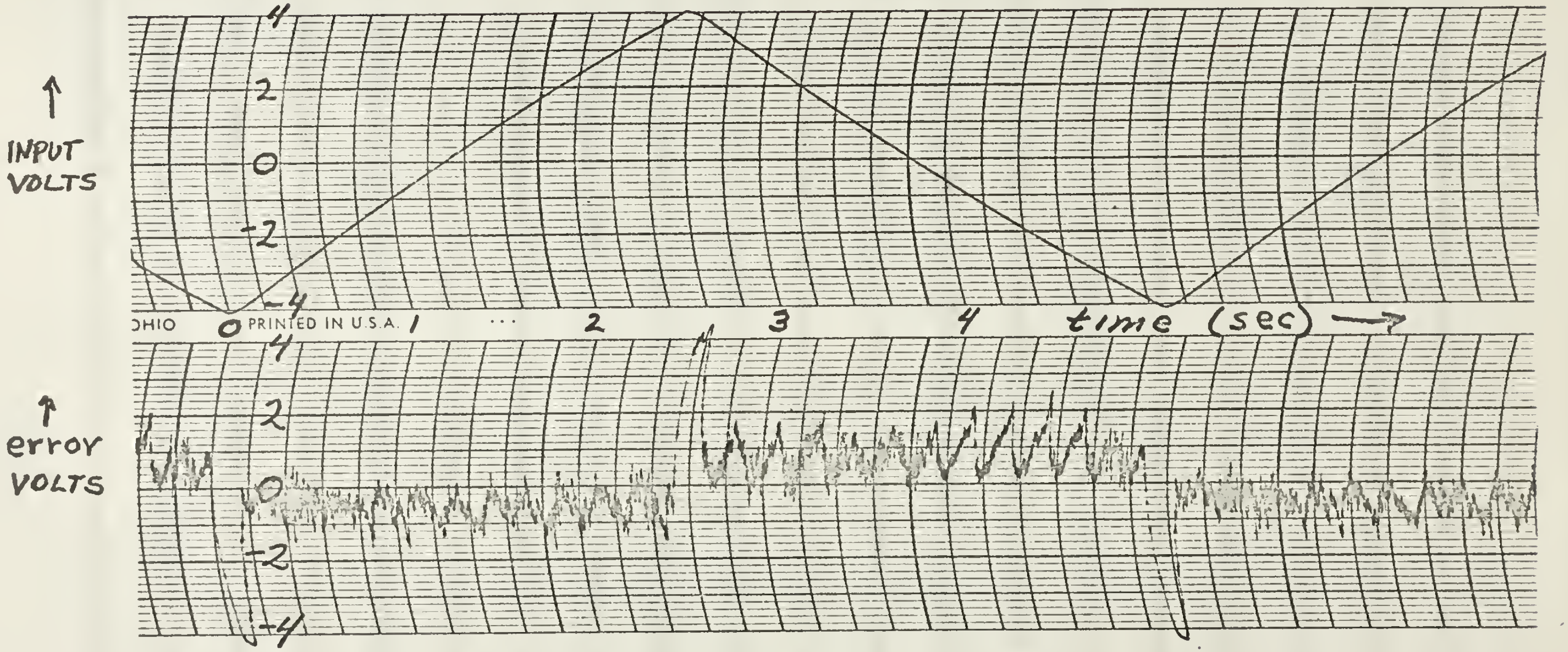

FIG. II-7-2 Error signal with triangular input.
$K_p = 42$, $K_A = 100$, $K'_t = 3K_t$

III

"BANG-BANG" CONTROL OF ANY DC MOTOR WITH A FOUR TRANSISTOR "RELAY"

To verify the hypothesis that the complementary symmetry transistor "relay" could be used to control any standard DC motor, a different test motor was obviously required. A split-field series motor manufactured by Universal Electric for Barber-Colman was substituted for the permanent magnet motor previously used. The field windings and the armature winding were made accessible so that any standard DC motor could be soft-wired. Name plate data was as follows: .0026 hp at 4100 RPM, 27 volts, 0.5 amps, continuous duty. The four transistor "relay" was then used as a "bang-bang" controller. Fig. III-1 shows each hook-up. The transistors are the equivalent transistors of the four transistor "relay." The driving amplifier, indicator lights, fuze, gear train, potentiometer, and tachometer, have all been omitted in Fig. III-1 to simplify the illustrations.

The switching characteristics were observed briefly on the oscilloscope to verify the ideality of the relay action. No attempt was made to eliminate or reduce the usual inductive transient effects with either diodes or a shunt resistor. Brief, visual observations were made to determine if bidirectional motion was achieved and if the response was sharp and tight. In every instance, the motor was controlled both open loop and closed loop, and the response appeared to be good. Hence it was concluded that it was feasible to use the four transistor relay as a "bang-bang" controller for any type of DC motor.

Fig. III-1(a), (b) and (c) are shunt motors and system performance is somewhat similar to the permanent magnet, DC motor. This is especially true, of course, with the circuit of Fig. III-1(a). However, the series motors of Fig. III-1(d), (e) and (f) have response characteristics which are markedly different from those of the shunt machines. Fig. III-2 shows phase trajectories and step responses for the split-series motor of Fig. III-1(d). The extreme non-linearity of the series motor is apparent from the behavior of the system. In general, it can be said that the current squared torque characteristic of the series motor makes it attractive for many fast response types of application. However, Fig. III-2 clearly illustrates that when tachometer feedback is used to eliminate the limit cycle, the time required to reach steady state is not significantly reduced any further. When selecting a DC motor for a particular application, it should be borne in mind that with the permanent magnet motor, or other shunt type machines, the time required to reach steady state is appreciably reduced by increasing the amount of tachometer feedback (up to the point yielding minimum time). The minimum time which may be thus achieved, with the permanent magnet motor, for example, is comparable to the inherently, much faster response of the series motor.

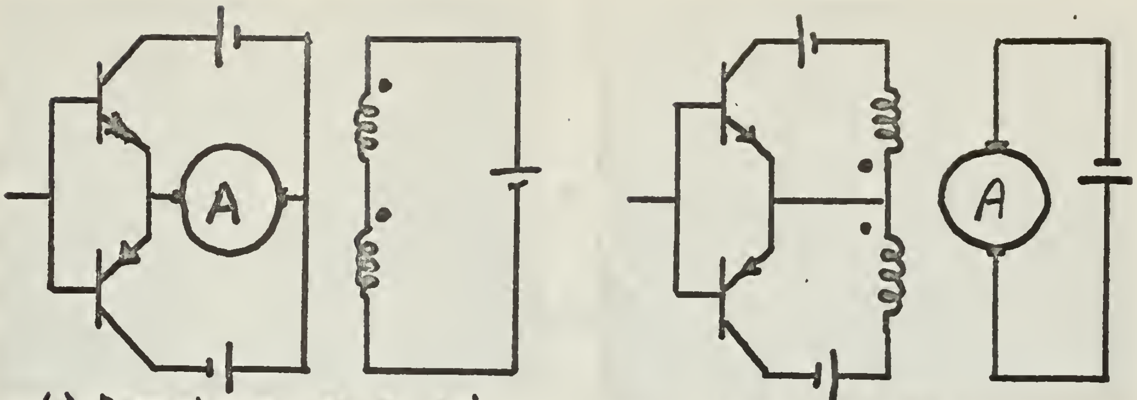

(a) Armature reversal, constant field current.

(b) Field reversal, constant armature current.

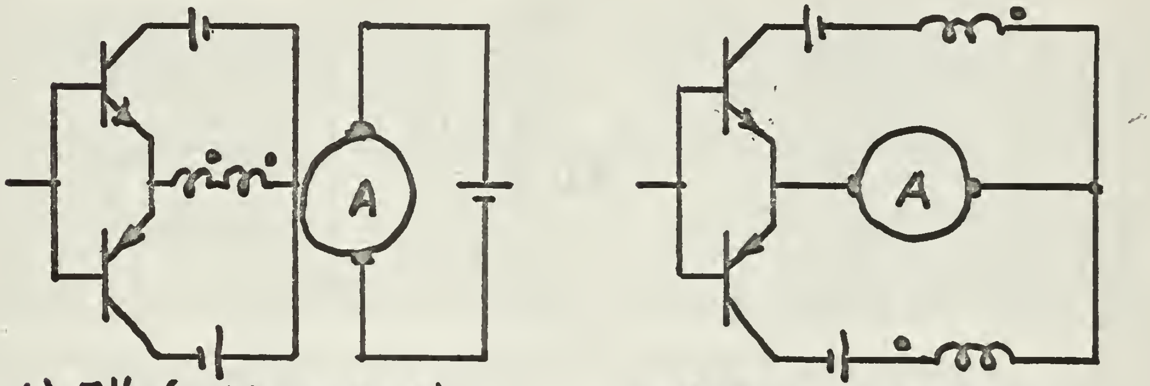

(c) Full field reversal, constant armature current.

(d) Armature reversal, split series.

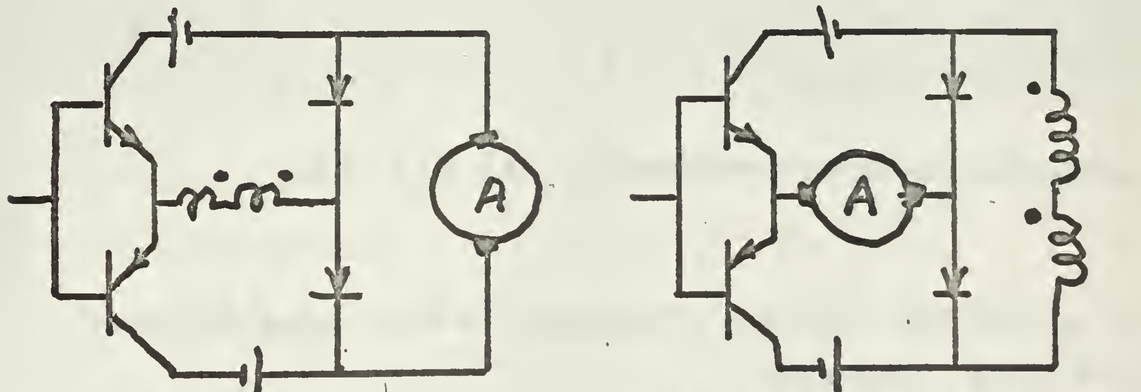

(e) Field reversal, full series

(f) Armature reversal full series.

FIG. III-1 "Bang-Bang" control of DC motors with a transistor "relay."

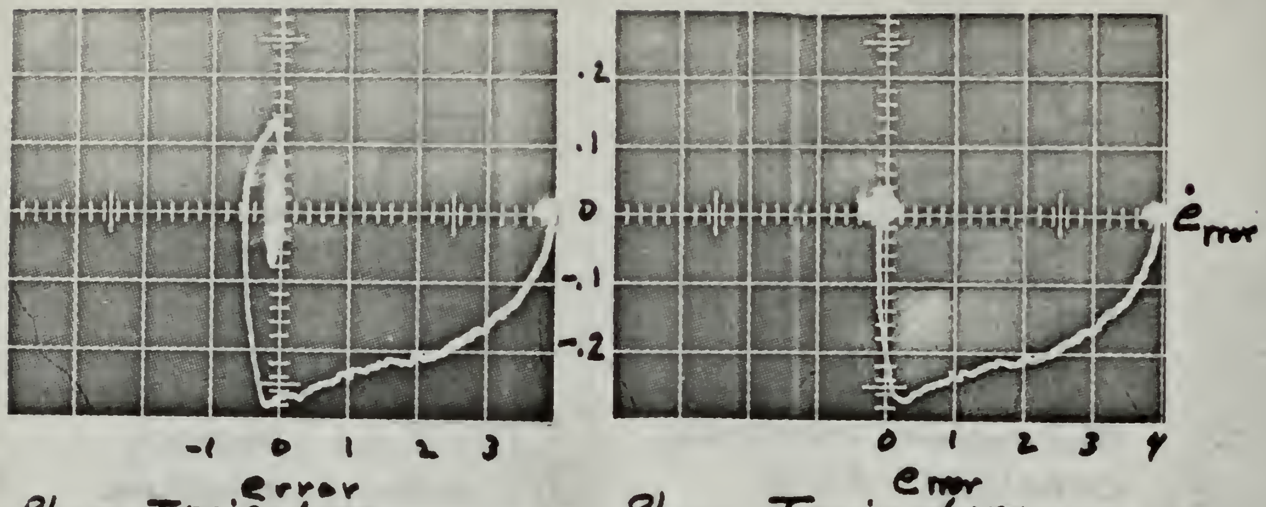

Phase Trajectory

Phase Trajectory

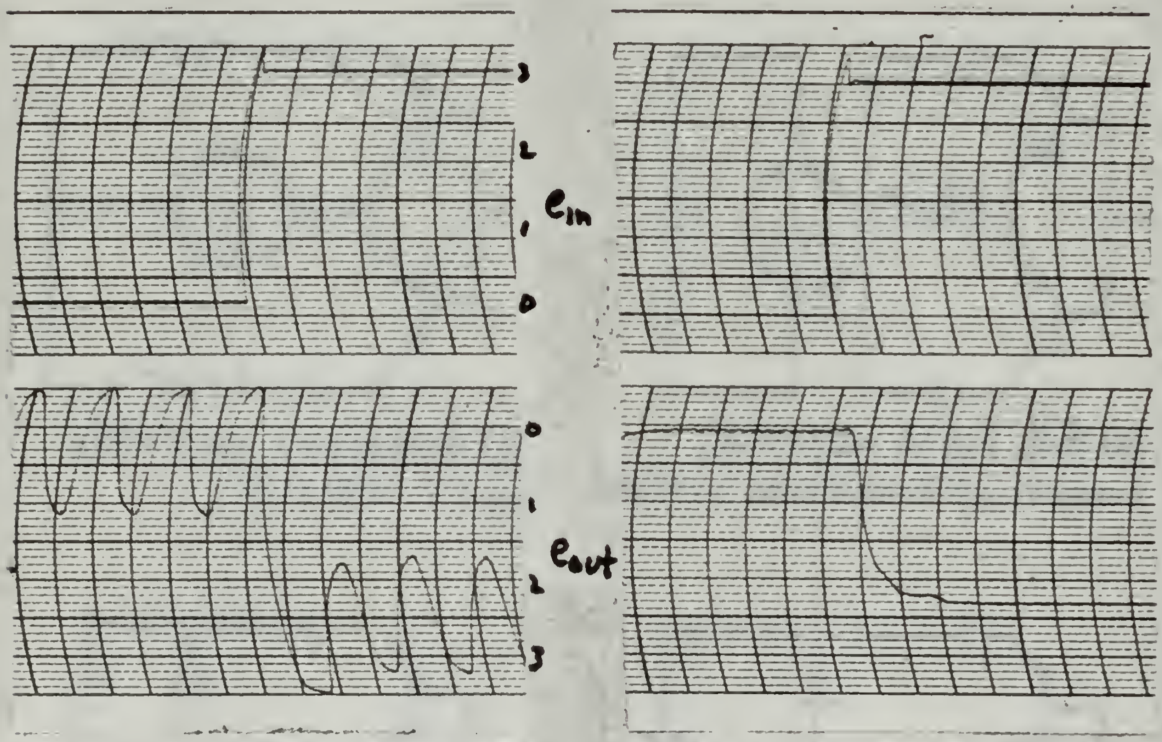

a) No tachometer feedback

b) $K'_t = .1\,K_t$

FIG. III-2 Step response of a split-field series motor.

CONCLUSIONS

The primary objective of transitor synthesizing a near-ideal relay was attained. An ideal relay can, in principle, be realized by an infinite gain, zero dead zone, saturated, symmetrical transistor amplifier. The final circuit, the four transistor "relay", has a dead zone of 10 millivolts at a current gain of about 250,000 and a voltage gain of 1200. Under these conditions the intrinsic hysteresis due to load effects on the collector voltages is negligible. Dead zone and hysteresis can be further reduced by increasing the forward gain.

The four transistor "relay" allows flexibility in switching characteristics. However, this flexibility is not likely to find wide application outside the classroom.

A relay servo system using the four transistor "relay" as the "bang-bang" controller, may be compensated by tachometer feedback or cascade compensation in the same manner and with the same general effect as with conventional mechanical relays.

The four transistor "relay" may be used to control any type of standard DC motor. The resulting system performance will be as expected for a near-ideal relay.

The only apparent limitation on the size of the DC motor which may be controlled with the four transistor "relay" is the state of the art limits on transistor maximum power, current and voltage ratings.

RECOMMENDATIONS

1. That dead zone be further reduced by development of a high power operational amplifier or by use of biased diodes in the output transistor stage.
2. That the state of the art be continuously monitored to ascertain the availability of high power transistors and silicon controlled rectifiers to provide control of large DC motors.
3. That the application of transistor "relays" for AC servo motor control be investigated.
4. That this four transistor "relay" be tested in a digital control loop.
5. That a joint thesis project be undertaken by an operations analyst and an electrical engineer to determine the cost effectiveness of a transistorized relay servo vs a mechanical relay servo.
6. That the current four transistor "relay" training aid being evaluated in the servo laboratory be further modified to increase its value as an aid to understanding various types of nonlinear control and as a test vehicle to implement the preceding recommendations.

The subject for this thesis was suggested by Professor George J. Thaler, Department of Electrical Engineering,

U. S. Naval Postgraduate School. The authors wish to extend their appreciation for his counsel and patience during the course of this investigation.

BIBLIOGRAPHY

1. Tou, J. T. Modern Control Theory. McGraw-Hill, 1964.
2. Chestnut, H. Systems Engineering Tools. Wiley, 1965.
3. RCA. Transistor Manual. RCA, 1964.
4. Thaler, G. J. and R. G. Brown. Analysis and Design of Feedback Control Systems. McGraw-Hill, 1960.
5. Thaler, G. J. and M. P. Pastel. Analysis and Design of Nonlinear Feedback Control Systems. McGraw-Hill, 1962.
6. Liu, C. C. Transistorized Relay Servo Optimization Using a Series Motor. Masters Thesis, USNPGS, 1960.
7. Thompson, R. G. An Experimental Study of Power Transistors As Switching Elements in DC Motor Relay Servos. Masters Thesis, USNPGS, 1960.
8. Texas Instruments. Transistor Circuit Design. McGraw-Hill, 1963.

INITIAL DISTRIBUTION LIST

		No. Copies
1.	Defense Documentation Center Cameron Station Alexandria, Virginia 22314	20
2.	Library U.S. Naval Postgraduate School Monterey, California	2
3.	Bureau of Naval Weapons Department of the Navy Washington, D. C. 20360	1
4.	Professor George J. Thaler Department of Electrical Engineering U.S. Naval Postgraduate School Monterey, California	24
5.	Jackson S. Sells Chairman, Department of Electrical Engineering University of Miami Coral Gables, Florida 33124	2

UNCLASSIFIED
Security Classification

DOCUMENT CONTROL DATA - R&D

(Security classification of title, body of abstract and indexing annotation must be entered when the overall report is classified)

1. ORIGINATING ACTIVITY *(Corporate author)*
U. S. Naval Postgraduate School

2a. REPORT SECURITY CLASSIFICATION
Unclassified

2b. GROUP
N.A.

3. REPORT TITLE
A Transistorized Relay Servo

4. DESCRIPTIVE NOTES *(Type of report and inclusive dates)*
Final Report - Thesis - May, 1966

5. AUTHOR(S) *(Last name, first name, initial)*
Johnson, Stephen (n), Jr., LT, USN
Pidgeon, Robert H., LT, USN

6. REPORT DATE
May 1966

7a. TOTAL NO. OF PAGES
108

7b. NO. OF REFS
8

8a. CONTRACT OR GRANT NO.

b. PROJECT NO. NA

c.

d.

9a. ORIGINATOR'S REPORT NUMBER(S)
NA

9b. OTHER REPORT NO(S) *(Any other numbers that may be assigned this report)*
NA

10. AVAILABILITY/LIMITATION NOTICES
Mennehen 11/25/69
[redacted]
This document has been approved for public release and sale; its distribution is unlimited.

11. SUPPLEMENTARY NOTES
None

12. SPONSORING MILITARY ACTIVITY
U. S. Navy

13. ABSTRACT

Bidirectional control of a DC motor is achieved with standard power transistors and a simple transistorized preamplifier. A permanent magnet, DC motor is used as the test vehicle to illustrate the feasibility of control without an amplidyne or mechanical relay. The"bang-bang" capability of the controller to operate as a near-ideal "relay" is emphasized The inherent flexibility allowed in selecting the switching characteristics is also demonstrated. The discussion points toward practical application and stresses the analysis of the switching characteristics and system performance. The feasibility of using this controller to operate any other type of standard DC motor is also studied.

DD FORM 1 JAN 64 **1473**

UNCLASSIFIED
Security Classification

14. KEY WORDS	LINK A		LINK B		LINK C	
	ROLE	WT	ROLE	WT	ROLE	WT
DESCRIBING FUNCTION						
JUMP RESONANCE						
BANG-BANG CONTROL						
DC MOTOR CONTROL						
RELAY						
TRANSISTOR RELAY						
RELAY SERVO						
TRANSISTORIZED CONTROLLER						
PERMANENT MAGNET MOTOR						
DARLINGTON						
NONLINEAR FEEDBACK CONTROL						

INSTRUCTIONS

1. ORIGINATING ACTIVITY: Enter the name and address of the contractor, subcontractor, grantee, Department of Defense activity or other organization *(corporate author)* issuing the report.

2*a*. REPORT SECURITY CLASSIFICATION: Enter the overall security classification of the report. Indicate whether "Restricted Data" is included. Marking is to be in accordance with appropriate security regulations.

2*b*. GROUP: Automatic downgrading is specified in DoD Directive 5200.10 and Armed Forces Industrial Manual. Enter the group number. Also, when applicable, show that optional markings have been used for Group 3 and Group 4 as authorized.

3. REPORT TITLE: Enter the complete report title in all capital letters. Titles in all cases should be unclassified. If a meaningful title cannot be selected without classification, show title classification in all capitals in parenthesis immediately following the title.

4. DESCRIPTIVE NOTES: If appropriate, enter the type of report, e.g., interim, progress, summary, annual, or final. Give the inclusive dates when a specific reporting period is covered.

5. AUTHOR(S): Enter the name(s) of author(s) as shown on or in the report. Enter last name, first name, middle initial. If military, show rank and branch of service. The name of the principal author is an absolute minimum requirement.

6. REPORT DATE: Enter the date of the report as day, month, year; or month, year. If more than one date appears on the report, use date of publication.

7*a*. TOTAL NUMBER OF PAGES: The total page count should follow normal pagination procedures, i.e., enter the number of pages containing information.

7*b*. NUMBER OF REFERENCES: Enter the total number of references cited in the report.

8*a*. CONTRACT OR GRANT NUMBER: If appropriate, enter the applicable number of the contract or grant under which the report was written.

8*b*, 8*c*, & 8*d*. PROJECT NUMBER: Enter the appropriate military department identification, such as project number, subproject number, system numbers, task number, etc.

9*a*. ORIGINATOR'S REPORT NUMBER(S): Enter the official report number by which the document will be identified and controlled by the originating activity. This number must be unique to this report.

9*b*. OTHER REPORT NUMBER(S): If the report has been assigned any other report numbers *(either by the originator or by the sponsor)*, also enter this number(s).

10. AVAILABILITY/LIMITATION NOTICES: Enter any limitations on further dissemination of the report, other than those imposed by security classification, using standard statements such as:

(1) "Qualified requesters may obtain copies of this report from DDC."

(2) "Foreign announcement and dissemination of this report by DDC is not authorized."

(3) "U. S. Government agencies may obtain copies of this report directly from DDC. Other qualified DDC users shall request through
____ ."

(4) "U. S. military agencies may obtain copies of this report directly from DDC. Other qualified users shall request through
____ ."

(5) "All distribution of this report is controlled. Qualified DDC users shall request through
____ ."

If the report has been furnished to the Office of Technical Services, Department of Commerce, for sale to the public, indicate this fact and enter the price, if known.

11. SUPPLEMENTARY NOTES: Use for additional explanatory notes.

12. SPONSORING MILITARY ACTIVITY: Enter the name of the departmental project office or laboratory sponsoring *(paying for)* the research and development. Include address.

13. ABSTRACT: Enter an abstract giving a brief and factual summary of the document indicative of the report, even though it may also appear elsewhere in the body of the technical report. If additional space is required, a continuation sheet shall be attached.

It is highly desirable that the abstract of classified reports be unclassified. Each paragraph of the abstract shall end with an indication of the military security classification of the information in the paragraph, represented as *(TS)*, *(S)*, *(C)*, or *(U)*.

There is no limitation on the length of the abstract. However, the suggested length is from 150 to 225 words.

14. KEY WORDS: Key words are technically meaningful terms or short phrases that characterize a report and may be used as index entries for cataloging the report. Key words must be selected so that no security classification is required. Identifiers, such as equipment model designation, trade name, military project code name, geographic location, may be used as key words but will be followed by an indication of technical context. The assignment of links, roles, and weights is optional.

[redacted]

thesJ634
A transistorized relay servo /
3 2768 002 10525 6
DUDLEY KNOX LIBRARY